The Role of Effective Action in Quantum Theories of Gravity

THESIS

Submitted in partial fulfillments
of the requirements for the degree of

DOCTOR OF PHILOSOPHY

by

Haridev S R
ID No: 2018PHXF0460H

Under the supervision of

Prof. Prasant Kumar Samantray

BITS Pilani
Pilani | Dubai | Goa | Hyderabad

BIRLA INSTITUTE OF TECHNOLOGY AND SCIENCE, PILANI
2024

BIRLA INSTITUTE OF TECHNOLOGY AND SCIENCE, PILANI

CERTIFICATE

This is to certify that the thesis titled, "**The Role of Effective Action in Quantum Theories of Gravity**" submitted by **Haridev S R** ID No. **2018PHXF0460H** for award of Ph.D. of the Institute embodies original work done by him under my supervision.

S. Prasanthkumar

Signature of the Supervisor

Name: Prof. Prasant Kumar Samantray

Designation: Associate Professor,

Department of Physics,

BITS Pilani, Hyderabad Campus

Date: 22/01/2024

DECLARATION

I, **Haridev S R**, affirm that the thesis entitled "**The Role of Effective Action in Quantum Theories of Gravity**," submitted under the guidance of **Prof. Prasant Kumar Samantray**, constitutes genuine research. I further confirm that it has not been previously submitted, either partially or in its entirety, to this University or any other academic institution for the award of any degree.

Signature of the student	:	
Name of the student	:	Haridev S R
ID number of the student	:	2018PHXF0460H
Date	:	22/01/2024

ACKNOWLEDGEMENTS

I want to express my most profound appreciation and gratitude to all those who have contributed to the completion of my Ph.D. thesis.

First and foremost, I would like to extend my heartfelt thanks to my supervisor, Prof. Prasant Kumar Samantray, for his invaluable guidance throughout my graduation period. His expertise and belief in my abilities have been truly transformative. Dear Sir, thank you for realizing me how to pinpoint the problems and solve them by breaking them into simpler ones. I might have my best research experience in your office while solving on your blackboard. Working with you has been a pleasure, and I am truly honored to be your first Ph.D. student.

I thank Prof. Pallab Basu, my collaborator, for his valuable suggestions and fruitful discussions. Also, I am grateful to Prof. Steven Strogatz for his support and inspiring discussions.

I would like to express my sincere gratitude to Dr. Swastik Bhattacharya and Prof. Rahul Nigam for being on my doctoral advisory committee. I would also like to thank all the faculty members in the Department of Physics at BITS-Hyderabad for their support and encouragement. Additionally, I am grateful to my friends in the department for their discussions and for creating a friendly and supportive atmosphere, making my Ph.D. period a stress-free and enjoyable experience.

I am grateful to all my teachers and friends who have supported me throughout my academic journey. A special thanks to Sai for all the discussions and for showing me how to ask questions to a physical problem.

Thank you, Sreeshna, for making numerous compromises throughout my graduation period and being my steadfast partner.

Finally, I would like to thank my parents for supporting all my life choices, including my career choice as a researcher.

ABSTRACT

This thesis explores the role of quantum effective action in understanding the vacuum states of a quantum field theory in curved spacetimes. The effective action is a powerful mathematical tool in the literature that explains fundamental phenomena like the Schwinger effect, Casimir effect, spontaneous symmetry breaking, etc. It also plays a significant role in understanding various approaches to quantum gravity.

We begin our study on the vacuum states of the field configuration by calculating the vacuum energy of a charged complex scalar field in the presence of a background electromagnetic field with nontrivial boundary conditions (periodic and finite boundary conditions). Understanding the vacuum energy under such nontrivial boundary conditions allows for a deeper understanding of the Casimir effect in scenarios involving extra compact dimensions and in the presence of background fields. Furthermore, these investigations aid in comprehending the role of boundary conditions in the Schwinger effect as well. From an experimental perspective, this research has the potential to facilitate the experimental realization of the Schwinger effect and the detection of extra compact dimensions.

Later we focus on understanding observer dependence of spontaneous symmetry breaking (SSB). SSB is fundamental, and it is nontrivial for such a phenomenon to depend on a class of observers. By general covariance, it is clear that a set of inertial observers would perceive the mechanism of SSB as universal. However, the situation is more complex when we consider this phenomenon from the perspective of a uniformly accelerating observer. In this thesis, we calculate a closed-form expression for the quantum effective potential in the frame of a uniformly accelerated observer for arbitrary dimensions. Using the effective potential, we show that the symmetry is restored from an accelerated observer's perceptive. We did this analysis for a single scalar field with $\lambda\phi^4$ interactions and in the $O(N)$ symmetric scalar field theory using large N limit approximation.

Focusing more on SSB, we study the role of curvature on SSB. The precise model we consider is the $O(N)$ symmetric scalar field theory in anti-de Sitter space (AdS) in the large N limit. We calculate the effective potential in arbitrary dimensional AdS and conclude that SSB exists in three dimensions but not in four-dimensional AdS.

Contents

List of Figures

Conventions

Speed of light	c	=	1
Reduced Planck constant	$\hbar$	=	1
Boltzmann constant	k_B	=	1
Minkowski metric	$\eta_{\mu\nu}$	=	(-,+,+,+)

Chapter 1

Introduction

The primary objective of theoretical physics is to establish a unified framework that encompasses all four fundamental forces, with a special emphasis on comprehending the quantum theory of gravity. Despite significant efforts to construct such a theory that unifies all interactions, it remains an elusive challenge. The quantization of gravity poses formidable difficulties, and its integration into a universal framework is complicated by its intrinsic connection to the spacetime on which quantum field theories are defined.

String theory [1] stands out as a promising candidate for a unified theory, representing all fundamental forces, including gravity, as excitations of one-dimensional strings. The mathematical elegance of the theory and its potential unification through M-theory [1] are compelling features. However, certain challenges, such as the need for supersymmetry for its consistency while lacking any experimental evidence, have raised questions about its validity. Another notable approach is loop quantum gravity [2], which utilizes the canonical quantization scheme. However, this approach fails to consistently unify the forces of nature and also runs into problems that have plagued earlier approaches to quantum gravity. However, both these theories predicted the existence of extra compact spatial dimensions and an experimental realisation of the same can give a valid test for these theories.

Tangentially, the AdS/CFT correspondence [3], also known as the holographic theory, stands as a unique quantum gravity theory in its own right. While it

was discovered from our understanding of string theory, most physicists believe that the correspondence is more general and is independent of string theory. The correspondence posits that a quantum gravity theory in $(d+1)$-dimensional anti-de Sitter (AdS) space is equivalent to a conformal field theory (CFT) without gravity residing on its (d)-dimensional conformal boundary. The AdS/CFT correspondence establishes a strong-weak duality between the two theories involved. This means that a strongly coupled theory in one description is equivalent to a weakly coupled theory in the other description. This duality is immensely valuable since strongly coupled quantum field theories are typically challenging to study, while weakly coupled theories are more amenable to analysis. The conjecture offers a nonperturbative approach to studying strongly coupled CFTs, providing novel insights into the nature of black holes, information theory, and resolving the information paradox [4, 5]. Furthermore, it finds applications in diverse areas, including condensed matter physics [6]. In fact, one can use this correspondence to compute features of strongly coupled quantum field theories by mapping it to the calculations involving classical general relativity in asymptotically anti-de Sitter spacetimes. One can also go the other way by studying quantum gravity aspects of theories in asymptotically anti-de Sitter spacetimes and relate it to weakly coupled quantum field theories at its boundaries. In all these analysis AdS spacetime plays a central role in the formulation of this correspondence.

Another spacetime which naturally emerges in the study of quantum gravity is Rindler space. This is the spacetime as perceived by a uniformly accelerating observer in Minkowski spacetime. Rindler space has been researched quite extensively and offers a simpler framework that captures essential aspects of non-extremal black hole spacetimes without the added mathematical complexities involving singularities. This analysis falls within the broader framework of quantum field theory in curved spacetime. This approach yields fascinating predictions, such as Hawking radiation [7] and the Unruh effect [8, 9]. Although not a fundamental theory, using this method in the context of black hole spacetime provides valuable insights into a quantum theory of gravity. In the absence of a fully developed quantum theory of gravity, this is a powerful tool [10]. Here, gravity is treated as a fixed background without dynamics, while other quantum fields interact within this background.

In summary, owing to the importance of these spacetimes in the context of quantum gravity, in this thesis, we shall investigate fundamental phenomena such as the Casimir effect [11] and Schwinger effect [11] in spacetimes with extra compact dimensions, as well as spontaneous symmetry breaking (SSB) [12, 13] in both Rindler and anti-de Sitter spacetimes. In our belief, these investigations contribute to a deeper understanding of quantum gravity and its underlying principles.

In the thesis, we employ quantum effective action or the quantum effective potential as an essential mathematical tool. The effective potential has been widely utilized in the literature to investigate Casimir effect [14], Schwinger effect [15], Hawking radiation [16], and SSB [17]. All these phenomena are closely linked to the vacuum state of the theory, and the effective potential serves as a powerful tool for defining and comprehending the vacuum state. Understanding vacuum states is crucial as they provide a description of the entire particle spectrum within the theory. Within the path integral formalism, the perturbative study of field dynamics involves expanding the action around the vacuum field configuration. In short, our research aims to explore the role of effective action in comprehending fundamental vacuum phenomena in spacetimes that hold significance for understanding the quantum theory of gravity.

By utilizing the methodologies of effective action, we investigate specific issues such as:

1. The means to detect the existence of additional compact dimensions, as postulated by theories like string theory. Also, how extra compact dimensions can modify the Casimir and Schwinger effects?

2. How to enhance the particle pair production in the Schwinger effect so that it is observable in a laboratory.

3. Does the occurrence of a fundamental phenomenon like SSB rely on the observer?

4. How does SSB depend on the curvature of the background spacetime?

Questions 1 and 2 are addressed in Chapter 3, where we revisit the calculations of vacuum energy of a charged massive complex scalar field in general $R^p \times S^1 \times ... \times S^k$

topology in the background of a constant electromagnetic gauge potential. The investigation of vacuum energy in the compact dimensions, characterized by periodic boundary conditions on the field, exhibits a natural connection to Casimir effect. Subsequently, it has been established that the inclusion of additional compact dimensions introduces modifications to the attractive Casimir force experienced between parallel plates. As an experimentally validated quantum field theory prediction, a more accurate measurement of the Casimir force can serve as a testing ground for confirming the existence of additional compact dimensions. Once we understood the vacuum energy of the complex scalar field in the background electric field, we can also study the role of boundary conditions on the Schwinger pair production rate using the same results. The analysis yields a conclusive finding that both periodic and finite boundary conditions can amplify the pair production rate, thereby facilitating the experimental manifestation of the Schwinger effect.

In Chapter 5, we investigate question 3 by examining the phenomenon of SSB within the frame of a uniformly accelerated observer (also called Rindler frame). The choice of the accelerated observer to study the observer dependence of the SSB is not random. The thermalization theorem or the Unruh effect establishes a connection between an accelerated frame and finite temperature field theory. Within the existing literature, it is known that broken symmetries can be restored at certain finite temperatures. Consequently, one can anticipate an analogous restoration of broken symmetries within the Rindler frame. We conclude the same through proper analysis in general dimensions, thereby further reinforcing the thermalization theorem. Hence, the broken symmetry state observed by an inertial observer manifests as a symmetric state for an observer accelerating beyond a critical acceleration. In our analysis we first employ a single scalar field with ϕ^4 interaction. The symmetry group of interest is the discrete symmetry group $\mathcal{Z}_2$. Furthermore, we expand our analysis by incorporating the $O(N)$ symmetric linear sigma model, encompassing N scalar fields (typically with $N \gg 1$). In this context, the symmetry group is a continuous one.

Finally, we address question 4 in Chapter 6 with explicit calculations of SSB in AdS space. As a constant curvature spacetime, AdS is a suitable setting to examine the curvature dependence of SSB. Moreover, given that we possess a quantum theory of

gravity in AdS facilitated by the AdS/CFT correspondence [3], this framework can contribute to a deeper comprehension of SSB by leveraging the holographic principle.

Chapter 2 presents a concise pedagogical review of the effective action and potential. Likewise, Chapter 4 offers an extensive analysis of SSB, rendering the thesis self-contained.

Chapter 2

The Effective Action

The effective action, commonly denoted as Γ, plays a crucial role in modern theoretical physics. It provides two equivalent descriptions: as the generating function for one-particle irreducible (1PI) Feynman diagrams, and as a reduced-action formalism that captures the essential physics of a system with fewer degrees of freedom. While the effective action is generally non-local, in many cases of interest, it can be expressed as a spacetime integral over the Lagrangian density, known as the effective Lagrangian or effective potential.

The effective potential plays a central role in understanding various aspects of vacuum field configurations, including the vacuum energy, vacuum polarizations, and the nature of symmetry in the vacuum state, such as spontaneous symmetry breaking. It serves as a fundamental mathematical tool that enables us to explore and analyze these phenomena. In this chapter, we present the basic formulation of the effective action and the effective potential, along with the associated mathematical tools that will be utilized in the subsequent chapters.

In this chapter we build the basic formalism of effective action in a way similar to that in [17, 18, 15].

2.1 As a Generating Functional

A fundamental quantity in quantum field theory is the transition amplitude ($\langle 0^+|0-\rangle_J$) between vacuum states in the presence of a source (J). Within the framework of Euclidean path integral formalism, this can be expressed as follows

$$\langle 0^+|0^-\rangle_J = Z[J] = \int [D\phi]\, e^{-\frac{1}{\hbar}[S_E[\phi]-J.\phi]}. \tag{2.1}$$

In this section, we maintain the explicit dependence on $\hbar$. However, it should be noted that in later parts of the thesis, we consider $\hbar = 1$. In the context of statistical field theory, the quantity $Z[J]$ assumes the role of a partition function. It is evident that $Z[J]$ serves as the generating functional for the n-point Feynman diagrams (or moments). However, by working with the connected Feynman diagrams, one can reduce the number of diagrams involved. The generating functional for the connected Feynman diagrams (or cumulants) is expressed as

$$W[J] = \hbar \log(Z). \tag{2.2}$$

$W[J]$ can be considered as the equivalent of the free energy (Helmholtz free energy) in the realm of statistical physics. By further employing the concept of one-particle irreducible ($1PI$) Feynman diagrams, it is possible to further reduce the number of diagrams involved. $1PI$ diagrams are those Feynman diagrams that cannot be separated into disconnected diagrams by cutting a single line. As the entire theory can be reconstructed using $1PI$ diagrams, they are regarded as the fundamental building blocks of the complete set of Feynman diagrams. To obtain the generating functional for $1PI$ diagrams, a functional Legendre transformation is employed. This transformation yields the following expression:

$$\Gamma[\phi_0] = W[J] - \int dv_x J(x)\, \phi_0(x), \tag{2.3}$$

where dv_x is the invariant volume element and ϕ_0 represents the vacuum expectation value of the field. The quantity Γ is referred as the effective action of the theory, which is analogous to the Gibbs free energy in statistical physics. It is important to

note that the effective action is not a functional of the external field, but rather a functional of the field configuration ϕ_0.

By considering Γ as the generating functional of $1PI$ diagrams, we can expand the effective action as follows

$$\Gamma = \sum_n \frac{1}{n!} \int dv_{x_1} ... dv_{x_n} \, \Gamma^{(n)} (x_1 ... x_n) \, \phi_0 (x_1) .. \phi_0 (x_n) . \tag{2.4}$$

The $\Gamma^{(n)}$ terms represent the one-particle irreducible Green's functions, also known as proper vertices. Additionally, it is possible to expand the effective action Γ in terms of derivatives of the field. In flat spacetime, this expansion is equivalent to expanding around the point where all external momenta vanish. In position space, the expansion of Γ can be written as follows:

$$\Gamma = \int dv_x \left(V (\phi_0) + \frac{1}{2} Z (\phi_0) (\partial_\mu \phi_0)^2 + ... \right) . \tag{2.5}$$

The term $V (\phi_0)$ is known as the effective potential and it is solely a function of ϕ_0, not a functional. In the context of flat spacetime, one can interpret the derivation of Eq. 2.5 as an expansion in terms of powers of momentum which can be found in Section 12.3 of [18]. In many physical scenarios, ϕ_0 can be treated as a constant, representing vanishing external momentum. In such cases, all the relevant information of the theory is encoded in the effective potential alone. The calculation including higher-order derivative terms of ϕ_0, can be found in [19]. Now, if we compare with Eq. 2.4, it becomes evident that the n-th derivative of the effective potential corresponds to the summation of all one-particle irreducible diagrams with vanishing external momenta.

Some of the important features of the effective potential are listed below.

1. **Effective potential as an energy density:** Similar to the classical potential, the effective potential can be interpreted as an energy density. Denoted as $V(\phi)$, the effective potential represents the energy density associated with the vacuum state characterized by the expectation value $\langle \phi \rangle = \phi_0$. A detailed derivation of this proposition can be found in Chapter 5, Section 3.7 [17] and

Section 2.3 of [20]. The outline of the proof is as follows . Analogous to the expansion in Eq. 2.5, the function $W(J)$ can be expanded in terms of derivatives of J, which, in the limit of constant J, yields $W(J) \sim TV\varepsilon(J)$, where V denotes the total volume of space and T represents the total time. Consequently, we can identify ε as the energy density of the vacuum state, as indicated in Eq. 2.1.

$$\langle 0^+|0^-\rangle_J = e^{-\frac{i}{\hbar}W} \sim e^{-\frac{i}{\hbar}TV\varepsilon(J)}. \tag{2.6}$$

The above result allow us to write the effective potential for constant ϕ_0 and constant source J as (using Eq. 2.3 and Eq. 2.5)

$$V(\phi_0) = \varepsilon(J) + J\phi_0. \tag{2.7}$$

The equation mentioned above (Eq. 2.7) represents the assertion that the effective potential corresponds to the energy density of the vacuum, subject to the constraint $\langle\phi\rangle = \phi_0$. Detailed information can be found in the aforementioned references for a comprehensive understanding of this concept.

In other words, $V(\phi_0)$ gives the ground state energy density with the classical field ϕ_0. One important point to note is that once we obtain the effective potential, the stationary points (not necessarily minima) of the effective potential corresponds to the vacuum field configuration. Also, if we have more than one local minima, the one that with lowest energy corresponds to the global minima.

2. **Everywhere convex:** Expressing the effective potential as a function of ϕ_0, it can be proven that it possesses convexity throughout. The proof of this statement can be outlined as follows, utilizing equations Eq. 2.1 and Eq. 2.6.

$$-\hbar TV\frac{\partial^2\varepsilon}{\partial J^2} = \left\langle \int dv_x\phi \right\rangle^2 - \left\langle \left(\int dv_x\phi \right)^2 \right\rangle. \tag{2.8}$$

We can observe that the variance of a distribution is consistently positive. Based on this fact, it is possible to demonstrate that the right-hand side of equation

Eq. 2.8 is always positive. As a result, we obtain the following expression

$$\frac{\partial^2 \varepsilon}{\partial J^2} \leq 0 \tag{2.9}$$

Also, from 2.7, one can show that

$$\frac{\partial \varepsilon}{\partial J} = -\phi_0; \qquad \frac{\partial V}{\partial \phi_0} = J. \tag{2.10}$$

Employing equations Eq. 2.8 and Eq. 2.10, it is possible to establish that the second derivative of the effective potential is always positive, thereby indicating the convexity of the effective potential. A comprehensive derivation of this result can be found in Section 13.5 of the reference [20]. Additional relevant sources for this topic include [21] and [22]. It should be noted that this assertion holds true even when the classical potential is non-convex, as is often the case in scenarios involving spontaneous symmetry breaking. The key element in the aforementioned derivation is the positivity of the distribution's variance, which holds significance not only in quantum field theory but also in the domain of statistical physics. Thus, within the context of statistical physics, the aforementioned statement is equivalent to the positivity of the specific heat of the system.

3. **Imaginary part of the effective potential:** Although one might expect the effective potential to be a real-valued function as an energy density, explicit calculations have revealed that it can possess an imaginary part [23]. This occurrence arises due to the instability of the field configuration with a fixed expectation value $\langle \phi \rangle = \phi_0$, as discussed in Section 45.1 of [24]. Consequently, the field configuration decays, and the imaginary part of the effective potential provides the probability of the decay rate per unit volume. Considering $V(\phi_0) = \mathcal{R} + i\mathcal{I}$, where $\mathcal{R}$ represents the real part and $\mathcal{I}$ denotes the imaginary part, we can deduce the following equation from Eq. 4.10.

$$\left| \langle 0^+ | 0^- \rangle_J \right|^2 = e^{-2 \int dv_x \mathcal{I}}. \tag{2.11}$$

Indeed, the imaginary part of the effective potential provides insight into

the number of particles produced per unit time and per unit volume. This concept will be particularly useful in comprehending the Schwinger effect [15]. Furthermore, once the explicit result for the one-loop effective potential is calculated, we can delve further into the discussion of its imaginary part.

2.2 One-loop Effective Potential

As previously mentioned, the calculation of the complete effective potential involves an infinite summation over all Feynman diagrams, which can be computationally challenging. To facilitate the calculation, an effective approximation method is the loop expansion. In this expansion, the leading order corresponds to the sum of all tree-level diagrams, representing the classical potential, while the next leading order corresponds to the sum of all one-loop diagrams, and so on. Calculation of V and Z upto second loop order can be seen in [22]. Now, let us explicitly calculate the effective potential of a scalar field in flat space up to the one-loop order. We consider the Euclidean Lagrangian in flat space.

$$\mathcal{L} = \frac{1}{2}\partial_\mu\phi\partial^\mu\phi + U(\phi)\,. \tag{2.12}$$

In our analysis, we consider a theory with broad generality, where $U(\phi)$ can represent any polynomial function of ϕ and may also include the mass parameter. As previously mentioned, the no loop approximation corresponds to the summation of all tree-level diagrams, which is simply the classical potential $U(\phi_c)$. On the other hand, the sum of all one-loop diagrams can be depicted diagrammatically as shown in Figure 2.1.

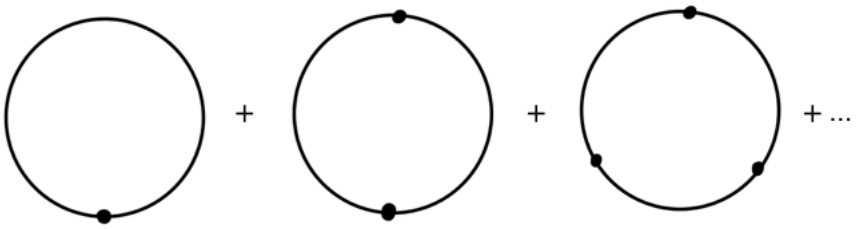

FIGURE 2.1: One loop diagrams

Given that $U(\phi)$ is an arbitrary polynomial function of ϕ, each vertex in Figure 2.1 corresponds to a sum of zero (representing the possible mass parameter), one (representing the cubic interaction), two (representing the quartic interaction), and so on, external lines. Since the effective potential includes terms with zero external momenta, each of these external lines carries zero external momenta. Consequently, the value of the vertex is determined by the second derivative of the potential evaluated at the classical field value, denoted as $U''(\phi_0)$. Hence, the sum of all one-loop diagrams can be expressed as follows:

$$V_1 = \int \frac{d^d k}{(2\pi)^d} \sum_{n=1}^{\infty} \frac{1}{2n} \left(\frac{U''(\phi_0)}{k^2 + i\epsilon} \right)^n , \tag{2.13}$$

where $2n$ is a combinatoric factor. Using this one can get

$$V = U(\phi_0) + \frac{1}{2} \int dv_k \log\left(k^2 + U''(\phi_0)\right) = U(\phi_0) + \frac{1}{2} \log\left(-\Box + U''(\phi_0)\right). \tag{2.14}$$

The operator $\Box$ represents the d'Alembert operator. By incorporating higher loop corrections, the calculations of the effective potential can be improved, as demonstrated in [25, 22]. It is worth mentioning that the results for the loop expansion of the effective potential in curved spacetime can be derived in a similar manner, as illustrated in Section 6.6 of [14]. In this thesis, our focus lies on problems where the one-loop effective potential serves as a satisfactory approximation. Additionally, it should be noted that for the case of free massive scalar field theory in four-dimensional spacetime

$$V_1 = \int \frac{d^4 k}{(2\pi)^4} \log\left(k^2 + m_0^2\right) = \int \frac{d\vec{k}^3}{(2\pi)^3} \sqrt{\vec{k}^2 + m_0^2}, \tag{2.15}$$

where the last equality is true upto an infinite constant. Indeed, equation Eq. 2.15 represents the minimum eigenvalue of the Hamiltonian obtained through the canonical formalism. In the case of free field theory, this minimum eigenvalue corresponds to the vacuum expectation value of the zero-zero component of the energy-momentum tensor, denoted as $\langle T^{00} \rangle$.

2.3 As an Effective Theory

Now we show that the loop expansion is equivalent to a power series expansion with respect to a constant multiple of the Lagrangian. For this purpose, introduce a parameter h in the Lagrangian density as

$$\mathcal{L}(\phi, \partial\phi, h) = \frac{1}{h}\mathcal{L}(\phi, \partial\phi). \tag{2.16}$$

Note that in the context of Feynman diagrams

- Propagator corresponds to the inverse of the differential operator associated with the equation of motion. Consequently, each propagator carries a factor of h.
- Each vertex in a diagram corresponds to an interaction, so each vertex carries a factor of h^{-1}.

With the considerations mentioned, the power of h in a one-particle irreducible diagram can be determined as $P = I - V$, where I corresponds to the number of internal lines and V corresponds to the number of vertices. The relationship between P and the number of loops, denoted as L, in a diagram can be established as follows. The number of loops, L, corresponds to the number of independent momentum integrations. Each internal line contributes to a momentum integral, while each vertex introduces a Dirac delta function that reduces the number of independent momentum integrations by one, except for the Dirac delta function associated with total momentum conservation. Thus, we have $L = I - V + 1$, which implies $P = L - 1$. Consequently, one can conclude that the loop expansion is equivalent to a power series expansion in terms of h.

Now we rederive Eq. 2.14 as the second leading order term in the power series expansion in $\hbar$. Consider a scalar field ϕ with the Euclidean action

$$S_E[\phi] = \frac{1}{\hbar}\int dv_x \left(\frac{1}{2}g^{\mu\nu}\partial_\mu\phi\partial_\nu\phi + U(\phi)\right). \tag{2.17}$$

In Eq. 2.17, ϕ represents the complete quantum field. However, we can express ϕ as $\phi = \phi_0 + \sqrt{\hbar}\eta$, where ϕ_0 is the classical field configuration or the vacuum expectation value of ϕ, and η represents the quantum fluctuation. The quantum fluctuation η is scaled by $\sqrt{\hbar}$ to ensure that the expansion around ϕ_0 is equivalent to a series expansion in $\hbar$. With this, we can expand the action around ϕ_0 as follows:

$$S_E[\phi] = \frac{1}{\hbar} S(\phi_0) + \frac{\hbar}{2} S''(\phi_0)\eta^2 + ... \tag{2.18}$$

In the above expression, the prime ($'$) denotes functional differentiation, and we utilize the fact that $S' = 0$ since ϕ_0 corresponds to the classical field. By substituting Eq. 2.18 into Eq. 2.1, we arrive at a functional Gaussian integral, assuming the translational invariance of the measure ($D\phi \to D\eta$). Employing the standard results of Gaussian integrals, one can obtain the following result (for detailed calculations, refer to Section 12.3 of [26])

$$\Gamma = S_{cl} + \frac{\hbar}{2} \int dv_x \log\left(-\Box + U''(\phi_0)\right), \tag{2.19}$$

The derived expression indeed reproduces the effective potential as given in Eq. 2.14. Thus, we have re-derived Eq. 2.14 as the leading-order term in an expansion in $\hbar$. This derivation highlights the fact that the classical theory corresponds to the $O(\hbar^0)$ order term of a general quantum theory.

Additionally, it is noteworthy that one can reinterpret $\phi_0 + \sqrt{\hbar}\eta$ as a separation of the field ϕ into low-energy modes (ϕ_0) and high-energy modes (η). Consequently, Eq. 2.19 provides a classical effective action for ϕ_0, which encodes the quantum information of the field. This explains the term "effective action" as it captures the effective behavior of the field.

The concept of an effective theory can be extended to include multiple fields. Let's consider an interacting field theory with two dynamical fields, denoted as Q and q. The full theory is described by the partition function, which can be written as

$$Z = \int DQ \int Dq\, e^{-S[Q,q]}, \tag{2.20}$$

where S is the total Euclidean action of the theory. In many physical situations, it is often reasonable to assume that one of the fields, let's say Q, varies slowly compared to the other field, denoted as q. In this case, we can construct a classical field theory for Q by integrating out the degrees of freedom associated with q. This leads to the formulation of an effective Euclidean action, denoted as Γ, which is given by

$$e^{-\Gamma} = \int Dq\, e^{-S[Q,q]}. \tag{2.21}$$

Now one can take Γ as classical action and study its properties. Now we list few well known examples where the idea of effective theory is used in the literature.

1. **Electric field as background field :** In the context of Quantum Electrodynamics (QED) with a slowly varying electric field, the electric field can be approximated as a classical field or background field. By calculating the effective action and effective potential for this background electric field, it is found that the effective potential exhibits an imaginary part, as discussed below Eq. 2.5. This imaginary part corresponds to the number of electron-positron pairs produced by the electromagnetic field per unit time per unit volume, which is known as the Schwinger effect [27]. Julian Schwinger utilized the effective action method to provide a complete quantum field theoretical description of this phenomenon. For more detailed calculations, you can refer to [28] for QED and section 4.2.1 of [15] for the case of a charged scalar field.

2. **Gravitational field as background field :** In the absence of a fully developed quantum theory of gravity, one can treat gravity as a background field within which the dynamics of other fields take place. This forms the basis of studying quantum field theory in curved spacetime. In the formalism we have established, the metric $g_{\mu\nu}$ can be treated as a classical field. By starting from the Lorentzian partition function (analogous to Eq. 4.10) and applying Schwinger's action principle [29], it is possible to demonstrate (as shown in section 12.2 of [26] or section 6.1 of [10]) that
$$\frac{\delta \Gamma_L}{\delta g^{\mu\nu}} = \frac{\sqrt{-g}}{2} \langle T_{\mu\nu} \rangle \,, \tag{2.22}$$

where Γ_L is the Lorentzian effective action, $T_{\mu\nu}$ is the energy momentum tensor and g is the determinant of the Lorentzian metric. $\langle T_{\mu\nu} \rangle$ account the back-reaction of quantum fields and including the back-reaction, one can write the Einstein field equation as $G_{\mu\nu} = 8\pi G \langle T_{\mu\nu} \rangle$. So in a semi-classical gravity theory, one can start defining the effective action as the one which gives the correct $\langle T_{\mu\nu} \rangle$ in Einstein's field equation.

In terms of the one-loop effective action, Eq. 2.19 involves the calculation of the trace of the logarithm of a differential operator. Mathematically, this calculation corresponds to finding all the eigenvalues of the differential operator. However, differential operators are infinite-dimensional operators, and therefore they have an infinite number of eigenvalues.

To extract meaningful physics from these infinite quantities, we follow two steps: regularization and renormalization. The first step, regularization, involves separating out the infinities in a controlled manner. This is typically achieved by introducing a regularization scheme that modifies the calculation in a way that renders the results finite. The second step is renormalization, which involves redefining the parameters of the theory in terms of physically measurable quantities. This is done to absorb the infinities and ensure that the theory is consistent with experimental observations.

In the case of free scalar field theory in Minkowski spacetime, the renormalization procedure can be simplified using a technique called normal ordering. Normal ordering involves subtracting an infinite constant, known as the zero-point energy, from the potential. This eliminates the infinite contributions and allows for meaningful calculations. In flat spacetime, subtracting an infinite quantity is valid because energy differences are physically meaningful, rather than the absolute values of energy. However, in the context of general relativity, where energy is the source of gravity, we cannot freely rescale the zero-point energy. The energy density associated with the quantum vacuum can have observable gravitational effects. Therefore, in gravitational theories, the renormalization procedure is more involved and requires careful treatment of the vacuum energy. Also, in interacting field theories, the renormalization procedure becomes more complex. Additional counterterms are

introduced to absorb the remaining divergences and ensure that physical observables are finite.

2.4 Regularization

We currently lack a theory that can fully explain the nature of the universe across all energy scales. However, quantum field theory has proven to be a powerful framework for understanding the behavior of elementary particles and their interactions within a certain range of energies. It is important to note that quantum field theory is an effective theory, which means it may break down at very high energy scales or small length scales where new physics is expected to emerge.

Nevertheless, this limitation does not hinder our ability to explain and understand the physics observed in our laboratories. The phenomena we observe and study typically occur at finite energy scales that fall within the domain where quantum field theory is applicable. Therefore, we can successfully utilize quantum field theory to describe and explain the experimental results within this energy range. The divergences that arise in our calculations within quantum field theory are a consequence of the fact the theory itself is not valid in all length scale. The two type of divergences we encounter in our calculations are

1. **Ultraviolet (UV) divergence:** The divergences of physical observables at very high energy or small length scales are called UV divergences. We will discuss how to handle these divergences in the next section.

2. **Infra red (IR) divergences:** The divergences occurring at low energy scales are referred to as IR (infrared) divergences. These divergences arise due to the absence of a upper bound on the length scale in the theory, particularly in massless theories where modes with infinite wavelengths are possible. In momentum space, this can be understood by observing that the propagator diverges as the momentum goes to zero in massless theories.

   In dealing with IR divergences, one common approach is to consider a massive theory and then take the limit of the mass tending to zero at the end of

the calculations. This effectively regularizes the IR divergences. However, in certain cases, such as in the high-temperature expansion of a finite temperature field theory, IR divergences can still arise. This is because the expansion is mathematically equivalent to an expansion about a massless theory, leading to the presence of IR divergences [30].

Below we go through some regularization techniques and in next Section 2.5 we describes the renormalization .

2.4.1 The Heat Kernel

The heat kernel associated with an operator $\hat{O}$, characterized by eigenvalues λ_n and eigenfunctions $|\psi_n\rangle$, is defined as

$$\hat{K}(s) = e^{-\hat{O}s} = \sum_n e^{-\lambda_n s} |\psi_n\rangle \langle\psi_n| . \tag{2.23}$$

In terms of the heat kernel one can write the one loop effective potential as (see section 12.3.3 of [26] or section 5.3.3 of [14])

$$V_1 = -\frac{1}{2}\int_0^\infty \frac{ds}{s}\hat{K}(s,x,x) , \tag{2.24}$$

where $\hat{K}(s,x,x)$ is the trace of the heat kernel. Calculating the heat kernel may initially appear challenging due to the involvement of both eigenvalues and eigenfunctions of the operator. However, it becomes more manageable when we realize that, in the position basis, it satisfies the following differential equation

$$\frac{d\hat{K}(s)}{ds} = -\hat{O}\hat{K}(s) , \tag{2.25}$$

with the boundary condition

$$\hat{K}(x,x',s=0) = \delta(x-x') . \tag{2.26}$$

One can calculate the heat kernel explicitly in some simple examples [31]. However, the significance of the heat kernel method arises from several properties, which are summarized below:

1. The heat kernel method can be applied to any self-adjoint, elliptic, second-order differential equation on a scalar function. Therefore, it can be used in various contexts, including general curved spacetime and gauge theories, where the differential operators are gauge invariant.

2. The heat kernel $\hat{K}(s, x, x')$ is non-singular for all $s > 0$ and $x \neq x'$. Additionally, in the limit $x \to x'$ and $s \to 0$, we can obtain an asymptotic expansion of the heat kernel given by:

$$\hat{K}\left(s, x, x'\right) \sim \frac{1}{\left(4\pi s\right)^{d/2}} e^{\frac{-u\left(x,x'\right)}{2s}} \sum_{n=0}^{\infty} a_n\left(x, x'\right) s^n, \tag{2.27}$$

where $u\left(x, x'\right)$ is half the square of the distance between x and x' (also known as Synge's function) and a_n are called the Seely-DeWitt coefficients. Especially in the coincidence limit $(x \to x')$

$$\hat{K}\left(s, x, x\right) \sim \frac{1}{\left(4\pi s\right)^{d/2}} \sum_{n=0}^{\infty} a_n\left(x\right) s^n. \tag{2.28}$$

The crucial aspect of the heat kernel method is that the coefficients $a_n(x)$ are independent of the coordinate system and gauge choice. These coefficients can be calculated explicitly using recursive relations, and the results are well-known in the literature. A recursive method for calculating these coefficients is provided in Chapter 9 of the book [32]. Alternatively, a non-recursive approach for calculating these coefficients in flat space is presented in the paper [33], which offers a comparatively easier method.

By employing Eq. 2.28 in Eq. 2.24, it is possible to regulate the one-loop effective potential and address the issue of ultraviolet divergence in its calculation. In curved spacetime, a different expansion of the heat kernel can be performed using curvature as demonstrated in Chapter 13 of [26]. This alternative expansion provides additional

information about the infrared structure of the theory, capturing its behavior at large distances.

2.4.2 Role of the Free Propagator

As mentioned earlier in Section 2.4.1, the heat kernel method allows us to separate out the divergent part of the effective potential. However, computing the finite remainder using the heat kernel can be a laborious task. In many cases of interest, we require the explicit form of the finite part of the effective potential, for which the heat kernel method may not be as useful. Therefore, we need an alternative regularization method that not only regulates the effective potential but also provides the finite terms. In this section, we introduce one such method that utilizes the propagator or the Green's function in the relevant spacetime. This method becomes particularly valuable when we have knowledge of the explicit form of the Green's function.

The Euclidean Green's function or propagator of a free massive scalar field with mass m in a general curved spacetime satisfies the following differential equation

$$\left(-\Box + m^2\right) G\left(x, x'\right) = \delta\left(x, x'\right). \tag{2.29}$$

Now we can rewrite Eq. 2.14 up to a term independent of the field configuration ϕ_0 using Eq. 2.29 as

$$V_1 = \frac{1}{2}\log\left(-\Box + M^2\right) = \frac{1}{2}\int_0^{M^2} dm^2 \lim_{u\to 0} G\left(u, m^2\right). \tag{2.30}$$

One can get Eq. 2.30 directly from Eq. 2.24 upto a constant by knowing the relation between the heat kernel and propagator as given below

$$G\left(x, x', m^2\right) = \int_0^{\infty} ds\, K\left(s, x, x'\right). \tag{2.31}$$

In situations where we know the explicit form of the Green's function, we can perform a series expansion of $G(u, m^2)$ around $u = 0$. This series expansion serves as

a regularization scheme for the effective potential and also provides the finite terms of the effective potential.

2.5 Renormalization

In the previous section, we discussed the separation of infinite and finite terms in the one-loop effective potential. In this section, we explore how to interpret these infinities in a consistent manner, as initially introduced by Kenneth G. Wilson [34, 35]. The general idea is as follows:

By imposing certain requirements such as symmetry and locality, we can construct a general Lagrangian for the theory, as shown in Eq. 2.12. Subsequently, following the approach described in Section 2.3, we can construct an effective theory that is valid for energies below a certain arbitrary energy scale μ. This process includes modifying the parameters in the Lagrangian (for example, $U(\phi)$ in Eq. 2.12 contains terms like $a_n\phi^n$ for $n = 2, 3, \ldots$, where a_n represents the bare parameters of the theory). In a renormalizable theory, the redefinition of these parameters address the divergences in the effective potential. However, the redefined parameters will depend on the arbitrary energy scale in such a way that the total effective potential or physical observables remains independent of the chosen scale.

2.5.1 $\lambda\phi^4$ Theory

To conclude our discussion on regularization and renormalization, let us consider the explicit calculation of the renormalized one-loop effective potential for a scalar field with quartic interactions ($\lambda\phi^4$ theory) in both flat spacetime and a non-trivial topology. The calculation of the one-loop effective potential for the $\lambda\phi^4$ theory has been extensively studied in the literature. A textbook calculation can be found in section 4.3 of [15] or chapter IV.3 of [36]. Here, we will reproduce these textbook results using the explicit form of the Euclidean propagator discussed in Section 2.4.2.

We consider the classical Euclidean Lagrangian

$$\mathcal{L} = \frac{1}{2}\partial_\mu\phi\partial_\mu\phi + \frac{1}{2}m_0^2\phi^2 + \frac{\lambda_0}{4!}\phi^4, \tag{2.32}$$

where m_0 and λ_0 are bare parameters which does not have any physical relevance. Quantum corrections in the classical Lagrangian introduce divergences in theory, which we can absorb by re-defining the parameters m_0 and λ_0. So we introduce the renormalized parameters m and λ such that both renormalized and bare parameters equate at leading order in λ. Generally, one has to replace ϕ with a renormalized field. However, as we are interested in one-loop calculations, this is fine (For a detailed discussion of our re-normalization procedure, see [37]). In terms of these renormalized parameters, one can write the finite Euclidean Lagrangian as

$$\mathcal{L} = \frac{1}{2}\partial_\mu\phi\partial_\mu\phi + \frac{1}{2}m^2\phi^2 + \frac{\lambda}{4!}\phi^4 + A\phi^2 + B\phi^4, \tag{2.33}$$

where A and B are the counter terms which are divergent and has to be calculated such a way that it make the complete Lagrangian as finite. The Euclidean propagator for a massive scalar field theory in a d dimensional flat space is given as [38]

$$G_E\left(u, m^2\right) = \frac{1}{(2\pi)^{d/2}}\left(\frac{m}{u}\right)^{\frac{d-2}{2}} K_{\frac{d-2}{2}}\left(mu\right), \tag{2.34}$$

where u is the invariant length and $K_\nu\left(z\right)$ is the modified Bessel function of second kind. As we are calculating one loop effective potential using Eq. 2.30, series expand the propagator about $u = 0$. In four dimensional spacetime ($d = 4$ in Eq. 2.34) the series expansion gives

$$\lim_{u\to 0} G_E\left(u, m^2\right) \sim \frac{1}{4\pi^2u^2} + \frac{m^2}{8\pi^2}\left(\gamma_E - \frac{1}{2}\right) + \frac{m^2}{16\pi^2}\log\left(\frac{m^2u^2}{4}\right) + O(u), \tag{2.35}$$

where γ_E is the Euler's constant. One can use the above expansion in Eq. 2.30 to obtain the regularized one loop effective potential as

$$\begin{aligned} V_{eff}^{un} = {} & \frac{1}{2}m^2\phi^2 + \frac{\lambda}{4!}\phi^4 + \frac{\lambda\phi^2}{64\pi^2}M^2\left(\log\left(\frac{M^2}{4\mu^2}\right) - \frac{3}{2} - 2\gamma_E\right) + \frac{\lambda\phi^2}{16\pi^2u} \\ & + \frac{m^4}{64\pi^2}\log\left(\frac{M^2}{4\mu^2}\right) + \frac{\lambda\phi^2}{64\pi^2}M^2\log\left(u^2\mu^2\right) + A\phi^2 + B\phi^4 \end{aligned} \tag{2.36}$$

where $M^2 = m^2/2 + \lambda\phi^2/2$, we introduced an arbitrary energy scale μ in order to separate out the divergent parts. Equation 2.36 is the regularized one loop effective potential. One can find the value of A and B using any physically observable parameters, we use the physical mass (m_p) and physical constant (λ_p) for this purpose. So the renormalization condition is

$$\frac{\partial^2 V_{eff}}{\partial\phi^2}\Big|_{\phi\to 0} = m_p^2 \tag{2.37a}$$

$$\frac{\partial^4 V_{eff}}{\partial\phi^4}\Big|_{\phi\to 0} = \lambda_p. \tag{2.37b}$$

The physical mass of the theory defined using Eq. 2.37a is equivalent to the poles of the complete propagator of the theory, which can be rigorously justified using Källen–Lehmann spectral representation [39, 40]. Similarly, one can experimentally validate the the coupling constant using collision experiments or four point function through S matrix which is equivalent to the definition of λ_p in Eq. 2.37b. Note that in some situations (for example for mass less theory, see chapter IV.3 of [36]), one can't take $\phi \to 0$ limit as the derivative blows up as $\phi \to 0$. In such situation we introduce an arbitrary energy scale and define the parameters accordingly. Using Eq. 2.37 in Eq. 2.36 including the classical contributions gives

$$\begin{aligned} m_p^2 &= m^2 + 2A + \frac{\lambda}{8\pi^2 u^2} + \frac{m^2\lambda}{16\pi^2}\left(\log(u\mu) + \log\left(\frac{m}{2\mu}\right) - \frac{1}{2} + \gamma_E\right) \\ \lambda_p &= \lambda + 24B + \frac{3\lambda^2}{16\pi^2}\left(\log(u\mu) + \log\left(\frac{m}{2\mu}\right) + \gamma_E\right) \end{aligned} \tag{2.38}$$

Choose the counter terms A and B such that it subtracts the divergent term as $u \to 0$ (minimal subtraction) which gives

$$\begin{aligned} m_p^2 &= m^2 + \frac{m^2\lambda}{16\pi^2}\left(\log\left(\frac{m}{2\mu}\right) - \frac{1}{2} + \gamma_E\right) \\ \lambda_p &= \lambda + \frac{3\lambda^2}{16\pi^2}\left(\log\left(\frac{m}{2\mu}\right) + \gamma_E\right). \end{aligned} \tag{2.39}$$

Note that the the physical parameters are independent of the arbitrary energy scale, so the renormalized parameters are dependent on the arbitrary energy scale μ. The dependence renormalized parameters on the μ can be shown be in terms of differential

equation as (from Eq. 2.39)

$$\begin{aligned} \frac{dm^2}{d\mu} &= \gamma(m) = \frac{\lambda_p m^2}{16\pi^2\mu} + O\left(\lambda^2\right) \\ \frac{d\lambda}{d\mu} &= \beta(\lambda) = \frac{3\lambda_p^2}{16\pi^2\mu} + O\left(\lambda^3\right), \end{aligned} \tag{2.40}$$

where we have used the fact that $\lambda = \lambda_p + O(\lambda^2)$. Equation 2.40 are called the renormalization group (RG) equation. The $\gamma(m)$ and $\beta(\lambda)$ tells how the parameters scale according to the energy scale μ. In terms of these renormalized parameters, one can write full renormalized effective potential as

$$V = \frac{1}{2}m^2\phi^2 + \frac{\lambda}{4!}\phi^4 + \frac{1}{64\pi^2}\left(m^2 + \frac{\lambda}{2}\phi^2\right)^2 \log\frac{1}{2\mu}\left(m^2 + \frac{\lambda}{2}\phi^2\right), \tag{2.41}$$

where we rescale the arbitrary energy scale μ. Now that we have the explicit form of the one-loop effective potential (Eq. 2.41), it is important to highlight some key points about the effective potential:

1. It seems that the effective potential is dependent on the arbitrary energy scale μ. But one can show that
$$\frac{dV}{d\mu} = 0, \tag{2.42}$$
using Eq. 2.40. Similarly one can find the RG equation by demanding Eq. 2.42.

2. The one-loop effective potential becomes complex when $m^2 + \frac{\lambda}{2}\phi^2 \leq 0$, as discussed in Section 2.1. In such cases, it is necessary to perform a field shift and calculate the effective potential by considering both the minima of the potential. This ensures a consistent treatment of the quantum corrections and provides a complete description of the system.

2.5.2 The Non Trivial Topology of $S^1 \times R^d$

In this section, we focus on the calculation of the renormalized effective potential for a free massive scalar field in the non trivial $S^1 \times R^d$ topology. In the next chapter, Chapter 2, we generalize this calculation to the case of $S^k \times R^p$ topology. In the case of a non-trivial topology, the renormalized effective potential can be obtained by

subtracting the contribution of the trivial topology. In our calculation, we employ the heat kernel method to evaluate the effective potential, as described in Eq. 2.24. For a free massive scalar field, the heat kernel in the coincident limit on the $S^1 \times R^{d-1}$ manifold is given by

$$K(s,x,x) = \frac{1}{(4\pi s)^{\frac{d}{2}}} \sum_{n=-\infty}^{\infty} e^{-\frac{n^2L^2}{4s}} e^{-sm^2}, \tag{2.43}$$

where s is the proper-time parameter, m is the mass of the scalar field, and L is the circumference of the S^1 direction. In this form, it is evident that $n = 0$ corresponds to the standard flat space heat kernel, and we renormalize the effective potential by subtracting the contribution from R^d. In terms of propagators (see Eq. 2.31), this corresponds to subtracting the flat space propagator. This subtraction yields the residual heat kernel as

$$K(s,x,x) = \frac{2}{(4\pi s)^{\frac{d}{2}}} \sum_{n=1}^{\infty} e^{-\frac{n^2L^2}{4s}} e^{-sm^2}. \tag{2.44}$$

This residual heat kernel captures the contributions arising from the non-trivial topology, allowing us to study the effects of the topology on the renormalized effective potential.

This renormalization works due to the fact that the divergent contributions of the of the non trivial topology is same as the trivial. From Eq. 2.24, one can write the corresponding one-loop effective potential as

$$V = -2\left(\frac{m}{2\pi L}\right)^{\frac{d}{2}} \sum_{n=1}^{\infty} \frac{1}{n^{\frac{d}{2}}} K_{\frac{d}{2}}(mnL), \tag{2.45}$$

where $K_\nu(z)$ is the modified Bessel function of second kind. Equation 2.45 gives the closed form expression for the complete one loop effective potential. Taking $d = 4$, $mL \to 0$ limit in Eq. 2.45 gives the vacuum energy of a massless scalar field with periodic boundary condition as

$$V = -\frac{\pi^2}{90L^2}. \tag{2.46}$$

Similarly one can calculate the vacuum energy in any arbitrary dimensions. We generalize these results in the next chapter.

Chapter 3

The Vacuum Energy

This chapter is based on our work on vacuum energy in compact spacetime [31]. In this study, we investigated the vacuum energy of a complex scalar field coupled to a constant electromagnetic gauge field in a general $R^p \times S^1 \times ... \times S^1_k$ ($R^p \times S^1_k$) topology. Additionally, we examined the Casimir force experienced by a parallel plate system situated in the topology, and we investigated the Schwinger pair production rate in this setting as well for completeness. Through our analysis, we aimed to gain insights into the effects of compact spacetime topologies on these physical phenomena.

The pursuit of unifying interactions has prompted the exploration of the concept of additional compact dimensions. This concept was initially introduced by Kaluza [41, 42, 43], and subsequently further developed in more promising endeavors such as supergravity and string theory. It is worth noting that the presence of boundary conditions and external background fields gives rise to phenomena such as the Casimir effect [11] and Schwinger effect [27]. By considering compact dimensions as periodic boundary conditions, the investigation of physics within extra compact dimensions becomes intertwined with the study of the Casimir effect [44, 45]. Consequently, comprehending fundamental phenomena like the Casimir effect and Schwinger effect within the framework of extra compact dimensions can serve as a platform for experimentally verifying the existence of these additional compact dimensions.

As discussed in Section 2.1, the effective potential provides the vacuum energy of the theory with constant field configuration. In Section 3.1, we compute the one-loop

effective potential for a complex scalar field coupled to a constant gauge potential in the topology of $R^p \times S^1_k$, utilizing Eq. 2.24. This one-loop effective potential enables us to determine the vacuum energy density of the complex scalar field within the specified topology. Subsequently, we employ the vacuum energy to calculate the Casimir force between parallel plates in this topology. Section 3.2 extends our analysis by introducing a coupling between the complex scalar field and constant electric and magnetic fields. Strong electric field results in the Schwinger effect, further explored within the context of finite and periodic boundary conditions in Section 3.3.

3.1 Constant Gauge Potential

The Euclidean Lagrangian density of complex scalar field of mass m and charge q minimally coupled to a vector potential A_μ is

$$\mathcal{L} = (D_\mu \phi)^* (D_\mu \phi) + m^2 \phi^2, \tag{3.1}$$

where $D_\mu = \partial_\mu - iqA_\mu$ is the gauge derivative. In our study, we adopt the Lorentz gauge condition ($\partial_\mu A^\mu = 0$). The k spatial dimensions are compactified within the range $0 < x_j < L_j$, where the index j spans from 1 to k. Given the non-trivial topology, the gauge potentials associated with the compact dimensions cannot be gauge-transformed away. Consequently, we treat the background gauge field as

$$A^\mu = \sum_{j=1}^{k} a_j \delta^\mu_j, \tag{3.2}$$

where a_j's are real. We required the Lagrangian to be single valued, which constrain the Lagrangian to satisfy the boundary condition as

$$\mathcal{L}(\vec{x}, x_1, x_2, ..., x_j + L_j, ..., x_k) = \mathcal{L}(\vec{x}, x_1, x_2, ..., x_k), \tag{3.3}$$

where $\vec{x}$ is the vector in the p dimensional flat Minkowski space and j can vary from 1 to k. The condition on the Lagrangian, where it involves the scalar field ϕ in the combination $\phi\phi^\dagger$ or its higher powers, can be satisfied if the field exhibits the

following generic properties:

$$\phi(\vec{x}, x_1, x_2, ..., x_j + L_j, ..., x_k) = e^{2\pi i \delta_j} \phi(\vec{x}, x_1, x_2, ..., x_k), \tag{3.4}$$

where all δ_j's are just real as of now undetermined phases. In this work we choose $\delta = 0$, corresponds to the periodic boundary condition.

In this section, our objective is to compute the one-loop effective potential utilizing Eq. 2.24. To achieve this, it is necessary to calculate the heat kernel as a solution to the differential Eq. 2.25, while considering the boundary condition given by Eq. 2.26. To solve the differential equation (Eq. 2.25), we employ the Fourier transform method. In a general d-dimensional space ($d = p + k$), the Fourier transform of the heat kernel can be expressed as follows

$$K(s; x, x') \propto \sum\!\!\!\!\!\!\int e^{ipx}\, \tilde{k}(s, p, ...), \tag{3.5}$$

where the summation is over the Fourier modes along the compact dimensions as the heat kernel satisfies the condition

$$K(s; \vec{x}, x_j + L_j; \vec{x}', x'_{j'} + L_{j'}) = K(s : \vec{x}, x_j; \vec{x}', x'_{j'}). \tag{3.6}$$

One can understand the above equation (Eq. 3.6) as follows, under any transformation, heat kernel must behave as $\phi(x)\,\phi^*(x')$ (see Eq. 2.23), and ϕ satisfy Eq. 3.4, which constrain the heat kernel by Eq. 3.6. In terms of the Fourier transform along compact dimensions, one can express the heat kernel as

$$K(\tau; x, x') = \frac{1}{\mathcal{V}_k} \sum_{n_1 ... n_k} \left[k_{n_1,...,n_k} \exp\left(\frac{2\pi i n_1}{L_1}(x_1 - x'_1)\right) ... \exp\left(\frac{2\pi i n_k}{L_k}(x_k - x'_k)\right)\right], \tag{3.7}$$

where $\mathcal{V}_k = L_1 L_2 ... L_k$. Now we proceed to calculate the heat kernel for our problem. The heat equation (Eq. 2.25) can be written as

$$\left(-D_\mu D^\mu + m^2\right) K(s; x, x') = -\frac{\partial}{\partial s} K(s; x, x')\,. \tag{3.8}$$

Using Eq. 3.2 we can expand Eq. 3.8 as

$$\begin{aligned}\Big(&- \nabla_p^2 - \partial_1\partial_1 - \partial_2\partial_2 ... - \partial_k\partial_k + 2iqa_1\partial_1 + 2iqa_2\partial_2 ... + 2iqa_k\partial_k \\ &+ q^2a_1^2 + q^2a_2^2 ... + q^2a_k^2 + M^2\Big)K = -\frac{\partial}{\partial s}K,\end{aligned} \tag{3.9}$$

where ∇_p^2 is the Laplacian in flat p dimensions. Using the Fourier trasform (Eq. 3.7) we can re write Eq. 3.9 as

$$\left(-\nabla_p^2 + M^2_{n_1n_2...n_k}\right) k_{n_1n_2...n_k} = -\frac{\partial}{\partial s}k_{n_1n_2...n_k}, \tag{3.10}$$

where $k_{n_1n_2...n_k}$ is the Fourier coefficients along compact dimensions and

$$\begin{aligned}M^2_{n_1...n_k} = &\left(\frac{2\pi}{L_1}\right)^2\left(n_1 - \frac{qaL_1}{2\pi}\right)^2 + \left(\frac{2\pi}{L_2}\right)^2\left(n_2 - \frac{qa_2L_2}{2\pi}\right)^2 ... \\ &+ \left(\frac{2\pi}{L_k}\right)^2\left(n_k - \frac{qa_kL_k}{2\pi}\right)^2 + m^2.\end{aligned} \tag{3.11}$$

But Eq. 3.10 is the heat kernel equation in flat p dimensional Euclidean space which is known in the literature [32]. Which concludes

$$k_{n_1n_2...n_k} = \frac{1}{(4\pi s)^{p/2}}\exp\left(-\frac{1}{4s}\left|\vec{x} - \vec{x}'\right|^2 - M^2_{n_1n_2...n_k}s\right). \tag{3.12}$$

We also require $k_{n_1...n_k}$ to satisfy the following boundary condition as

$$\lim_{s\to 0} k_{n_1n_2...n_k}(s, \vec{x}, \vec{x}') = \delta^p(\vec{x} - \vec{x}'). \tag{3.13}$$

Now as a heat kernel $K(s, x, x')$ should satisfy similar boundary condition. From (Eq. 3.7) one can show that

$$\begin{aligned}\lim_{s\to 0} K(s, x, x') &= \delta^p(\vec{x} - \vec{x}')\sum_{n_1...n_k}\frac{1}{\mathcal{V}_k}\exp\left(\frac{2\pi in_1}{L_1}(x_1 - x_1')\right)...\exp\left(\frac{2\pi in_k}{L_k}(x_k - x_k')\right) \\ &= \delta^p(\vec{x} - \vec{x}')\delta(x_1 - x_1')...\delta(x_k - x_k').\end{aligned} \tag{3.14}$$

Thus we have the complete heat kernel. Now using Eq. 3.7 and Eq. 3.12 in Eq. 2.24 we can rewrite the one loop correction to the effective potential as

$$\begin{aligned} V_1 &= \int_0^\infty \frac{ds}{s}\frac{1}{\mathcal{V}_k}\sum_{n_1\ldots n_k}\frac{1}{(4\pi s)^{p/2}}\exp\left(-M^2_{n_1\ldots n_k}s\right), \\ &= \frac{1}{\mathcal{V}_k}\frac{1}{(4\pi)^{\frac{p}{2}}}\Gamma\left(\frac{-p}{2}\right)\sum_{n_k\ldots n_1}\left(M^2_{n_1\ldots n_k}\right)^{\frac{p}{2}}. \end{aligned} \tag{3.15}$$

One can do the summation in Eq. 3.15 using

$$\sum_{n=-\infty}^{\infty}\left((n+\beta)^2+\alpha^2\right)^{-\lambda} = \sqrt{\pi}\frac{\Gamma\left(\lambda-\frac{1}{2}\right)}{\Gamma(\lambda)}\alpha^{(1-2\lambda)} + 4\sin(\lambda\pi)f_\lambda(\alpha,\beta), \tag{3.16}$$

where

$$f_\lambda(\alpha,\beta) = \mathcal{R}\left\{\int_\alpha^\infty \frac{(x^2-\alpha^2)^{-\lambda}}{\exp(2\pi x+2\pi i\beta)-1}\right\}. \tag{3.17}$$

Here, $\mathcal{R}$ represents the real part of the complex-valued function. The summation in (Eq. 3.16) converges only when $\mathcal{R}(\lambda) > \frac{1}{2}$. However, the right-hand side expression is valid for all values of λ. For k compact spatial dimensions, we have k summations in Eq. 3.15, and each summation converges. Consequently, we have $k!$ ways to perform this summation, which considers the symmetry related to the exchange of compact dimensions ($L_i \leftrightarrow L_j$). The 'sym' in the equations below represents this symmetry consideration. It's important to note that the Euclidean effective potential (V) is related to the Lorentzian effective potential (V_L) as $V = -V_L$. Therefore, the effective potential for a complex scalar field in a d-dimensional spacetime with k compact spatial dimensions is given by

$$V_L = V_0 - \frac{4\pi\hbar}{\mathcal{V}_k}\sum_{s=1}^{k}\left[\frac{(\pi)^{\frac{d-s}{2}}}{\Gamma\left(\frac{d-s}{2}+1\right)}\left(\frac{1}{L_{k+1-s}}\right)^{d-s}\left(\prod_{r=1}^{k-s}L_r\right)\sum_l{}^{*} f_{\frac{s-d}{2}}\left(\alpha^k_{k+1-s},\beta_{k+1-s}\right)\right] + \text{sym}, \tag{3.18}$$

where $\sum^*$ is a multiple summation and we have to sum over all $l \in (n_k,\ldots,n_{k+2-s})|s \geq 2$ in the range $(-\infty,\infty)$, $\mathcal{V}_k = L_1\ldots L_k$ and

$$\alpha^k_{k+1-s} = L_{k+1-s}\left(L^{-2}_{k+2-s}\left(n_{k+2-s}+\beta_2\right)^2\ldots + L_k^{-2}\left(n_k+\beta_k\right)^2 + \left(\frac{m}{2\pi}\right)^2\right)^{\frac{1}{2}}, \tag{3.19}$$

where $\beta_k = -qa_kL_k/2\pi$. To get Eq. 3.18 we used the mirror identity $\Gamma(-x)\sin(-\pi x) = \pi/x\Gamma(x)$. In Eq. 3.18, V_0 is an infinite quantity corresponds to the contribution

from non compact spacetime. As we discussed at the end of Section 2.5, one can renormalize the effective potential by subtracting the contribution from the non compact spacetime, which corresponds to the trivial topology (R^d). Then the renormalized one loop correction to the effective potential is given as

$$V_{ren} = -\frac{4\pi\hbar}{\mathcal{V}_k}\sum_{s=1}^{k}\left[\frac{(\pi)^{\frac{d-s}{2}}}{\Gamma\left(\frac{d-s}{2}+1\right)}\left(\frac{1}{L_{k+1-s}}\right)^{d-s}\left(\prod_{r=1}^{k-s}L_r\right)\sum_{l}{}^{*} f_{\frac{s-d}{2}}\left(\alpha^k_{k+1-s},\beta_{k+1-s}\right)\right] + \text{sym}, \tag{3.20}$$

3.1.1 Vacuum Energy

The effective potential corresponds to the energy density of the vacuum state (see Section 2.1). But in our system we have an arbitrary parameter corresponds to the constant guage potential. One can choose the guage such that it minimises the effective potential and can call the corresponding effective potential as the vacuum energy of the field. The minimum of the effective potential (Eq. 3.20) is at the maximum of $f_\lambda(\alpha,\beta)$. The a dependence of effective potential is through β. So, we are interested in finding the maximum of $f_\lambda(\alpha,\beta)$ with respect to β when $\lambda<0$. From Eq. 3.17

$$\frac{\partial f}{\partial\beta} = 2\pi\mathcal{I}\left\{\int_\alpha^\infty dx\frac{(x^2-\alpha^2)^{-\lambda}e^{2\pi x+2\pi i\beta}}{\left(e^{2\pi x+2\pi i\beta}-1\right)^2}\right\}, \tag{3.21}$$

where $\mathcal{I}$ gives the imaginary part of the function inside. But,

$$\frac{e^{2\pi x+2\pi i\beta}}{\left(e^{2\pi x+2i\pi\beta}-1\right)^2} = \frac{1}{(2\cos(2\pi\beta)\cosh(2\pi x)-2)+2i\sin(2\pi\beta)\sinh(2\pi x)}.$$

Which gives,

$$\frac{\partial f}{\partial\beta} = -4\pi\int_\alpha^\infty dx\left(x^2-\alpha^2\right)^{-\lambda}\frac{\sin(2\pi\beta)\sinh(2\pi x)}{\left(2\cos(2\pi\beta)\cosh(2\pi x)-2\right)^2+\left(2\sin(2\pi\beta)\sinh(2\pi x)\right)^2}. \tag{3.22}$$

Then,

$$\frac{\partial f}{\partial\beta} = 0 \quad \forall \quad \beta = \frac{n}{2} \quad \text{where} \quad n\in\mathbf{Z}. \tag{3.23}$$

Checking the second derivative at these critical points,

$$\frac{\partial^2 f}{\partial \beta^2}\Big|_{\beta=\frac{n}{2}} = 4\pi \int_\alpha^\infty dx \left(x^2-\alpha^2\right)^{-\lambda} \frac{2\pi(-1)^{n+1}}{\left(2\cos(2\pi\beta)\cosh(2\pi x)-2\right)^2+\left(2\sin(2\pi\beta)\sinh(2\pi x)\right)^2}\,.$$

Which gives

$$\text{Sign}\left(\frac{\partial^2 f}{\partial \beta^2}\right) = (-1)^{n+1} = (-1)^{2\beta+1} \quad \forall \quad n \in \mathbf{Z}.$$

From this we can conclude that f is maximum when $\beta = n$ and is minimum when $\beta = n + \frac{1}{2}$. In our calculations we choose $n = 0$. Then, the renormalized effective potential obtains its minimum value when $a = 0$. Then changing the integration variable in Eq. 3.17 to $y = x/\alpha$ and using the modified Bessel function of second kind $K_\nu(z)$ we can write

$$f_\lambda(\alpha,0) = \frac{\Gamma(1-\lambda)}{\pi^{1-\lambda}\alpha^{\lambda-\frac{1}{2}}} \sum_{n=1}^{\infty} n^{\lambda-\frac{1}{2}} K_{\lambda-\frac{1}{2}}(2\pi n\alpha). \tag{3.24}$$

Using Eq. 3.24 the vacuum energy of a massive complex scalar field is

$$V_{min} = -\frac{4\hbar}{L^d}\sum_{s=1}^{k}\sum_{l}^{*}\sum_{n=1}^{\infty}\left(N^k_{k+1-s}\right)^{\frac{d-s+1}{2}} n^{\frac{s-d-1}{2}} K_{\frac{d-s+1}{2}}\left(2\pi n N^k_{k+1-s}\right) + \text{sym}, \tag{3.25}$$

where

$$N^k_{k+1-s} = \sqrt{n^2_{k+2-1}+\ldots+n^2_{k+1-s}+(mL/2\pi)^2}. \tag{3.26}$$

In obtaining Eq. 3.26 we assume $L_1 \approx L_2 \ldots \approx L_k \approx L$. Now we do some explicit calculation of vacuum energy of a complex scalar field using Eq. 3.18 in some specific spacetimes.

$1+3$ dimensional flat spacetime with two compact dimensions

The zero point energy of the massless complex scalar field in $\mathbb{R}^{(1,1)} \times \mathbb{S}^1 \times \mathbb{S}^1$ topology is given by Eq. 3.25 with $p = 2$ and $k = 2$. This leads to

$$\begin{aligned} V_{min} &= -4\hbar\pi^2 \left(\frac{4 f_{-\frac{3}{2}}(0,0)}{3L_2^4} + \frac{\sum_{n_2} f_{-1}(N_{n_2},0)}{L_2 L_1^3} \right) + \text{sym}, \\ &= -2\hbar\pi^2 \left(\frac{4 f_{-\frac{3}{2}}(0,0)}{3L_2^4} + \frac{4 f_{-\frac{3}{2}}(0,0)}{3L_1^4} + \frac{\sum_{n_2} f_{-1}(N_{n_2},0)}{L_2 L_1^3} + \frac{\sum_{n_1} f_{-1}(N_{n_1},0)}{L_1 L_2^3} \right), \\ &= -\frac{\hbar}{10} \left(1.2 \left(\frac{1}{L_1^4} + \frac{1}{L_2^4} \right) + 1.96 \left(\frac{1}{L_2 L_1^3} + \frac{1}{L_1 L_2^3} \right) \right). \end{aligned} \tag{3.27}$$

In this expression, if we take the limit of either L_1 or L_2 approaching infinity and consider the symmetry factor appropriately, we will recover the standard result for one compact space dimension i.e., $V_{min} = -\hbar\pi^2/45L^4$ [14]

$1+5$ dimensional flat spacetime with two compact dimensions

As we are interested in four-dimensional Minkowski spacetime, consider the topology $\mathbb{R}^{(1,3)} \times \mathbb{S}^1 \times \mathbb{S}^1$. This consists of four flat dimensions ($p = 4$) and two compact dimensions ($k = 2$). Then, using equation (Eq. 3.25), the zero-point energy of a massless complex scalar field in this topology is as follows:

$$\begin{aligned} V_{min} &= -2\hbar\pi^3 \left(\frac{16 f_{\frac{-5}{2}}(0,0)}{15L_2^6} + \frac{\sum_{n_2} f_{-2}(N_{n_2},0)}{L_1^5 L_2} \right) + \text{sym}, \\ &= -\hbar\pi^3 \left(\frac{16 f_{\frac{-5}{2}}(0,0)}{15L_2^6} + \frac{16 f_{\frac{-5}{2}}(0,0)}{15L_1^6} + \frac{\sum_{n_2} f_{-2}(N_{n_2},0)}{L_1^5 L_2} + \frac{\sum_{n_1} f_{-2}(N_{n_1},0)}{L_2^5 L_1} \right), \\ &= -\frac{\hbar}{100} \left(6.6 \left(\frac{1}{L_2^6} + \frac{1}{L_1^6} \right) + 8.5 \left(\frac{1}{L_2 L_1^5} + \frac{1}{L_1 L_2^5} \right) \right). \end{aligned} \tag{3.28}$$

$1+6$ dimensional flat spacetime with three compact dimensions

Now include one more extra compact dimension (i.e., $p = 4$ and $k = 3$). Then the vacuum energy of the massless complex scalar field is,

$$\begin{aligned} V_{min} &= -4\hbar\pi^3\left(\frac{\pi f_{-3}(0,0)}{6L_3^7} + \frac{8\sum_{n_3} f_{-\frac{5}{2}}(N_{n_3},0)}{15L_2^6L_3} + \frac{\sum_{n_2}\sum_{n_3} f_{-2}\left(N_{n_2,n_3},0\right)}{2L_1^5L_2L_3}\right) + \text{ sym}, \\ &= -\frac{\hbar}{10}\left(\frac{1.21}{L_3^7} + \frac{1.45}{L_2^6L_3} + \frac{1.83}{L_1^5L_2L_3}\right) + \text{sym}. \end{aligned} \tag{3.29}$$

These results are accurate when all compact spatial dimensions are of same size. But summations in renormalised effective potential (Eq. 3.20) converges very fast and the leading order itself is a good approximation and it simplifies the calculations drastically. So in the next section, we take this approximation and also check the validity of the approximation by comparing it with the results above.

3.1.2 Approximation Scheme for the Vacuum Energy

The function $z^\lambda K_\lambda(z)$ rapidly decays as z ranges from 0 to ∞. This enables us to approximate the sum $\sum^*$ using its leading order term as follows

$$V_{min} \approx -\frac{4\hbar}{\mathcal{V}_k}\sum_{s=1}^{k}\left(\frac{\prod_{r=1}^{k-s}L_r}{L_{k+1-s}^{d-s}}\right)\left(\frac{mL_{k+1-s}}{2\pi}\right)^{\frac{d-s+1}{2}}\sum_{n=1}^{\infty} n^{\frac{s-d-1}{2}}K_{\frac{d-s+1}{2}}(nmL_{k+1-s}) + \text{sym}. \tag{3.30}$$

The above equation (Eq. 3.30), simplifies the effective potential considerably. This approximation is valid even for compact dimensions of difference size. Also using the result $\lim_{z\to 0} z^\nu K_\nu(z) = 2^{\nu-1}\Gamma(\nu)$ we can use Eq. (3.30) for calculating the vacuum energy of massless scalar field in the same spacetime. Now we can check the validity of our approximation by calculation the vacuum energy of the massless complex scalar field using Eq. 3.30 and comparing the results with results with the one calculated using Eq. 3.25. The vacuum energy of the massless complex scalar field in different spacetime are as follows

$p = 2,\ k = 2$

$$\begin{aligned} V_{min} &\approx -2\hbar\pi^2 \left(\frac{1}{180} \left(\frac{1}{L_1^4} + \frac{1}{L_2^4} \right) + \frac{\zeta(3)}{4\pi^3} \left(\frac{1}{L_2 L_1^3} + \frac{1}{L_1 L_2^3} \right) \right), \\ &= -\frac{\hbar}{10} \left(1.2 \left(\frac{1}{L_1^4} + \frac{1}{L_2^4} \right) + 1.91 \left(\frac{1}{L_2 L_1^3} + \frac{1}{L_1 L_2^3} \right) \right). \end{aligned} \tag{3.31}$$

$p = 4,\ k = 2$

$$\begin{aligned} V_{min} &\approx -\hbar\pi^3 \left(\frac{2}{945} \left(\frac{1}{L_2^6} + \frac{1}{L_1^6} \right) + \frac{3\zeta(5)}{4\pi^5} \left(\frac{1}{L_2 L_1^5} + \frac{1}{L_1 L_2^5} \right) \right), \\ &= -\frac{\hbar}{100} \left(6.6 \left(\frac{1}{L_2^6} + \frac{1}{L_1^6} \right) + 7.9 \left(\frac{1}{L_2 L_1^5} + \frac{1}{L_1 L_2^5} \right) \right). \end{aligned} \tag{3.32}$$

$p = 4,\ k = 3$

$$\begin{aligned} V_{min} &\approx -4\hbar \left(\frac{15\zeta(7)}{16\pi^3 L_3^7} + \frac{\pi^3}{945 L_2^6 L_3} + \frac{3\zeta(5)}{8\pi^5 L_1^5 L_2 L_3} \right) + \text{sym}, \\ &= -\frac{\hbar}{10} \left(\frac{1.21}{L_3^7} + \frac{1.30}{L_2^6 L_3} + \frac{1.57}{L_1^5 L_2 L_3} \right) + \text{sym}. \end{aligned} \tag{3.33}$$

Now we have the vacuum energy of a massless complex scalar field obtained using the exact formula Eq. 3.25 (see 3.1.1) and using the approximation Eq. 3.30 in different spacetime. Comparing these results, one can conclude that for masseless scalar field, the approximation (Eq. 3.30) gives a relative error of 1.3%, 3.9% and 9% for $\mathbb{R}^{(1,1)} \times \mathbb{S}^1 \times \mathbb{S}^1$, $\mathbb{R}^{(1,3)} \times \mathbb{S}^1 \times \mathbb{S}^1$ and $\mathbb{R}^{(1,3)} \times \mathbb{S}^1 \times \mathbb{S}^1 \times \mathbb{S}^1$, respectively. The relative error increases as we increase the number of dimensions but we can consider higher order corrections in the same way. In this work we are only interested in the qualitative nature of the Casimir force between parallel plates placed in different spacetime having extra compact dimension. So for our purpose we will use the approximate result (Eq. 3.30) as our formula for the vacuum energy of the complex scalar field.

3.1.3 Casimir Force on a Piston

Armed with an approximate expression for V_{min} (Eq. 3.30), we now turn our attention to calculate the Casimir force on a piston (or two parallel plates) placed in various compact spacetime dimensions. The energy density ρ of a complex scalar field

satisfying Dirichlet boundary condition (i.e., the field vanishing at boundaries $x = 0$ and $x = L$) can also inferred from our results by replacing L by $2L$ (where $L \in \{L_1, ..., L_k\}$)[14, 46] as

$$\rho(L) = V_{min}(2L). \tag{3.34}$$

For calculating the Casimir force on a piston we consider the finite box boundary condition as shown in Figure 3.1 and eventually take the limits $l_1, l_2, l_3 \to \infty$. The importance of taking the finite box boundary condition is well discussed in the literature [44, 45, 47, 48, 49].

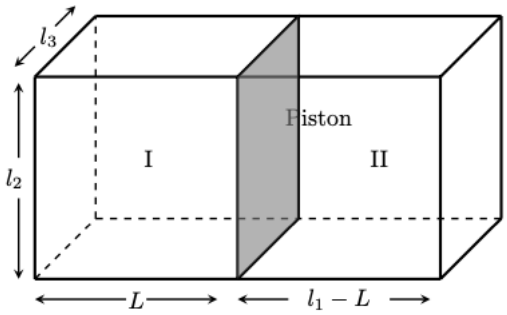

FIGURE 3.1: A Rectangular piston

The Casimir force has contributions from both regions I and II as

$$\frac{F}{\mathcal{V}_k} = -\frac{d}{dL}\left(L\rho_1\right) - \frac{d}{dL}\left((l_1 - L)\rho_2\right)\Big|_{l_1 \to \infty}, \tag{3.35}$$

where ρ_1 and ρ_2 are the energy densities in the region I and II respectively. Considering $d = 4$ and $k = 1$ in Eq. 3.30 and using Eq. 3.34 and Eq. 3.35, the Casimir force acting on the piston is

$$F = -\frac{m^2}{4L^2\pi^2}\sum_{n=1}^{\infty}\left(\frac{2mL}{n}K_1(\xi) + \frac{3}{n^2}K_2(\xi)\right), \tag{3.36}$$

Here, $\xi = 2mnL$. This expression represents the force per unit area acting on the piston due to vacuum fluctuations of a massive complex scalar field in a Minkowski spacetime. It's worth noting that this result (Eq. 3.36) for the Casimir force is well known in the literature [46]. In the limit as m approaches zero, it converges to the standard result initially derived by H. B. G. Casimir [11]. Furthermore, we can extend this analysis to calculate the force per unit area on the piston when extra compact dimensions are present. Each additional compact dimension introduces corrections

to Eq. 3.36, as illustrated in Figure 3.2 for a massless scalar field. These corrections vanish in the limit as R, the size of the extra compact dimension, approaches both zero and infinity. The limit $R \to 0$ corresponds to the case of compact dimensions collapsing to a point, while $R \to \infty$ yields results consistent with a d-dimensional flat topology [50]. A similar examination of corrections to the Casimir force from extra compact dimensions in a massless scalar field is presented in [45].

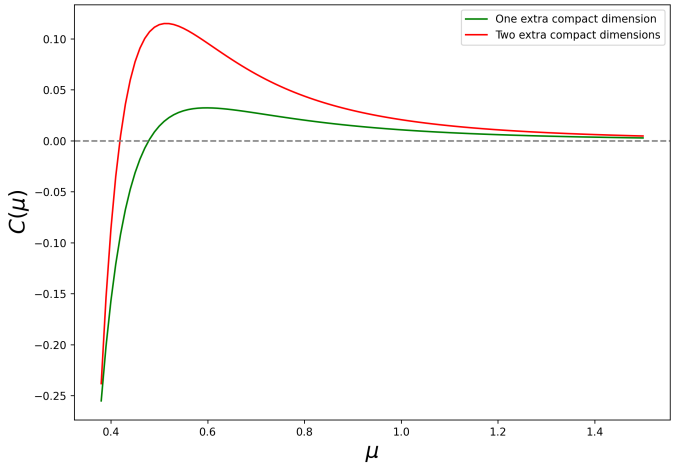

FIGURE 3.2: Corrections in the Casimir force due extra compact dimensions for a massless scalar field. $C(\mu)$ is the correction and $\mu = L/R$.

The Casimir force between the parallel plates due a massive complex scalar field depends on different parameters like the mass of the field, number of extra compact dimensions, separation between the parallel plates and the size of extra compact dimensions. The role of each parameter in the Casimir force can be analysed by plotting the Casimir force as a function of these parameters.

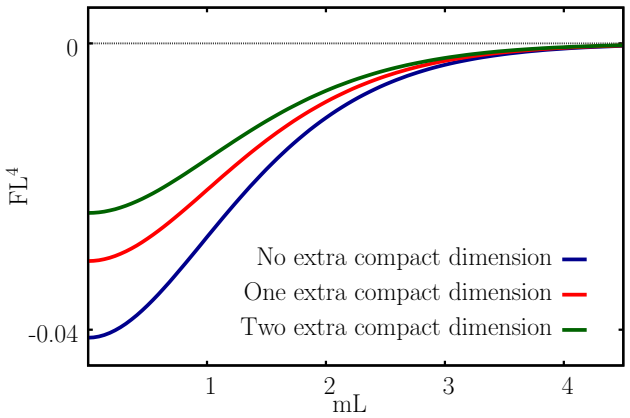

FIGURE 3.3: Shows the variation of Casimir force with respect to Lm, where we assume $R = L$.

From Figure 3.3 we can conclude few features of the Casimir force as follows

1. The Casimir force is always attractive, irrespective of mass, separation between the plates, number of extra compact dimensions and the size of extra compact dimensions.

2. Having extra compact dimensions reduces the attractive Casimir force. This effect can be attributed to the following phenomenon: in the presence of extra dimensions, vacuum fluctuations have the opportunity to escape into these additional dimensions. Consequently, there are fewer modes available within the confined space between the plates. This hypothesis gains support from the observation that the Casimir force per unit area per unit length of extra compact dimension is maximized when the size of the extra compact dimension is smaller than the separation between the plates. The impact of these extra compact dimensions is most pronounced when $Lm < 1$.

3. As a function of mass, Casimir force is maximal for a massless scalar field and decreases as mass increases. Casimir force vanishes to zero as $m \to \infty$ as there are no more quantum fluctuations in this limit.

Experimentally, the Casimir effect has been observed for a parallel plate separation of the order 10^{-7}m [51, 52]. For the Higgs field (mass $\approx 10^{-25}$Kg [53]), using the above values, the Casimir force per unit area on the piston without any extra compact

dimension is $-4.318 \times 10^{-8} N$. Now from phenomenological models, if we consider the upper bound on the size of one extra compact dimension as $R \leq 10$ nm [54], we see from our Eq. (3.59) that the presence of one extra compact dimension almost halves the intensity of attraction to $-2.262 \times 10^{-8} N$. These qualitative numbers can in fact provide us with a test bed to probe for existence of compact extra dimensions.

3.2 Constant Magnetic and Electric Fields

A non trivial boundary condition disturbs the vacuum state of field and this leads to the Casimir force and all the effect of extra compact dimensions on the Casmir force is also due to the same. Any general interactions of the field can also disturb the vacuum configurations and leads to non trivial effects, one simple example of this is the presence of an external background field. In this section we study both the effect of constant background elctro magnetic field and the non trivial boundary conditions in the vacuum state of a massive complex scalar field.

We start our study by considering a complex scalar field in $1+3$ spacetime where one of the spatial dimension is compact under the identification $x_1 \sim x_1 + L$. We choose the guage potential $A_\mu = (0, a, 0, Bx_2)$ such that there exist a constant magnetic field B along the compact dimension along with a constant guage potential a. One can solve Eq. 2.25 with Eq. 2.26 by expanding $K(s; x, x')$ in Fourier modes.The Fourier transform of the heat kernel is given as

$$K(s; x, x') = \frac{1}{L_1} \sum_n \exp\left(\frac{2\pi i}{L} n(x_1 - x_1')\right) \int \frac{d\omega}{2\pi} \frac{dp_3}{2\pi} e^{i\omega(\tau - \tau')} e^{ip_3(x_3 - x_3')} \tilde{k}(s, x_2). \quad (3.37)$$

Where we choose periodic boundary condition for the field. In this context, one write the heat equation (Eq. 2.25) as

$$\partial_2^2 \tilde{k} - \left(\omega^2 + \left(\frac{2\pi n}{L_1}\right)^2 + p_3^2 - 2qa\left(\frac{2\pi n}{L_1}\right) - 2qBx_2 p_3 + q^2 a^2 + q^2 B^2 x_2^2 + m^2\right)\tilde{k} = \frac{\partial \tilde{k}}{\partial s}. \quad (3.38)$$

By completing the square we can re write this as

$$\frac{\partial^2 \tilde{k}}{\partial y^2} - q^2 B^2 y^2 \tilde{k} - \left(M_n^2 + \omega^2\right) = \frac{\partial \tilde{k}}{\partial s}, \quad (3.39)$$

where $qBy = p_3 - qBx_2$ and $L_1^2 M_n^2 = L_1^2 m^2 + 4\pi^2 \left(2\pi n - qaL_1\right)^2$. Equation 3.39 is a standard differential equation satisfied by the Mehler kernel. So,

$$\tilde{k}(s; y, y') = \mathcal{A} \exp\left(\frac{-\coth(2qBs)}{2} qB(y^2 + y'^2) + qB\,\mathrm{coseh}(2qBs)yy' - \left(M_n^2 + \omega^2\right)s\right), \tag{3.40}$$

where $\mathcal{A} = \left[qB/\left(2\pi \sinh(2qBs)\right)\right]^{\frac{1}{2}}$. Using Eq. 3.40 in Eq. 3.37 gives the complete heat kernel in the coincidence limit $(x \to x')$ as

$$K(s; x, x) = \frac{qB\mathcal{A}}{L_1} \sum_{n=-\infty}^{\infty} e^{-M_n^2 s} \int \frac{d\omega}{2\pi} \frac{dy}{2\pi} e^{-\omega^2 s} \exp\left(-\tanh(qBs) qBy^2\right), \tag{3.41}$$

where we have used $dp_3 = qBdy$. We can do the integration in Eq. 3.41 using the standard Gaussian integral as

$$K(s; x, x) = \frac{qB}{8\pi^{\frac{3}{2}} L} \frac{1}{\sqrt{s}\sinh(qBs)} \sum_{n=-\infty}^{\infty} e^{-M_n^2 s}. \tag{3.42}$$

Substituting Eq. 3.42 in Eq. 2.24 gives the Euclidean effective potential as

$$V = \frac{1}{8\pi^{3/2} L} \sum_{n=-\infty}^{\infty} \int_0^{\infty} \frac{ds}{s^{5/2}} \frac{qBs}{\sinh(qBs)} e^{-M_n^2 s}. \tag{3.43}$$

The above expression for the effective potential (Eq. 3.43) diverges a $s \to 0$. So one has to implement a proper renormalization procedure. One can series expand the effective potential (Eq. 3.43) around $s = 0$ as

$$V \approx v_0 + \frac{1}{8\pi^{3/2} L_1} \sum_n \left(\frac{B^2 q^2}{6} \int_0^{\infty} \frac{ds}{\sqrt{s}} e^{-M_n^2 s}\right) + V_{finite}, \tag{3.44}$$

where v_0 corresponds to terms independent of B and V_{finite} corresponds to the finite contribution to the effective potential. We can subtract out the v_0 term as it only rescale the energy. Then the remaining diverging term is proportional to B^2, which can be renormalized by re defining the parameters in the bare Lagrangian Eq. 3.1 (see Section 2.5). For a weak magnetic field the renormalized Euclidean effective potential is

$$V_{ren} \approx \frac{7q^4 B^4}{2880\pi^{3/2} L} \sum_n \int_0^{\infty} ds s^{3/2} e^{-M_n^2 s} + O(B^6), \tag{3.45}$$

where we neglect the higher order terms in B. The s integral in Eq. 3.45 is the integral representation Gamma function, so we can re write this as

$$V_{ren} = \frac{7q^4B^4}{3840L\pi}\left(\frac{L}{2\pi}\right)^5 \sum_{n=-\infty}^{\infty}\left(\frac{m^2L^2}{4\pi^2} + \left(n - \frac{qaL}{2\pi}\right)^2\right)^{-\frac{5}{2}} + O(B^6). \tag{3.46}$$

Using Eq. 3.16 we can do the summation which leads to,

$$V_{ren} = \frac{7B^4q^4}{5760m^4\pi^2} + \frac{7B^4L^4q^4}{30720\pi^6} f_\lambda(\alpha,\beta) + O(B^6), \tag{3.47}$$

where $\alpha = mL_1/2\pi$, $\beta = -qaL_1/2\pi$ and $\lambda = 5/2$. The first term in V_{ren} is the contribution from $1+3$ flat spacetime [15]. Similar to the above Section 3.1, we choose the constant gauge potential $a = 0$, such that it minimizes the Lorentzian effective potential. Then one can re-express the vacuum energy of the massive complex scalar field using Eq. 3.24 as

$$V_{min} = -\frac{7B^4q^4}{5760m^4\pi^2}\left(1 + m^2L^2\sum_{n=1}^{\infty} n^2K_2(\xi/2)\right) + O(B^6). \tag{3.48}$$

As we have an idea on the effect of weak background magnetic field on the effective potential, now we can add the higher order corrections in the magnetic field. The higher order corrections can be expressed in the form form a converging summation as

$$\begin{aligned} V_{min} = &\sum_{k=2}^{\infty}\frac{(2^{2k}-2)}{16\pi^2(2k)!}m^{4-4k}B^{2k}q^{2k}B_{2k}\Gamma(2k-2) \\ &+ \sum_{k=2}^{\infty}\left(\frac{(1-2^{1-2k})}{\pi^2(2k)!}\left(\frac{L}{m}\right)^{2k-2}B^{2k}q^{2k}B_{2k}\sum_{n=1}^{\infty}n^{2k-2}K_{2k-2}(\xi/2)\right), \end{aligned} \tag{3.49}$$

where B_k is the $(k)^{th}$ Bernoulli number. This matches with the results in [55]. First part of the equation is the contribution from flat space topology [56]. Now we calculate the Casimir force acting on piston as discussed in Section 3.1.3. Substituting Eq. 3.48 in Eq. 3.34 and using Eq. 3.35 , the Casimir force per unit area on the piston is

$$F = \frac{7B^4q^4L^2}{5760m^4\pi^2}\sum_{n=1}^{\infty}\left(3\xi^2K_2(\xi) - \frac{1}{2}\xi^3\left[K_1(\xi)+K_3(\xi)\right]\right). \tag{3.50}$$

where $\xi = 2mnL$. Similarly, we can calculate the Casimir force per unit area on the piston with extra compact spatial dimensions, and the results are as shown in the Figure 3.4.

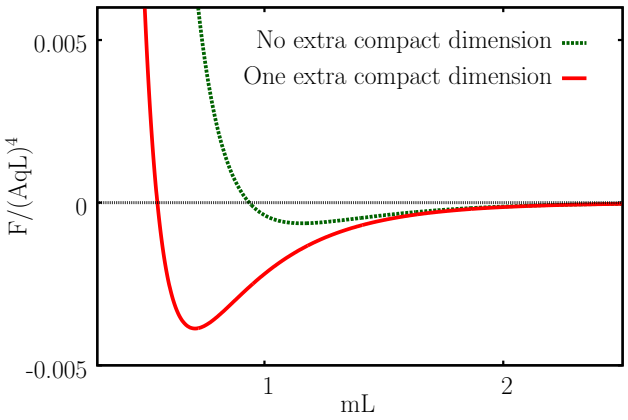

FIGURE 3.4: Shows the qualitative behaviour of Casimir force in the presence of weak external field and extra compact dimensions. On the y-axis A can be electric field E parallel to the plates or magnetic field B perpendicular to the plates. In this plot we assume that the size of extra compact dimension is same as the seperation between the plates.

We study the effect of constant magnetic field perpendicular to the piston on the Casimir force. Now we focus on the effect of constant electric field parallel to the piston on the Casimir force. Due the duality between the electric and magnetic field [57, 58], one can simply repeat the calculations as above and the results are qualitatively same.

Consider the guage potential $A_\mu = (0, a, 0, E\tau)$, a constant guage potential along the compact dimension and a constant electric field along the non compact dimension. Proceeding the same way as discussed above, one can get the effective potential as

$$V_L = -\frac{1}{8\pi^{3/2}L_1}\sum_{n=-\infty}^{\infty}\int_0^\infty \frac{ds}{s^{5/2}}\frac{qEs}{\sin(qEs)}e^{-M_n^2 s}. \tag{3.51}$$

Following the calculations as in the case of constant magnetic field, for a weak electric field $E \to 0$, one can calculate the Casimir force per unit area on the piston as

$$F = \frac{7E^4q^4}{5760m^4\pi^2}\sum_{n=1}^{\infty}\Big(3\xi^2K_2(\xi) - \frac{1}{2}\xi^3\left[K_1(\xi) + K_3(\xi)\right]\Big). \tag{3.52}$$

Similar calculations can be extended to d dimensional spacetime with k compact spatial dimensions. For the case of one extra compact dimension, the corresponding

Casimir force is

$$F = -\frac{7E^4q^4}{11520\pi^2m^4}\sum_{n=1}^{\infty}\left(\xi^2K_2(\xi) + \frac{Rm}{\sqrt{2\pi}}\xi^{\frac{3}{2}}K_{\frac{3}{2}}(\xi) - \xi^3K_1(\xi) - \frac{Rm}{\sqrt{2\pi}}\xi^{\frac{5}{2}}K_{\frac{1}{2}}(\xi)\right), \quad (3.53)$$

where $\xi = 2mnL$ as usual and R is the size of extra compact dimension. A plot showing the influence of extra compact dimension on the Casimir force is given in Figure 3.4.

That completes our study on the effect of constant background fields on the Casimir force between the parallel plates in the presence of extra compact spatial dimensions. The conclusions are as follows

1. Large magnetic field can inhibit the Casimir force between two parallel plates [55]. We can inferred this conclusion from Eq. 3.43, as $B \to \infty$ the effective potential vanishes. On the contrary, a similar analysis on the electric field (Eq. 3.51) concludes that a large electric field enhances the Casimir force.

2. In the weak field approximation, both the electric field and magnetic field enhances the Casimir force (see Eq. 3.52 and Eq. 3.50).

3. From the Figure 3.4, we can see that there is repulsive contribution to the Casimir force for $Lm < 1$. For the case of a weak magnetic field, this repulsive contribution is noted in [59].

4. Also, Figure 3.4 illustrates that even though the extra compact dimension does not change the qualitative behavior of Casimir force, it does decrease its magnitude.

3.3 The Schwinger Effect

The Schwinger effect is the creation of particle-antiparticle pairs from the vacuum in the presence of a strong electric field. It was proposed by physicist Julian Schwinger in 1951 [27] and has important implications in quantum field theory, high-energy physics, cosmology, and quantum gravity. The effect occurs when a strong electric

field separates virtual particles before they annihilate, resulting in the production of real particles. It is difficult to observe experimentally but has been studied using ultra-intense lasers and strong electric fields in condensed matter systems. Understanding Schwinger effect in the presence of parallel plates can help in the experimental realization of it. Here, we calculate the Schwinger pair production rate from the imaginary part of the effective potential as follows. The complete effective potential is give by Eq. 3.51 and we have to do the integral

$$I = \int_0^\infty \frac{ds}{s^{5/2}} \frac{qEs}{\sin(qEs)} e^{-M_n^2 s}. \tag{3.54}$$

The integrand has branch points at $s = 0$ and $s = \infty$ and has singularities at $s_k = k\pi/qE$ as shown in Figure 3.5. But the singularity at $s = 0$ is already considered for calculating Casimir energy or the real part of the effective potential. Then the contribution to the imaginary part of the effective potential might be coming from other poles. One can do the integral in Eq. 3.54 using Cauchy's theorem.

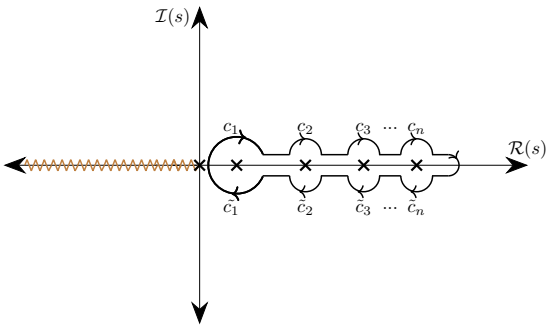

FIGURE 3.5: The contour of s integration for Eq. 3.54

Take

$$f(z) = \frac{1}{z^{5/2}} \frac{qEz}{\sin(qEz)} e^{-M_n^2 z}, \tag{3.55}$$

and using Cauchy's theorem we can say that

$$\oint f(z)dz = 2\pi i \sum_{k=1}^{\infty} (-1)^k \left(\frac{qE}{k\pi}\right)^{\frac{3}{2}} e^{-\frac{M_n^2 k\pi}{qE}}, \tag{3.56}$$

along the closed contour given in the Figure 3.5. From this we can write

$$\oint f(z)dz = \int_{c_1} f(z)dz + \int_{s_1+\epsilon}^{s_2-\epsilon} f(z)dz + ... + \int_{-\infty}^{s_n+\epsilon} + \int_{\tilde{c_n}} f(z)dz + ... \int_{s_1-\epsilon}^{\epsilon} f(z)dz.$$

In the fourth quadrant or in the lower half plane the function will have an extra 2π phase which gives

$$f(z) = \frac{e^{-i\pi}}{z^{5/2}} \frac{qEz}{\sin(qEz)} e^{-M_n^2 z} = -f(z). \tag{3.57}$$

Then in the limit $\epsilon \to 0$ this gives

$$\oint f(z)dz = 2I + \int_{c_1} f(z)dz + \int_{c_2} f(z)dz + ... + \int_{c_n} f(z)dz + \int_{\tilde{c_n}} f(z) + ... \int_{\tilde{c_1}} f(z)dz.$$

Then for integration over c_1, take $z = s_1 + \epsilon e^{i\theta}$

$$\begin{aligned}\int_{c_1} f(z)dz &= \int_{\pi}^{0} \frac{i\epsilon e^{i\theta} d\theta}{s_1^{5/2}} \frac{qEs_1}{\cos(qEs_1)\epsilon e^{i\theta}} e^{-M_n^2 s_1}, \\ &= -i \frac{\pi qE e^{-M_n^2 s_1}}{s_1^{\frac{3}{2}} \cos(qEs_1)}.\end{aligned}$$

The integration over c_1 and $\tilde{c_1}$ add up to zero, similarly for all other $c_n's$. From this we can write

$$I = \pi i \sum_{k=1}^{\infty} (-1)^k \left(\frac{qE}{k\pi}\right)^{\frac{3}{2}} e^{-\frac{M_n^2 k\pi}{qE}}. \tag{3.58}$$

Now we can use this result of the integration in the effective potential (Eq. 3.51). The summation over n in Eq. 3.51 can be done in terms of elliptic theta function, which gives the imaginary part of the effective potential as

$$Im(V) = \sum_{k=1}^{\infty} \frac{(-1)^{k+1}}{2(2\pi)^3} e^{\frac{-k\pi m^2}{qE}} \left(\frac{qE}{k}\right)^2 \Theta\left(3, 0, e^{\frac{-qEL^2}{4k\pi}}\right), \tag{3.59}$$

where Θ is the elliptic theta function. Here we used $M_n^2 = m^2 + \frac{4\pi^2}{L^2}\left(n - \frac{qaL}{2\pi}\right)^2$ and also took $a = 0$ as that choice minimizes the potential. The imaginary part of the effective potential gives the number of pairs of charged scalar particles created by the electric field per unit time per unit volume. The functional behaviour of elliptic theta is given Figure 3.6

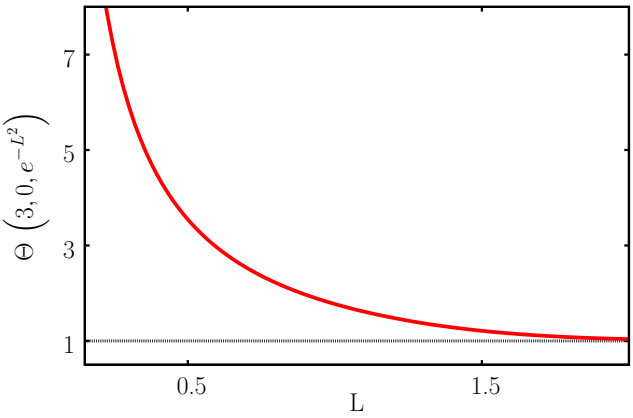

FIGURE 3.6: Shows the variation of imaginary part of the effective potential with respect to the separation between the parallel plates.

In the limit $L \to \infty$, $\Theta \to 1$ and gives the standard Schwinger effect result in $3+1$ dimension [28, 27]. Presence of extra compact dimensions, along with the piston, add the number of Θ functions corresponding to each extra compact dimensions. But if we consider extra compact dimensions without the piston, i.e., $A_\mu = (0,0,0,E\tau,a)$. The corresponding effective potential is

$$V = -\frac{qE}{16\pi^2 R}\sum_{n=-\infty}^{\infty}\int_0^\infty \frac{ds}{s^2}\frac{e^{-M_n^2 s}}{\sin(qEs)}, \tag{3.60}$$

where R is the size of extra compact dimension and $M_n^2 = (\frac{2\pi n}{R} - qa)^2 + m^2$. There are no branch cuts in the integral and using the results in [28, 15]

$$Im(V) = \sum_{k=1}^{\infty}\frac{(-1)^{k+1}}{4(2\pi)^3}e^{\frac{-k\pi m^2}{qE}}\left(\frac{qE}{k}\right)^{\frac{5}{2}}\Theta\left(3,0,e^{\frac{-qER^2}{4k\pi}}\right). \tag{3.61}$$

The limit $R \to \infty$ gives the Schwinger effect in $1+4$ flat dimension. In the same way, one can calculate the pair production in a higher compact and non-compact dimensions, with or without pistons.

The conclusions are as follows

1. The functional behaviour of the theta function (Figure 3.6) explicitly shows that the presence of parallel plates and the extra compact dimensions can enhance the particle pair production

The Schwinger effect still awaits experimental confirmation in the laboratory as it requires extreme electric fields. Our results in this work can help in the experimental realization of the Schwinger effect via enhancement mechanism. Also, once we have an experimental realization of the Schwinger effect, we can use it to put constraints on the extra compact dimensions.

Chapter 4

Spontaneous Symmetry Breaking

The foundation of constructing fundamental theories relies on the concept of symmetry. It is believed that nature favors symmetry, and all fundamental laws exhibit symmetry. However, the world we observe is not entirely symmetrical. The central notion to comprehend an asymmetrical world by employing symmetrical laws is the concept of spontaneous symmetry breaking (SSB).

In this chapter, we delve into the topic of spontaneous symmetry breaking (SSB) in real scalar fields, employing the methodologies of effective potential. Our approach aligns with standard textbooks such as [24, 17, 36], capturing the essence of SSB in a comprehensive manner. While discussing SSB, we draw connections to condensed matter physics as explored in [60, 18]. However, we do not venture into the SSB of gauge theories or its renormalization, which holds significance in the renormalization of weak interactions.

In Section 4.1, we provide a definition of SSB and present a list of its key features. Moving on to Section 4.2, we outline the explicit calculation of SSB in the context of discrete symmetry, utilizing both classical and quantum theories. Subsequently, in Section 4.3, we extend the quantum analysis of SSB to continuous symmetry and highlight notable features such as the Goldstone theorem and the Coleman-Mermin-Wagner theorem. Section 4.4 focuses on discussing the $O(N)$ symmetric theory, utilizing the $1/N$ expansion (Large-N expansion) and demonstrating SSB within this

framework. Finally, we conclude this chapter by exploring symmetry restoration at finite temperature in Section 4.5.

4.1 Introduction

Definition : The phenomenon in which a state of a system (usually the vacuum state or in statistical physics a thermal equilibrium state) is not symmetric under the symmetry transformation of the theory (means symmetry of the action, Lagrangian or Hamiltonian.)

It is not difficult to see spontaneous symmetry breaking in nature, all the material around us are made up of atoms that obey rotationally symmetric laws, but most objects around us are not rotationally symmetric (see section 19. 1 of [61]). One can see similar intuitive examples of spontaneous symmetry breaking like bending of thin rod in section 8.1 of [62] and a little man in a ferromagnet in section 43.1 of [24].

Some general features of spontaneous symmetry breaking are listed below

1. **Degenerate Vacuum :** A theory exhibiting SSB is invariably connected with the degeneracy of vacuum states. As mentioned earlier (refer to Section 2.2), the vacuum expectation value of the field is determined by the minimum of the effective potential. Let's consider a symmetry transformation T of the theory, implying that the effective potential remains invariant under the action of T. However, in the presence of SSB, we find that $T\phi_0 \neq \phi_0$, where ϕ_0 represents the vacuum expectation value of the field. Simultaneously, we have $V(\phi_0) = V(T\phi_0)$, which implies the existence of degenerate vacua. This statement reflects the fact that different vacuum states, related to one another through the symmetry transformation T, possess the same energy given by the value of the effective potential. So, symmetry is not broken, but is hidden by the choice of the vacuum state.

2. **Non-zero ϕ_0 :** An essential and mathematically useful characteristic of SSB is the existence of a non-zero vacuum expectation value of the field

($\phi_0 \neq 0$). This signifies that when $\phi_0 \neq 0$, SSB is present in the system. In the context of SSB for continuous symmetry, we can establish the validity of the aforementioned statement through the following proof: Consider a continuous symmetry transformation T of the theory. According to Noether's theorem, for every continuous symmetry, a conserved current J^μ and an associated conserved charge Q can be constructed. This conserved charge also serves as the generator of the symmetry. Then the statement of SSB, that vacuum field configuration ϕ_0 varies under the symmetry transformation can be written as

$$\delta\phi_0 = i\,[Q, \phi_0]\,\delta\omega \neq 0, \tag{4.1}$$

where ω is the parameter of the symmetry transformation. Then taking vacuum expectation value of Eq. 4.1 gives

$$\langle 0|\, Q\phi_0\,|0\rangle - \langle 0|\,\phi_0 Q\,|0\rangle \neq 0. \tag{4.2}$$

So one can conclude that $Q\,|0\rangle \neq 0$ means $\langle\phi_0\rangle \neq 0$, which completes the proof.

3. **Phase transition** : Spontaneous symmetry breaking is associated with phase transitions occurring in a system, specifically the transition from a symmetric state to a broken symmetry state. At these phase transitions, a parameter, often referred to as an order parameter, reaches its critical value. This critical value separates different phases of matter, such as magnetic phases, superconducting phases, and others.

   The concept of SSB provides a powerful framework for understanding and studying these phases of matter. It allows us to analyze the behavior of systems where the symmetries are broken in certain phases, leading to the emergence of unique properties and phenomena. For instance, in a ferromagnetic material, the alignment of magnetic spins breaks the rotational symmetry, resulting in a magnetized state. The transition from a paramagnetic phase to a ferromagnetic phase can be explained using the ideas of SSB. Similarly, in superconductors, the breaking of gauge symmetry leads to the expulsion of magnetic fields and the emergence of zero resistance. The study of this phase transition and the

properties of superconducting materials can be approached through the lens of SSB.

Now let's dive into the mathematical details of SSB using some examples and study them using the one-loop effective potential.

4.2 Discrete Symmetry Breaking: The Z_2 group

We start with the spontaneous breaking of a discrete symmetry Z_2. Consider the Lagrangian

$$\mathcal{L} = \frac{1}{2}(\partial\phi)^2 + \frac{m^2}{2}\phi^2 + \frac{\lambda}{4!}\phi^4 = \frac{1}{2}(\partial\phi)^2 + U(\phi)\,. \tag{4.3}$$

Few points to note about the system are

1. The Lagrangian density of the theory exhibits an invariance under the transformation $\phi \to -\phi$, indicating that the symmetry group associated with the theory is the cyclic group Z_2.

2. The variables denoted by m^2 and λ represent parameters within the theory, capable of assuming any value. However, when considering a bounded system, it is necessary for λ to have a positive value.

4.2.1 Classical Field Theory

In order to investigate SSB in classical theory, it is necessary to determine the ground state field configuration. If the ground state field configuration changes under the symmetry group Z_2, it indicates the presence of SSB. To determine the ground state of the theory, we can note that the Euclidean Lagrangian density is equivalent to the Hamiltonian density or the energy density of the system. Consequently, the terms involving derivatives of the field ϕ in the Lagrangian contribute positively to the energy density. Therefore, the state of minimum energy or the ground state should be described by a constant field configuration denoted as ϕ_0, which corresponds to the minimum of the potential $U(\phi)$. It is important to note that the potential

may possess multiple minima depending on the $U(\phi)$. At this point, two distinct situations arise depending on the sign of m^2.

In the case of $m^2 \geq 0$, the potential is concave everywhere, and the minimum occurs at $\phi_0 = 0$, as depicted in Figure 4.1a. The field configuration at the ground state (ϕ_0) exhibits symmetry under Z_2, indicating the absence of SSB.

In contrast, for $m^2 < 0$, the situation is significantly different. As illustrated in Figure 4.1b, the potential has two minima at $\phi_0 = \pm v$, while $\phi_0 = 0$ becomes a local maximum. The value of v can be explicitly calculated by determining the minimum of the potential, yielding $v^2 = 6m^2/\lambda$. The system has the freedom to choose either $\pm v$ as its ground state, and one can't distinguish between these ground states through any physical experiments.

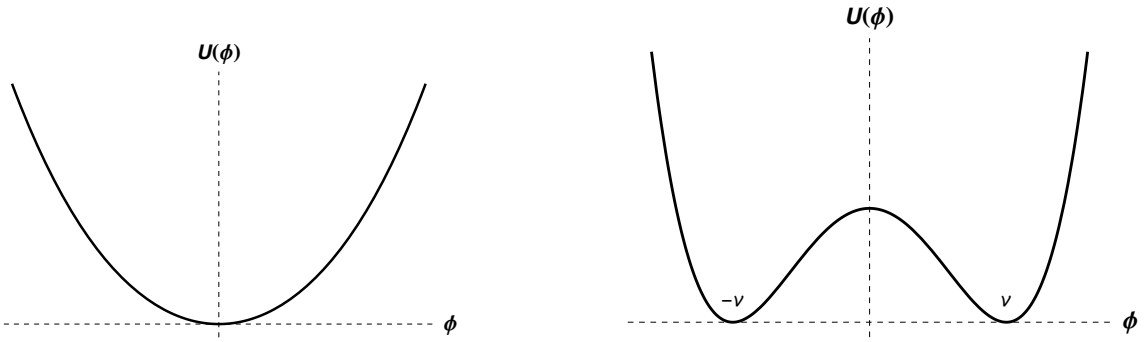

(A) For $m^2 \geq 0$. Minimum of the potential is at $\phi = 0$

(B) For $m^2 < 0$. Minimum of the potential is at $\phi = \pm v$

FIGURE 4.1: Potential $U(\phi)$ as a function of ϕ.

Whichever value ($\pm v$) the system selects as its ground state, it no longer possesses symmetry under Z_2, indicating SSB. However, it is important to note that each ground state configuration is related to the other through a Z_2 transformation. Hence, one can argue that the symmetry is hidden due to the random choice of vacuum state.

An intriguing question arises regarding the critical point $m^2 = 0$. In classical theory, there is no SSB for $m^2 = 0$. However, one may wonder if quantum fluctuations can induce symmetry breaking. The answer is affirmative, and we will delve into the details in next section.

4.2.2 SSB in Quantum Field Theory

Spontaneous Symmetry Breaking gives rise to degenerate vacuum states. In a quantum theory, within a finite volume, these distinct vacuum states can communicate through the phenomenon of tunneling. However, in the infinite volume limit, the energy barrier between different vacuum states becomes infinitely high, preventing any tunneling from occurring. As a result, in quantum field theory, all of these degenerate vacuum states are considered distinct and equally probable. One can choose to construct perturbation theory around any of these vacuum states.

As discussed in Section 2.1, in quantum field theory, the effective potential takes the role of classical potential. So, one has to find the vacuum state configuration of the field as the minimum of the effective potential (here, we consider the one-loop effective potential). The one-loop correction to the effective potential for the Lagrangian Eq. 4.3 is already calculated in Section 2.5 (Eq. 2.41). Including the classical term, the effective potential upto one loop correction is

$$V = \frac{1}{2}m^2\phi^2 + \frac{\lambda}{4!}\phi^4 + \frac{1}{64\pi^4}\left(m^2 + \frac{\lambda}{2}\phi^2\right)^2 \log\frac{1}{2\mu}\left(m^2 + \frac{\lambda}{2}\phi^2\right). \tag{4.4}$$

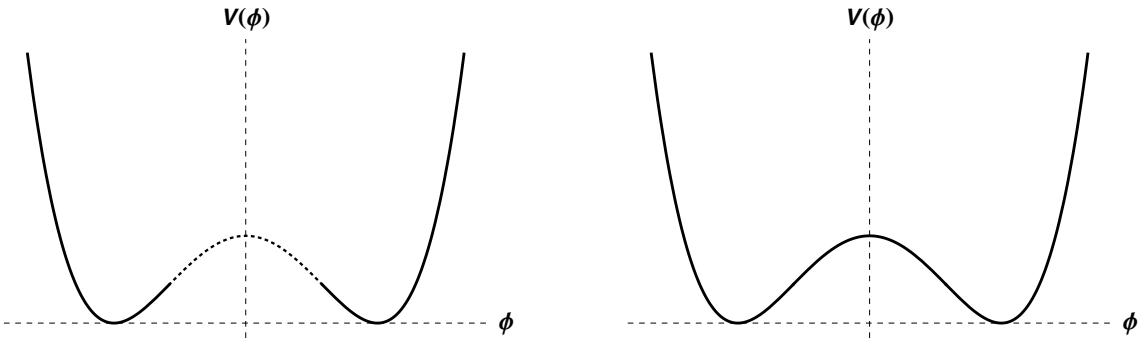

(A) For $m^2 < 0$. The dotted part corresponds to the imaginary part.

(B) For $m^2 = 0$. Plotted for very low values of ϕ.

FIGURE 4.2: Potential $U(\phi)$ as a function of ϕ.

The vacuum field configuration is the minimum of the effective potential. Looking at Eq. 4.4 one can conclude the following

1. For $m^2 > 0$, the qualitative behaviour of $V(\phi)$ remains the same as Figure 4.1a. So, there is a unique minimum at $\phi = 0$ which is symmetric under Z_2, so there is no spontaneous symmetry breaking upto one loop order

2. In the case of $m^2 < 0$, it is observed that the effective potential becomes complex when $m^2 > \frac{\lambda}{2}\phi^2$. As explained in Section 2.2, the presence of the complex part in the potential indicates the system's instability. Consequently, $\phi = 0$ cannot be a possible minimum. By referring to Figure 4.2a, it can be observed that the minimum of the effective potential occurs at $\phi \neq 0$. Thus, the vacuum field configuration is not symmetric under Z_2, indicating the presence of SSB.

   (a) **Word of caution :** The effective potential appears not convex between v and $-v$. However, this is a consequence of directly substituting $m^2 \to -m^2$ in equation Eq. 4.4, which is not a justified procedure. When $m^2 \to -m^2$, the potential exhibits two minima, and in the saddle point approximation (as seen in equation Eq. 2.19), it is necessary to consider a sum over both minima. By taking this into account, it becomes evident that between v and $-v$, the vacuum expectation value of the field does not coincide with the classical field, and the classical field serves as a mean field. This leads to the appearance of the complex part in the effective potential, and it can be demonstrated that the effective potential is indeed convex in all regions. Additionally, for the calculations we are performing, which are centered around the minima, the use of equation Eq. 4.4 can be justified. For more comprehensive explanations and detailed arguments, please refer to section 13.6 of [20].

3. We now turn our attention to the question of whether quantum fluctuations can induce symmetry breaking for $m^2 = 0$. To investigate this, we calculate the one-loop effective potential by substituting $m^2 \to 0$ in Eq. 4.4. The resulting plot of the one-loop effective potential for the massless theory is depicted in Figure 4.2b. From this analysis, it can be concluded that quantum fluctuations indeed break the symmetry. For a more comprehensive understanding, please refer to chapter 4.3 of the book by A. Zee [36].

4.3 Continuous Symmetry Breaking: The $O(2)$ group

In this section, we explore the spontaneous symmetry breaking of a continuous symmetry, specifically the rotational symmetry (belonging to the $O(2)$ group) within the configuration space of the field. We examine a Lagrangian similar to Eq. 4.3, which can be expressed as follows:

$$\mathcal{L} = \frac{1}{2}(\partial\Phi)^2 + \frac{m^2}{2}\Phi^2 + \frac{\lambda}{4!}\Phi^4 = \frac{1}{2}(\partial\Phi)^2 + U(\Phi), \tag{4.5}$$

where $\Phi = (\phi_1, \phi_2)$ represents a pair of scalar fields. Alternatively, one can also perform the same analysis using a single complex scalar field. We can replicate all the analyses outlined in Section 4.2, with Figure 4.2 being replaced by its higher-dimensional counterparts, as depicted in Figure 4.3. This leads us to the same conclusions, indicating that the system exhibits SSB for $m^2 \leq 0$, while no SSB occurs for $m^2 > 0$.

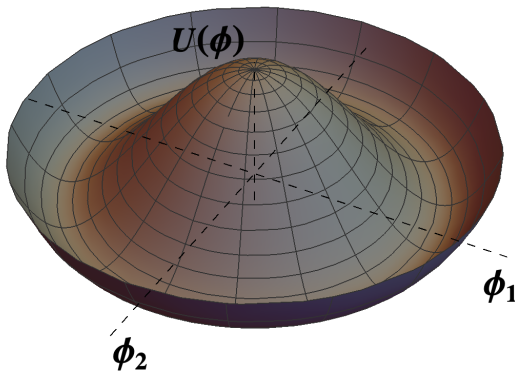

FIGURE 4.3: Plot of classical potential in Eq. 4.5 with $m^2 < 0$.

But there are some crucial difference between spontaneous symmetry breaking of discrete symmetry and continuous symmetry which are listed below

1. **Infinitely degenerate vacuum:** There exist infinitely degenerated vacuum associated with every continuous symmetry breaking. The SSB of a continuous symmetry means

$$S|0\rangle = e^{i\theta Q}|0\rangle \neq |0\rangle, \tag{4.6}$$

where S is the symmetry transformation and Q is the generator or the conserved current associated with the symmetry. As Q represents a conserved charge, it follows that $[Q, H] = 0$, which implies $[S, H] = 0$ as well. Utilizing these relations, one can observe that the state $S|0\rangle$ also possesses the same energy (zero) as the vacuum state $|0\rangle$. In simple terms, this implies that if a continuous symmetry is broken, there exists a curve of points through the vacuum state that corresponds to the symmetry transformation of the vacuum, all having the same energy. This argument holds true for any continuous symmetry, as explained in chapter 5 of the book by Coleman [17]. In the case of the $O(2)$ symmetry, all the degenerate vacuum states lie on valley of the Mexican hat potential (see Figure 4.3).

2. **Goldstone's theorem:** Goldstone's theorem, first established by Goldstone, Salam, and Weinberg [63, 12, 13], asserts that in the presence of SSB of a continuous symmetry, massless fields called Nambu-Goldstone bosons emerge. This statement can be proven in various ways. One approach involves demonstrating that the mass matrix associated with SSB has zero eigenvalues, as illustrated in section 11.1 of [39]. Alternatively, the theorem can be established by employing the techniques of quantum field theory, as explained in chapter 4.1 of [36]. Additionally, a proof utilizing group theory and geometry can be found in section 5.2.3 of [17] or section 43.3 of [24]. These proofs establish the emergence of Nambu-Goldstone bosons in the context of SSB.

   Explicitly considering the $O(2)$ Lagrangian given by equation Eq. 4.5, one can investigate SSB by imposing the transformation $\phi_1 = \phi_1 + v$ and $\phi_2 = \phi_2$. Substituting these expressions into equation Eq. 4.5, it becomes apparent that ϕ_2 remains massless, providing a concrete illustration of Goldstone's theorem.

3. **Coleman-Mermin-Wagner theorem :** The theorem postulates that the spontaneous breaking of a continuous symmetry in spacetime dimension $d \leq 2$ is implausible [64, 65, 66]. The derivation of the theorem, closely following [66], can be outlined as follows. The Goldstone theorem ensures the presence of massless bosons as a characteristic feature of SSB of a continuous symmetry. Consequently, the coincident limit of the propagator for the massless boson in

d-dimensional spacetime is

$$G(x,x) = \lim_{x\to 0} \int \frac{d^d k}{(2\pi)^d} \frac{e^{ikx}}{k^2}. \tag{4.7}$$

The ultraviolet divergence in this propagator can be effectively addressed by utilizing previously discussed renormalization techniques. However, it is important to note that in cases where $d \leq 2$, an infrared divergence emerges ($k \to 0$), which cannot be reconciled through renormalization procedures, resulting in the absence of massless bosons in $d \leq 2$ and, consequently, the spontaneous breaking of continuous symmetry. For a comprehensive explanation of this argument, please refer to section *IV*.1 of [36].

4.4 $O(N)$ Symmetric Theory in the large N limit

In Section 4.3 we investigated a system that possesses an $O(2)$ symmetry. To extend this symmetry group to $O(N)$, we consider the same Lagrangian as in equation Eq. 4.5, but now with $\phi = (\phi_1, ..., \phi_N)$. Perturbative studies of these models can be approached in two distinct ways: the ordinary expansion in λ for a fixed value of N , or the perturbation in $1/N$ for a fixed value of λ. In this section, our focus lies on the latter approach, the $1/N$ perturbation, as it encompasses a more nonlinear structure of the theory. We aim to understand the phenomenon of SSB in the context of $O(N)$-symmetric theory, utilizing the large N approximation.

A thorough and comprehensive analysis of the $1/N$ expansion for $O(N)$-symmetric theories can be found in chapter 8 of [17], which serves as our reference for this discussion. Since we utilize the results of this section in the study of SSB in Anti de Sitter space, we consider the theory in a general curved spacetime with minimal coupling to gravity. In the $1/N$ perturbation approach, it is advantageous to introduce a scaled coupling constant, denoted by λ, which yields the following action:

$$S = \int dv_x \left(\frac{1}{2} g^{\mu\nu} \partial_\mu \phi \partial_\nu \phi + \frac{1}{2} m_0^2 \phi^2 + \frac{\lambda_0}{8N} \left(\phi^2\right)^2 \right), \tag{4.8}$$

where m_0, λ_0 are bare parameters of the theory and $dv_x = d^d x\sqrt{g}$ is the d dimensional invariant measure. One can introduce an axillary field to the theory which gives the new action as

$$S[\phi,\sigma] = \int dv_x \left(\frac{1}{2}\phi\left(-\nabla^2+\sigma\right)\phi - \frac{N}{2\lambda_0}\sigma^2 + \frac{Nm_0^2}{\lambda_0}\sigma\right), \tag{4.9}$$

where ∇^2 is the d dimensional Laplacian. Then the partition function for the theory is

$$Z = \int D\phi D\sigma e^{-S[\phi,\sigma]}. \tag{4.10}$$

One can do the path integral over σ in Eq. 4.10 as

$$\begin{aligned} Z &= \int D\phi \int D\sigma e^{-\int dv_x\left(-\frac{1}{2}\phi\nabla^2\phi+\frac{1}{2}\sigma\left(\phi^2+\frac{Nm_0^2}{\lambda_0}\right)-\frac{N}{2\lambda_0}\sigma^2\right)} \\ &= \int D\phi\, e^{-\int dv_x\left(-\frac{1}{2}\phi\nabla^2\phi\right)} \int D\sigma e^{-\int dx\sqrt{g}\left(\frac{1}{2}\sigma\left(\phi^2+\frac{Nm_0^2}{\lambda_0}\right)-\frac{N}{2\lambda_0}\sigma^2\right)} \\ &= \int D\phi\, \exp\left\{-\int dv_x\left(-\frac{1}{2}\phi\nabla^2\phi+\frac{1}{2}m_0^2\phi^2+\frac{\lambda_0}{8N}\phi^4\right)\right\}. \end{aligned} \tag{4.11}$$

Which is the same partition function with Eq. 4.8 as our action. By utilizing the result of a Gaussian integral and neglecting terms that are independent of the fields, we arrive at the final line of equation Eq. 4.11. This implies that the introduction of the auxiliary field σ does not alter the partition function of the actual theory. In other words, both the actions presented in equations Eq. 4.8 and Eq. 4.9 describe the same dynamics. Considering equation Eq. 4.9 as our action simplifies our calculations, enabling us to construct an effective theory for σ by integrating out the ϕ field.

$$\begin{aligned} Z &= \int D\sigma\, e^{\int dv_x\left(\frac{N}{2\lambda_0}\sigma^2-\frac{Nm_0^2}{\lambda_0}\sigma\right)}\left(\det\left(-\nabla^2+\sigma\right)\right)^{\frac{-N}{2}} \\ &= \int D\sigma\, e^{-\frac{N}{2}\log\left(\det\left(-\bar{\nabla}^2+\bar{\sigma}\right)\right)-\int dv_x\left(-\frac{N}{2\lambda_0}\sigma^2+\frac{Nm_0^2}{\lambda_0}\sigma\right)} \\ &= \int D\sigma\, e^{-S_{eff}}, \end{aligned} \tag{4.12}$$

where $\bar{O} = O/\mu^2$, μ is some arbitrary constant with the dimension of mass inserted, so the logarithm argument is dimensionless and S_{eff} is the effective action and is

given as

$$\begin{aligned} S_{eff} &= \frac{N}{2}\log\left(\det\left(-\bar{\nabla}^2+\bar{\sigma}\right)\right)+\int dv_x\left(-\frac{N}{2\lambda_0}\sigma^2+\frac{Nm_0^2}{\lambda_0}\sigma\right) \\ &= \frac{N}{2}\int dv_x\ \log\left(-\bar{\nabla}_x^2+\bar{\sigma}\right)+\int dv_x\left(-\frac{N}{2\lambda_0}\sigma^2+\frac{Nm_0^2}{\lambda_0}\sigma\right). \end{aligned} \tag{4.13}$$

If the theory consists of a large number of scalar fields ($N \to \infty$), the dominant contribution to Z comes from the saddle point of S_{eff}. One can evaluate the effective action and the corresponding effective potential around the saddle point as

$$V_{eff} = \frac{N}{2}\left(\log\left(-\bar{\nabla}_x^2+\bar{\sigma}\right)-\frac{1}{\lambda_0}\sigma^2+\frac{2m_0^2}{\lambda_0}\sigma\right). \tag{4.14}$$

Now for notational simplicity we take

$$\begin{aligned} V_1 &= \frac{N}{2}\log\left(-\bar{\nabla}_x^2+\bar{\sigma}\right) \\ &= \frac{N}{2}\lim_{u\to 0}\int_0^{\sigma} dm^2\ G\left(u,m^2\right). \end{aligned} \tag{4.15}$$

Here, $G\left(u,m^2\right)$ represents the Euclidean Green's function of a scalar field with mass m in d-dimensional space, and u denotes the invariant distance (see Section 2.4.2). In the limit where u approaches zero (the coincident limit), the propagator diverges. Consequently, it is necessary to employ an appropriate renormalization procedure. By examining the classical action (Eq. 4.9), we can establish the renormalization conditions as follows:

$$\left.\frac{dV_{eff}}{d\sigma}\right|_{\sigma\to\mu^2} = \frac{Nm^2}{\lambda}, \tag{4.16a}$$

$$\left.\frac{d^2V_{eff}}{d\sigma^2}\right|_{\sigma\to\mu^2} = -\frac{N}{\lambda}, \tag{4.16b}$$

where λ and m are the renormalized parameters. Here μ is an arbitrary constant with dimensions of energy and in possible cases we take $\mu = 0$. After renormalization, the total potential (V) is

$$V = \frac{1}{2}\sigma\phi^2 + V_{eff}^{ren}, \tag{4.17}$$

where V_{eff}^{ren} is the renormalized effective potential. As discussed in Section 2.2, the minima of the total potential is determined by stationary points of V, *i.e.*,

$$\frac{\partial V}{\partial \sigma} = 0, \tag{4.18a}$$

$$\frac{\partial V}{\partial \phi} = 0. \tag{4.18b}$$

Utilizing Eq. 4.18a, we can express σ as a function of ϕ, allowing us to subsequently write V as a function solely dependent on ϕ. Therefore, the condition for the minima of the potential can be expressed as follows:

$$\begin{aligned} \frac{dV}{d\phi} &= \frac{\partial V}{\partial \phi} + \frac{\partial V}{\partial \sigma}\frac{\partial \sigma}{\partial \phi} \\ &= \frac{\partial V}{\partial \phi} = 0, \end{aligned} \tag{4.19}$$

where in the second line of Eq. 4.19 we use Eq. 4.18a. Using Eq. 4.19 in Eq. 4.17 gives

$$\frac{dV}{d\phi} = \sigma\phi = 0. \tag{4.20}$$

The minima of the potential can manifest at either $\phi = 0$ or $\sigma = 0$. The field configuration associated with the $\phi = 0$ minima is characterized by $O(N)$ symmetry. However, the field configuration corresponding to $\sigma = 0$ does not possess $O(N)$ symmetry. Therefore, if the global minima of the potential are found at $\sigma = 0$, it indicates the occurrence of SSB in the theory.

4.4.1 Spontaneous Symmetry Breaking

In this subsection, we investigate the phenomenon of SSB in the linear sigma model (LSM) as described in [67, 68, 69]. Following a similar approach as in the simple $\lambda\phi^4$ theory (see Section 4.2.2), we examine the SSB in the LSM by computing the one-loop effective potential. Our analysis is carried out in various spacetime dimensions.

Four dimensions

In the case of four dimensions, we have already derived the renormalized effective potential. By comparing equation Eq. 4.14 with equation Eq. 2.14, we can obtain the renormalized one-loop effective potential from equation Eq. 2.41 by replacing M^2 with σ, yielding:

$$V = \frac{1}{2}\sigma\phi^2 - \frac{N}{2\lambda}\sigma^2 + \frac{Nm^2}{\lambda}\sigma + \frac{N\sigma^2}{64\pi^2}\log\frac{\sigma}{2\mu^2}. \tag{4.21}$$

To determine the global minimum of the effective potential, we can utilize equation Eq. 4.18a to write

$$\phi^2 = \frac{2N\sigma}{\lambda} - \frac{2Nm^2}{\lambda} - \frac{N\sigma}{16\pi^2}\log\left(\frac{\sigma}{\mu^2}\right). \tag{4.22}$$

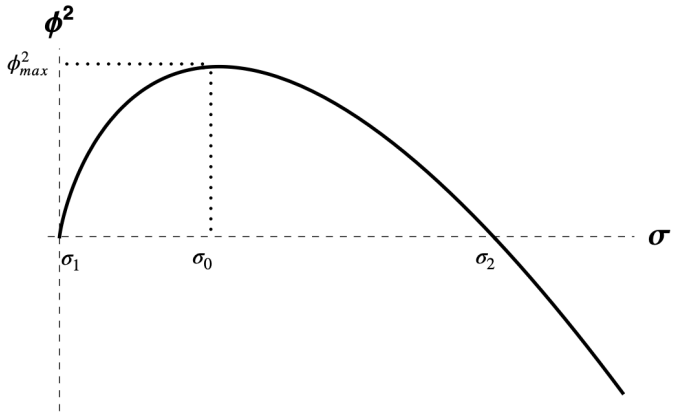

FIGURE 4.4: ϕ^2 as a function of σ.

In order to obtain equation Eq. 4.22, we rescaled the arbitrary parameter μ^2. The plot depicting ϕ^2 as a function of σ according to equation Eq. 4.22 can be found in Figure 4.4.

The maximum value that ϕ can reach is $\phi_{\max}$, as for $\phi > \phi_{\max}$ the effective potential becomes complex. Additionally, it is important to note that for $\phi < \phi_{\max}$, ϕ^2 and the effective potential are double-valued. Now, when $\sigma = 0$

$$\phi^2 = -\frac{2Nm^2}{\lambda}. \tag{4.23}$$

As we are considering a real scalar field, this is possible only if $m^2/\lambda < 0$. So for $m^2/\lambda < 0$ the system can have minima at $\sigma = 0$ or at $\sigma = \sigma_1$. The magnitude of V at $\sigma = 0$ and $\sigma = \sigma_2$ is determined by $V_{eff}^{ren}(\sigma)$ (see Eq. 4.17). Also, as function of σ, $V_{eff}^{ren}(\sigma)$ has its turning points at σ_1 and σ_2 and for $m^2/\lambda < 0$, $\sigma_1 < 0$ which is not in the possible range of $\sigma \in [0, \infty)$. The slope of V_{eff}^{ren} at $\sigma = 0$ is negative for $m^2/\lambda < 0$, so the magnitude of V_{eff}^{ren} decreases from $\sigma = 0$ to $\sigma = \sigma_2$ which means

$$V(\sigma = 0) > V(\sigma = \sigma_2). \tag{4.24}$$

Therefore, the global minimum of the effective potential occurs at $\sigma = \sigma_2$ or $\phi = 0$. The global minima of the system exhibit symmetry under $O(N)$ transformations, indicating the absence of SSB in four dimensions for any values of m^2/λ. For a more detailed analysis, please refer to [68, 69].

Three dimensions

The renormalized effective potential in three dimensions can be calculated by following the steps outlined in Section 2.5.1. First, expand the propagator around $u = 0$ using equation Eq. 2.34 with $d = 3$. Then, perform the integration over m^2 using equation Eq. 2.30. Finally, apply the renormalization conditions as specified in equation Eq. 4.16. This procedure yields the following expression for the renormalized effective potential

$$V = \frac{1}{2}\sigma\phi^2 - \frac{N}{2\lambda}\sigma^2 + \frac{Nm^2}{\lambda}\sigma - \frac{N\sigma^{3/2}}{12\pi}. \tag{4.25}$$

Note that here the renormalized $\lambda = \lambda_0$, so $\lambda > 0$. Following the same way as in four dimension one can use 4.18a to get

$$\phi^2 = \frac{2N\sigma}{\lambda} - \frac{2Nm^2}{\lambda} + \frac{2N\sigma^{1/2}}{4\pi} \tag{4.26}$$

In three dimensions, similar to the four-dimensional case, $\sigma = 0$ is only possible for $m^2 < 0$ in the context of a real scalar field. Furthermore, $\phi^2(\sigma)$ is a monotonically increasing function of σ. For $m^2 < 0$, $\phi^2(\sigma = 0)$ is positive, and as a monotonically increasing function, it implies that $\phi = 0$ is not possible for any value of σ. The only viable vacuum state of the theory is at $\sigma = 0$, which breaks the $O(N)$ symmetry and is

asymmetric. Therefore, it can be concluded that SSB occurs in the $O(N)$-symmetric linear sigma model in three dimensions for $m^2 < 0$, while there is no SSB for $m^2 \leq 0$. Detailed analysis can be found in [67].

Similar analysis can be carried out in two dimensions; however, it is important to note that the Coleman-Mermin-Wagner theorem, as discussed in Section 4.1, already guarantees the absence of SSB in two dimensions. The formalism presented here is general and can be readily extended to higher dimensions.

4.5 Symmetry Restoration

The concept of the restoration of broken symmetries at finite temperature was initially proposed by D.A. Kirzhnits and A.D. Linde, inspired by the Meissner effect [70]. Subsequently, L. Dolan, R. Jackiw, and Steven Weinberg provided a quantum field theory-based understanding of this phenomenon [71, 72]. In this section, we revisit and explore these effects in a manner similar to the approach presented in [71]. An intuitive perspective on the restoration of symmetry at finite temperature can also be found in [73].

In this section, we investigate the phenomenon of symmetry restoration at finite temperature within the context of a single real scalar field with $\lambda\phi^4$ self-interaction, which exhibits SSB (for $m^2 < 0$, as discussed in Section 4.2.1). The analysis presented here can be extended to other models discussed in this chapter. The procedure is outlined as follows. First, we calculate the one-loop effective potential at finite temperature for a free massive scalar field using the heat kernel method (similar calculations using the propagator can be found in [30]). We then utilize these results to calculate the one-loop effective potential for the $\lambda\phi^4$ interaction, demonstrating that the broken symmetry is restored beyond a critical temperature T_c.

4.5.1 Free Massive Scalar Field Theory at $T \neq 0$

To demonstrate the symmetry restoration, one could directly consider the $\lambda\phi^4$ theory and proceed. However, since we require the results of this section for comparison

with the results of an accelerated observer in the next chapter, we will examine it in detail. In a d-dimensional finite temperature quantum field theory at equilibrium, the system is equivalent to a Euclidean field theory where the periodicity of imaginary time corresponds to the inverse temperature. Therefore, it is necessary to study the field theory on the manifold $S^1 \times R^{d-1}$. By taking $L = \beta = 1/T$ in Eq. 2.45, we can obtain the one-loop effective potential as follows:

$$V = -2\left(\frac{m}{2\pi\beta}\right)^{\frac{d}{2}} \sum_{n=1}^{\infty} \frac{1}{n^{\frac{d}{2}}} K_{\frac{d}{2}}(mn\beta)\,, \tag{4.27}$$

where $K_\nu(z)$ is the modified Bessel function of second kind. The Eq. 4.27 provides a closed-form expression for the complete one-loop effective potential in arbitrary dimensions. We will utilize this result to examine the influence of temperature on the effective potential by considering extreme cases such as $m\beta \to 0$ (high temperature expansion) and $m\beta \to \infty$ (low temperature expansion). Consequently, we will analyze different dimensions separately.

For three dimension, taking $d = 3$ in Eq. 4.27, the leading order high temperature expansion ($m\beta \to 0$ in Eq. 4.27) gives

$$\lim_{m\beta\to 0} V = -\frac{\zeta(3)}{2\pi\beta^3} + \frac{m^2 T}{8\pi} - \frac{m^2 T}{4\pi}\log\left(\frac{m}{T}\right). \tag{4.28}$$

This is in agreement with the results in [74, 75]. The leading term $1/\beta^3$ leads to the Stefan-Boltzan law. Similar calculations in four dimensions ($d = 4$ in Eq. 4.27) gives

$$\lim_{m\beta\to 0} V = -\frac{\pi^2}{90\beta^4} + \frac{m^2}{24\beta^2}. \tag{4.29}$$

Similarly, we can study the low temperature expansion. For three dimension, with $d = 3$ and $m\beta \to \infty$ in Eq. 4.27, gives

$$\lim_{m\beta\to\infty} V = -\frac{m\beta}{2\pi\beta^3} e^{-m\beta}. \tag{4.30}$$

Similar expansions in four dimensions gives

$$\lim_{m\beta\to\infty} V = -\frac{m\beta^{\frac{3}{2}}}{(2\pi)^{\frac{3}{2}}\beta^4} e^{-m\beta}. \tag{4.31}$$

These findings are consistent with the outcomes presented in [30]. Similar computations can be conducted in other dimensions as well. It can be observed that at low temperatures $T << m$, the finite temperature contributions are exponentially suppressed, allowing us to approximate the results with those obtained at $T = 0$. The exponential decay appears to be attributed to the functional behavior of $K_\nu(z)$ and remains independent of the spacetime dimensions.

4.5.2 $\lambda\phi^4$ Interaction

If we consider the $\lambda\phi^4$ theory and aim to calculate the one-loop effective potential, we can simply replace m^2 in Eq. 4.27 with $M^2 = m^2 + \frac{\lambda}{2}\phi^2$. Here, m and λ represent the renormalized parameters of the scalar field, and ϕ denotes the constant field configuration. For our qualitative analysis of symmetry restoration, we only need to examine what occurs at high temperatures, specifically when $m\beta \to 0$ [71]. In three dimensions, according to Eq. 4.28, we can express the one-loop effective potential at the high-temperature limit as follows:

$$V = \frac{m^2}{2}\phi^2 + \frac{\lambda}{4!}\phi^4 + \frac{M^2T}{8\pi} - \frac{M^2T}{8\pi}\log\left(\frac{M^2}{T^2}\right). \tag{4.32}$$

The total mass of the system is defined as

$$\frac{\partial^2 V}{\partial\phi^2}\Big|_{\phi\to 0} = \mu^2. \tag{4.33}$$

This gives

$$\mu^2 = m^2 + \frac{\lambda T}{4\pi}\log\left(\frac{T}{m}\right). \tag{4.34}$$

This is in agreement with Eq. 3.4 of [74] and Eq. 4 of [75]. So if we start from a system with SSB ($m^2 < 0$), after some critical temperature T_c, where T_c can be defined as

$$m^2 = \frac{\lambda T_c}{4\pi}\log\left(\frac{T_c}{m}\right), \tag{4.35}$$

the effective mass of the theory takes positive values or one can say that symmetry is restored. One do similar calculations in four dimensions, comparing with Eq. 4.29

$$V = \frac{m^2}{2}\phi^2 + \frac{\lambda}{4!}\phi^4 + \frac{\lambda}{24\beta^2}\phi^2. \tag{4.36}$$

Similar to the three dimensional case, one can calculate the mass corrections in $\lambda\phi^4$ theory due to temperature as

$$\mu^2 = m^2 + \frac{\lambda T^2}{12}. \tag{4.37}$$

In four dimensions, if we start with $m^2 < 0$ (SSB), then the effective mass takes positive values for $T > T_c$

$$T_c^2 = 12\frac{m^2}{\lambda}. \tag{4.38}$$

So one can conclude that the broken symmetry is restored at finite temperature after some critical temperature T_c.

Chapter 5

Spontaneous Symmetry Breaking and the Uniformly Accelerated Observer

In this chapter, we address the question, do the spontaneous symmetry breaking and associated phase transitions depends on the observer? This chapter is based on our work on calculating one-loop effective potential in the frame of an accelerated observer [76].

An accelerated observer is of particular interest in theoretical physics because of the equivalence principle: "The effects of a uniform gravitational field is equivalent to the effects observed in a non-inertial uniformly accelerated frame". Later, this interest is reinforced by the observation that the accelerated observer perceives an observer dependent horizon that essentially captures all the salient features of black hole spacetime without the associated mathematical complexity. Due to the horizon, an accelerated observer has no access to the information outside the horizon, and this ignorance makes the observables of an accelerated observer equivalent to that of a thermal ensemble of an inertial observer. This is the statement of Fulling-Davies-Unruh effect [9, 8, 77] or simply the Unruh effect. Specifically, the Unruh effect is the statement that the observations of an accelerated observer with acceleration a are equivalent to the observations of an inertial observer at temperature $T = a/2\pi$. As we

saw in the previous chapter 4, the broken symmetry is restored at a finite temperature. So, one can expect a similar restoration of broken symmetries in the accelerated frames. Indeed we will conclude the same, which means the broken symmetry state of an inertial observer is a symmetric state for an accelerated observer with acceleration above some critical acceleration. Along with confirming the observer dependence of SSB, this demonstrates the ontic nature of the Unruh effect.

One can understand the Unruh effect using different methods, like using an accelerated detector [8] (section 3.3 of [10]), using Bogoliubov transformation [9] (chapter 8 of [26]), using thermalization theorem [78], using Euclidean propagators [79], using flat space propagator [80] etc. Some reviews on the topic are [81, 82, 83].

In Section 5.1, we demonstrate the Unruh effect closely following [79]. In Section 5.2, we calculate the one loop effective potential in Rinder frame and in Section 5.3 we use the effective potential to study the symmetry restoration. We conclude this chapter with 5.4, where we extend this analysis to linear sigma model using the large N approximation.

5.1 The Euclidean Rindler Observer

Consider the theory in the frame of an accelerated observer in $1+3$ dimensional spacetime with the metric

$$ds^2 = -\xi^2 d\tau^2 + d\xi^2 + d\vec{x}^2, \tag{5.1}$$

where $\vec{x}$ is a vector in 2 dimensional flat spacetime. Extending to arbitrary $d+2$ dimensional spacetime is trivial by considering $\vec{x}$ as a vector in R^d dimensional spacetime. In the metric, there is no acceleration parameter as it can be absorbed into the Euclidean Rinlder time, which makes the Euclidean time dimensionless. With this choice of Euclidean time, the only relevant quantity is the inverse invariant horizon temperature given by 2π. From the standard flat Minkowski spacetime given by

$$ds^2 = -dT^2 + dX^2 + dY^2 + dZ^2, \tag{5.2}$$

one can reach the Rindler metric (Eq. 5.1) using the standard transformation given by

$$\begin{aligned} T &= \xi \sinh(\tau) \\ X &= \xi \cosh(\tau) . \end{aligned} \tag{5.3}$$

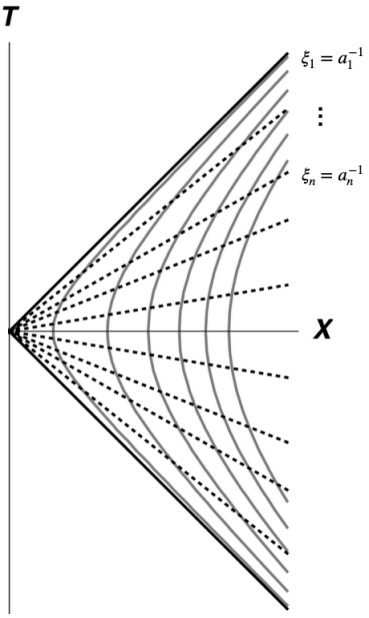

FIGURE 5.1: The coordinate system prepared by an accelerated observer. Each dotted line corresponds to constant τ and hyperbolic lines corresponds to constant ξ. Light cone in the Minkowski coordinates act as the horizon for the accelerated observer.

Some interesting features of this coordinate transformation is listed below

1. The Rindler coordinates only cover quarter of the Minkowski coordinates, the region $X^2 - T^2 = \xi^2 > 0$ as shown in Figure 5.1.

2. $X^2 - T^2 = \xi^2 = 0$ is a coordinate singularity, which forms an observer dependent horizon to the accelerated observer. So, the accelerated observer cannot access the regions beyond this horizon.

3. Each hyperbola $\xi = a^{-1}$ shown in Figure 5.1, corresponds to an accelerated observer moving along X direction with constant acceleration a and proper time τ.

4. The time-like Killing vector is different for an accelerated and inertial observer, which leads to different vacuum states for accelerated and inertial observers. Then the statement of the Unruh effect is that the accelerated observer perceives the vacuum of an inertial observer as thermal.

5. The Rinlder frame is a coordinate transformation from the flat Minkowski frame, so the spacetime remains flat (vanishing Riemann tensor).

Now we do the standard Wick rotation to get the Euclidean Rindler space by taking $T \to iT$ and $\tau \to i\tau$. The Euclidean Rindler metric is given by

$$ds^2 = \xi^2 d\tau^2 + d\xi^2 + d\vec{x}^2, \tag{5.4}$$

with the coordinate transformation

$$\begin{aligned} T &= \xi \sin(\tau) \\ X &= \xi \cos(\tau). \end{aligned} \tag{5.5}$$

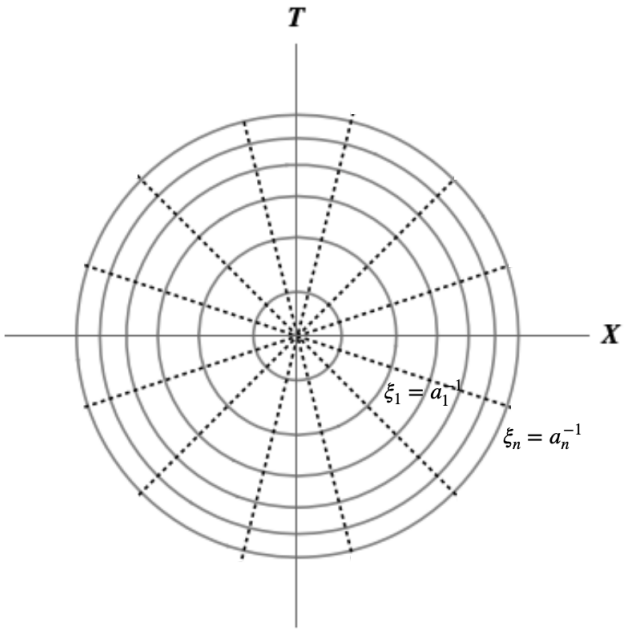

FIGURE 5.2: The coordinate system prepared by the Euclidean Rindler (or the polar coordinate chart). Each dotted line corresponds to constant τ and circles corresponds to constant ξ. The entire horizon is mapped to a single point at the center.

Note the following

1. The new metric Eq. 5.4 is the Euclidean flat space represented in polar coordinates through transformation Eq. 5.5. An inertial observer in these coordinates can be described as having coordinates $\xi = \xi_0$ and $\tau = \tau_0$. A uniformly accelerating/Rindler observer in the same coordinate system can be characterized as $\xi = \xi_0$ and τ not constant but uniformly varying.

2. The Euclidean time is an angular coordinate, so is periodic with periodicity 2π.

3. The word line of constant accelerated observer is circles with radius $1/a$ as shown in Figure 5.2

4. The crucial observation is that the entire horizon is mapped to a single point at the origin. The topology perceived by an inertial observer is standard R^4, but for an accelerated observer, it is $S^1 \times R^3$, which is multiply connected. The accelerated observer perceives a hole at the origin.

5. So in the Euclidean signature, the difference between the inertial and accelerated observer is topological.

6. As the topology is different, the inertial observer and accelerated observer perceive different vacuum states distinguished by topologically invariant parameters, as $|0\rangle_i$ for the inertial observer and $|0\rangle_r$ for the Euclidean Rindler observer.

Now consider as a free massive scalar field ϕ. In the Euclidean Rindler frame, one can define the propagator of the scalar field with respect to the $|0\rangle_i$ given by $G_{2\pi}$ or with respect to the vacuum of an accelerated observer $|0\rangle_r$ given by G_∞. Both these propagator or Green's functions satisfy the same differential equation given by

$$\left(-\Box + m^2\right) G_{\infty/2\pi}\left(x, x'\right) = \delta\left(x, x'\right). \tag{5.6}$$

As a solution to the above differential equation, the difference between the propagator comes from the different boundary conditions they satisfy. The $G_{2\pi}$ is uniquely defined by the condition that it is periodic in τ with periodicity 2π. However, G_∞ lives in a multiply connected space and it posses an infinite periodicity in τ and for

an accelerated observer with acceleration a , G_∞ can be obtained by

$$G_\infty = \lim_{a\to 0} G_{2\pi}. \tag{5.7}$$

Now let us look at the explicit expression for $G_{2\pi}$ and G_∞. We can compute these propagators by directly using the Rindler modes [82] or using the optical metric [84, 85]. For a $d+2$-dimensional Euclidean Rindler space the propagators are given by [86],

$$G_{2\pi}^{d+2}(x, x_0; m) = \int \frac{d^d k}{(2\pi)^d} e^{i\vec{k}.\Delta\vec{x}} \int_0^\infty \frac{d\nu}{\pi^2} \cosh\left(\nu\left(\pi - \Delta\tau\right)\right) K_{i\nu}\left(\mu_k \xi\right) K_{i\nu}\left(\mu_k \xi_0\right) \tag{5.8}$$

and

$$G_\infty^{d+2}(x, x_0; m) = \int \frac{d^d k}{(2\pi)^d} e^{i\vec{k}.\Delta\vec{x}} \int_0^\infty \frac{d\nu}{\pi^2} \sinh\left(\pi\nu\right) e^{-\nu\Delta\tau} K_{i\nu}\left(\mu_k \xi\right) K_{i\nu}\left(\mu_k \xi_0\right) \tag{5.9}$$

where $\Delta y = y - y_0$, $\mu_k^2 = k^2 + m^2$ and $K_\nu(z)$ is the modified Bessel function of the second kind. We can explicitly calculate the integrals in Eq. 5.8, which yield the flat space propagator with invariant length written in Rindler coordinates. This indeed confirms that $G_{2\pi}$ is the flat space propagator written in Rindler coordinates. Also, using Eq. 5.8 and Eq. 5.9 one can see that

$$G_{2\pi}\left(\tau - \tau_0\right) = \sum_{n=-\infty}^{\infty} G_\infty\left(\tau - \tau_0 + 2\pi n\right). \tag{5.10}$$

Examining Eq. 5.10, it becomes apparent that $G_{2\pi}$ exhibits periodicity in $\tau - \tau_0$, with a period of 2π . One can understand Eq. 5.10 in the following manner: The propagator of an accelerating observer relating to their vacuum is G_∞. However, due to the observer inhabiting a multiply connected space, they obtain their actual propagator by summing over all the inequivalent closed paths around the origin, which gives $G_{2\pi}$. Drawing a parallel with analogous findings in finite temperature field theory, $G_{2\pi}$ can be seen as the thermally equilibrated counterpart of G_∞ [79]. Therefore, in relation to the vacuum state of an accelerated observer, the inertial vacuum assumes a thermal nature for an accelerated observer, which elucidates the Unruh effect.

5.2 One-loop Effective Potential

Within this section, we employ the methodology outlined in Eq. 2.4.2 to compute the one-loop effective potential of a free massive scalar field from the perspective of an accelerated observer. The resultant calculation yields the complete one-loop effective potential, which is expressed as follows:

$$\begin{aligned} V_{eff} &= \frac{1}{2}m_0^2\phi^2 + \frac{1}{2}\int_0^{m_0^2} dm^2 \lim_{u\to 0} G\left(u, m^2\right) \\ &= \frac{1}{2}m_0^2\phi^2 + V_1, \end{aligned} \tag{5.11}$$

where m_0 is the bare mass of the theory. From Section 5.1, topologically the problem of calculating effective potential in the Euclidean Rindler frame is similar to the calculation of the energy-momentum tensor in $R^{d+1} \times S^1$ (same as finite temperature field theory) space in d+2 spatial dimensions. We address this problem in Section 2.5.2, and using the results in Section 2.5.2, we calculate the renormalized one-loop effective potential by using $G_\Delta = G_{2\pi} - G_\infty$. The physical condition we are imposing through this renormalization procedure is to set the vacuum energy with respect to the Rinlder vacuum to zero, as we should. Also, in finite temperature field theory, we renormalize the free energy by subtracting the zero temperature contribution [30], comparing with this, the above renormalization is justified as $\lim_{a\to 0} G_{2\pi} = G_\infty$ [79].

To avoid potential confusion among readers, we emphasize an important point. Specifically, $G_{2\pi}$ represents the standard flat space propagator expressed in polar coordinates (as discussed below Eq. 5.9). Hence, one can calculate the standard flat Euclidean space one-loop effective potential using the same $G_{2\pi}$. However, the renormalization process must be executed in a manner that sets the vacuum energy to zero with respect to the vacuum of an inertial observer. This involves taking the coincidence limit in the usual space with a topology of R^{d+1} and eliminating singular contributions by including counterterms. In our study, given that inertial and accelerated observers possess distinct vacuum states, the renormalization of vacuum energy must be approached differently to ensure consistency with their respective vacua. Consequently, for a comprehensive investigation of physical effects from the perspective of an accelerated frame in Euclidean signature, one must

calculate operator expectation values with respect to $G_\Delta = G_{2\pi} - G_\infty$ instead of solely employing $G_{2\pi}$.

Furthermore, it is essential to note that both $G_{2\pi}$ and G_∞ exhibit finite and infinite components. Remarkably, the infinite part of $G_{2\pi}$ precisely matches that of G_∞ and elegantly cancels out in the expression for G_Δ. However, the significance lies in that G_Δ also involves a non-trivial subtraction of the finite components, yielding the correct finite contribution to the effective potential (see Section 2.5.2 for more details). As a means of ensuring consistency, the effective potential derived from G_Δ successfully reproduces the correct free energy as demonstrated in [87], as well as the Rindler entropy density illustrated in [88]. In this light, we can confidently conclude that the effects arising from the presence of an event horizon, as perceived by the accelerating observer, are accurately captured by adhering to this consistent renormalization protocol.

Now using Eq. 5.8 and Eq. 5.9, one can write G_Δ in the coincidence limit as

$$G_\Delta = \int \frac{d^d k}{(2\pi)^d} \int \frac{d\nu}{\pi^2} e^{-\pi\nu} K^2_{i\nu}(\xi\mu_k)\,. \tag{5.12}$$

One can do the 'ν' and 'k' integral in Eq. 5.12 by separating the 'ν' dependence in $K_{i\nu}(z)$ using Eq. 2.1 in [89] and the integral identity (p.693, Eq.6.596,3 in [90]). The resulting integral can be expressed in terms of elementary functions using (p.917, Eq. 8.432,6 in [90]) as

$$G_\Delta = \frac{1}{2\pi\,(4\pi)^{\frac{d}{2}}\,\xi^d} \int_0^\infty \frac{du}{\pi^2+u^2} \int_0^\infty \frac{ds}{s^{\frac{d}{2}+1}} e^{-\xi^2 m^2 s} e^{\frac{-\cosh(u/2)^2}{s}}, \tag{5.13}$$

where we introduced renormalized mass m. One can calculate one-loop effective potential using Eq. 5.13 in Eq. 5.11 as

$$V_1 = \frac{-1}{(4\pi)^{\frac{d}{2}+1}\,\xi^{d+2}} \int_0^\infty \frac{du}{\pi^2+u^2} \int_0^\infty \frac{ds}{s^{\frac{d}{2}+2}} e^{-\alpha^2 s} e^{\frac{-\cosh(u/2)^2}{s}}, \tag{5.14}$$

where $\alpha = m\xi$. It turns out that there is no closed-form expression for the complete integral in Eq. 5.14. However, one can derive an approximate result as follows. First

scale s as $s = \alpha^2 t$ and then splitting the integral into two parts as

$$V_1 = \frac{-1}{(4\pi)^{\frac{d}{2}+1}\xi^{d+2}\alpha^{d+2}}\left(\int_0^{1/\alpha^2}\frac{dt}{t^{\frac{d}{2}+2}}e^{-\alpha^4 t}\int_0^\infty \frac{du}{\pi^2+u^2}e^{\frac{-\cosh(u/2)^2}{\alpha^2 t}} + \int_{1/\alpha^2}^\infty \frac{dt}{t^{\frac{d}{2}+2}}e^{-\alpha^4 t}\int_0^\infty \frac{du}{\pi^2+u^2}e^{\frac{-\cosh(u/2)^2}{\alpha^2 t}}\right). \tag{5.15}$$

In the first term in Eq. 5.15 α^2 is less than 1, so one can do the u integral using Laplace method and the resulting t integral in the leading order can be done in terms of Bessel function of the second kind. The leading order approximation is

$$V_1 \approx -\frac{2}{(4\pi)^{\frac{d+2}{2}}\pi^{\frac{3}{2}}}\frac{\alpha^{\frac{d+1}{2}}}{\xi^{d+2}}K_{\frac{d+1}{2}}(2\alpha)\,. \tag{5.16}$$

The correction from the second integral in Eq. 5.15 is of the order $O(\alpha^4)$, so one can safely neglect that in comparison with the leading order term. In order to obtain the other extreme limit for the parameter α, we now scale $s = t/\alpha^2$ in Eq. 4.15 to get

$$V_1 = \frac{-\alpha^{d+2}}{(4\pi)^{\frac{d}{2}+1}\xi^{d+2}}\left(\int_0^{\alpha^2}\frac{dt}{t^{\frac{d}{2}+2}}e^{-t}\int_0^\infty \frac{du}{\pi^2+u^2}e^{\frac{-\alpha^2\cosh(u/2)^2}{t}} + \int_{\alpha^2}^\infty \frac{dt}{t^{\frac{d}{2}+2}}e^{-t}\int_0^\infty \frac{du}{\pi^2+u^2}e^{\frac{-\alpha^2\cosh(u/2)^2}{t}}\right). \tag{5.17}$$

Now as $\alpha \to \infty$, one can do the first integral in Eq. 5.17 using the Laplace method which gives the same result as Eq. 5.16. Therefore, for the two extreme conditions considered in this paper, Eq. 5.16 is a good approximation to Eq. 5.14.

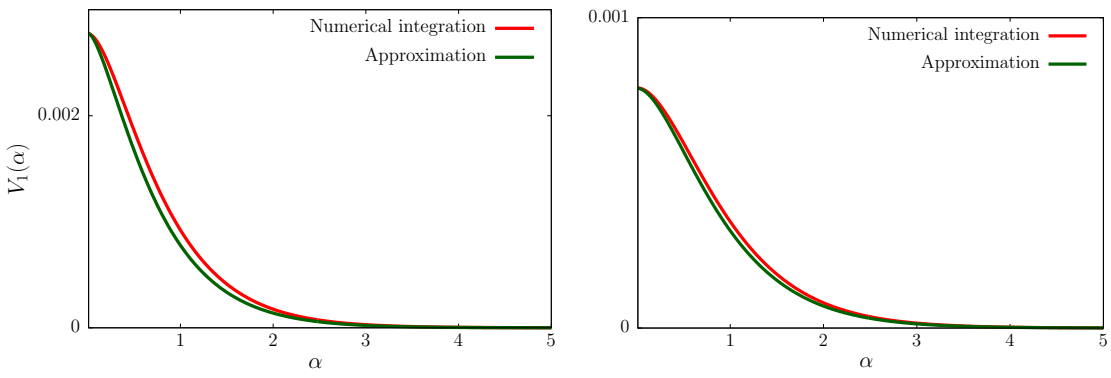

(A) Three dimensions (B) Four dimensions

FIGURE 5.3: Plot and compare the approximate result (Eq. 5.16) with the numerically integration result for Eq. 5.14 in the cases of $d = 1$ and $d = 2$..

In order to assess the accuracy of the approximation presented in Eq. 5.16, we can directly compare it to the entire function described by Eq. 5.14 through numerical integration for specific values of d. The resulting comparison plot is depicted in Figure 5.3. Analysis of the figure indicates that disregarding a scaling factor, the approximation Eq. 5.16 provides an adequate representation of the function Eq. 5.14. Notably, this scaling factor relies on numerical coefficients, implying that by substituting Eq. 5.16 for Eq. 5.14, we can obtain reasonably accurate qualitative insights. This approximation proves particularly effective when considering limiting values of α, successfully capturing the qualitative behavior. Utilizing this approximation, we can further investigate the characteristics of the effective potential for observers experiencing both high and low acceleration. Furthermore, to verify the validity of our approximation, we can compare these results with those obtained from field theory at finite temperatures.

5.2.1 Observers with High Values of Acceleration for $d = 1, 2$

Considering near horizon observers characterized by high acceleration, we can examine this regime by taking the limit $\alpha \to 0$ in Eq. 5.14. Notably, this limit corresponds to the high-temperature limit in finite temperature field theory. Although performing a Taylor series expansion around $\alpha = 0$ in Eq. 5.14 may appear tempting, caution must be exercised. As a function of α, V_1 is not analytically defined at $\alpha = 0$ due to the divergence of the 's' integral for terms with $n \geq \frac{d}{2} + 1$. However, this expansion still yields the correct leading-order term for the case of four dimensions, where $d = 2$. Specifically, the second term in the series expansion around $\alpha = 0$ in Eq. 5.14 yields the following expression (after reintroducing m and ξ),

$$\lim_{\alpha \to 0} V_1 = \frac{m^2}{6\,(4\pi)^2\,\xi^2}. \tag{5.18}$$

An interesting interpretation arises when considering an observer following a trajectory with a constant ξ. In this case, the observer perceives an Unruh temperature given by $\xi = \frac{1}{2\pi T}$. Remarkably, we observe that Eq. 5.18 aligns with the results

obtained from field theory at finite temperature (see Eq. 4.29). However, this interpretation and agreement do not hold for dimensions other than four. Therefore, for general dimensions, the near horizon limit can be investigated effectively by utilizing Eq. 5.16 as a reliable approximation for the effective potential. Specifically, for the case of three dimensions with $d = 1$ and $\alpha \to 0$, Eq. 5.16 yields the following expression:

$$\lim_{\alpha\to 0} V_1 \approx \frac{m^2}{8\pi^3\xi}\left(1-\gamma_E\right) - \frac{m^2}{8\pi^3\xi}\log\left(m^2\xi^2\right), \tag{5.19}$$

where γ_E is the Euler's constant. By considering the Unruh temperature $\xi = \frac{1}{2\pi T}$, we can compare Eq. 5.19 with the finite temperature results in Eq. 4.28. Notably, the temperature dependence of the effective potential in Eq. 5.19 perfectly matches that of the finite temperature results in Eq. 4.28, albeit with some disagreement in the coefficients at this order of approximation. However, it is possible to refine the agreement by considering higher-order corrections. Analogous calculations in four dimensions, i.e., for $d = 2$ and $\alpha \to 0$ in Eq. 5.16, yield the following expression,

$$\lim_{\alpha\to 0} V_1 \approx \frac{m^2}{16\pi^3\xi^2}. \tag{5.20}$$

Which is a sufficiently good approximation of Eq. 5.18. Also, Eq. 5.16 can in fact be used to study the behavior of effective potential in Euclidean Rindler space in general dimensions.

5.2.2 Observers with Low Values of Acceleration for $d = 1, 2$

Let us now examine the opposite limit, where the observer accelerates slowly and remains far from the horizon (denoted as $\alpha \to \infty$ in Eq. 5.16). Specifically, for three dimensions with $d = 1$ and $\alpha \to \infty$, Eq. 5.16 yields the following expression:

$$\lim_{\alpha\to\infty} V_1 \approx -\frac{e^{-2\alpha}\alpha^{\frac{1}{2}}}{8\pi^{\frac{5}{2}}\xi^3}. \tag{5.21}$$

To analyze this result, we can compare it with the finite temperature results in Eq. 4.30 by considering the Unruh temperature ($\xi = 1/(2\pi T)$). We observe that the leading exponential decay behavior remains the same as in the finite temperature

case. However, the polynomial powers of the temperature are altered by a factor of half. This discrepancy may be attributed to the approximation scheme employed. For the case of four dimensions, a similar limit yields the expression:

$$\lim_{\alpha\to\infty} V_1 \approx -\frac{e^{-2\alpha}\alpha}{16\pi^3\xi^4}. \tag{5.22}$$

In conclusion, we find that for a slowly accelerating observer with proper acceleration 'a', the corrections to the effective potential exhibit exponential suppression characterized by the Boltzmann factor $e^{-m/a}$. This behavior arises from the leading order behavior of the modified Bessel function ($\lim_{z\to\infty} K_\nu(z) \sim e^{-z}$). Based on Eq. 5.16, we can expect this exponential suppression to also be present in arbitrary dimensions.

5.3 Symmetry Restoration in $\lambda\phi^4$ Theory

We now turn our attention to the investigation of whether the breakdown of discrete $\mathbb{Z}_2$ symmetry is restored for a specific class of observers. To study SSB, it is customary to employ the effective potential [17, 36]. Leveraging the insights gained from Chapter 4, we can now elucidate the phenomenon of spontaneous symmetry breaking in the Rindler frame. Since the Rindler frame can be regarded as another coordinate system for standard flat space, a comparison with results obtained in standard flat space enables us to discern the frame dependence of SSB. To this end, we consider a self-interacting massive scalar field theory characterized by the following action:

$$S = \int dv_x \left(\frac{1}{2}g^{\mu\nu}\partial_\mu\phi\partial_\nu\phi + \frac{m_0^2}{2}\phi^2 + \frac{\lambda_0}{4!}\phi^4\right). \tag{5.23}$$

The corresponding renormalized one loop effective potential for this action can be calculated using G_Δ in Eq. 5.13 in the formula for one loop effective potential as in Eq. 2.30. Proceeding the same as in Section 5.2, we can get the approximate result of renormalized one loop effective potential as

$$V_1 \approx -\frac{2}{(4\pi)^{\frac{d+2}{2}}\pi^{\frac{3}{2}}}\frac{(m^2+\lambda\phi^2/2)^{\frac{d+1}{4}}}{\xi^{\frac{d+3}{2}}}K_{\frac{d+1}{2}}\left(2\xi\sqrt{m^2+\frac{\lambda}{2}\phi^2}\right), \tag{5.24}$$

where m and λ are now the renormalized parameters. From Eq. 5.24, it is evident that the effective potential explicitly depends on ξ, which corresponds to the trajectory of the accelerated observer [91]. This observation implies that the re-normalized parameters of the theory, such as the mass, can also exhibit dependence on the observer, thus indicating the observer dependence of SSB in the system.

Furthermore, we can provide an interpretation of the effective potential result as follows: Let us consider discretizing the radial coordinate in the Euclidean Rindler frame. At each radial lattice point, denoted by index "i" (with the usual rotational invariance), the effective potential takes on a distinct form that depends on the label "i". In other words, each observer situated at a specific lattice point "i" perceives a different effective potential and, consequently, a distinct coefficient of ϕ^2.

In the literature, it is well-established that in standard flat space, the vacuum state configuration of a scalar field governed by $\lambda\phi^4$ interaction exhibits a breakdown of $\mathbb{Z}_2$ symmetry for $m^2 < 0$ [36, 17]. Additionally, it is known that at finite temperatures, this symmetry is restored above a critical temperature [70, 71, 72]. Drawing upon the thermalization theorem [81], we can thus anticipate a similar restoration of broken symmetries in accelerated frames, as demonstrated in previous works [92, 93]. Analogous to finite temperature calculations, we can determine the critical acceleration for symmetry restoration by imposing [71]:

$$\frac{\partial^2 V_{eff}}{\partial \phi^2}\Big|_{\phi=0} = 0. \tag{5.25}$$

The hallmark of SSB is the emergence of a nonvanishing vacuum state field configuration. Consequently, the equation for the critical acceleration can be interpreted as the point at which the minimum of the effective action or effective potential occurs with $\phi_0 = 0$, indicating the restoration of symmetry. Furthermore, the critical acceleration can be interpreted as the point at which the renormalized mass attains a value of zero. Viewed from the perspective of the effective potential discretized along the radial direction, the condition given by Eq. 5.25 can be regarded as imposing a renormalization condition to absorb the quadratic divergence at each lattice point. By employing this condition (Eq. 5.25) in Eq. 5.24 with $m^2 < 0$, one can estimate

the approximate critical acceleration in four dimensions as follows:

$$a_c^2 = \frac{16\pi^3}{\lambda} m^2 e^{2im\xi} \xrightarrow{m\xi\to 0} \frac{16\pi^3 m^2}{\lambda} \tag{5.26}$$

where we choose the trajectory $\xi = 1/a_c$. The value of the critical acceleration obtained in Eq. 5.26 shows good agreement with the results found in [92, 93], considering the limitations of our approximation. It is crucial to emphasize that the methods employed in [93, 92] do not generalize to arbitrary dimensions and yield incorrect outcomes for dimensions other than four. In [93], the authors calculated the critical acceleration using a Taylor expansion, as discussed in Section 5.2. However, this approach fails in two distinct ways when applied to dimensions other than four.

Firstly, it fails to capture the correct functional dependence of the effective potential in the $m\xi \to 0$ limit. Secondly, in four dimensions, the divergence part of the effective potential naturally separates even when performing the Taylor expansion in $m\xi$ at the leading order. However, this separation does not occur in other dimensions, necessitating the specification of a renormalization procedure. This becomes evident when considering three dimensions, where the critical acceleration can be calculated by setting $d = 1$ in Eq. 5.24 and utilizing Eq. 5.25:

$$-\frac{m^2}{2} + \frac{\lambda a_c}{8\pi^3} K_0\left(\frac{2m}{a_c}\right) = 0. \tag{5.27}$$

In the limit of $\lim_{z\to 0} K_\nu(z) \to +\infty$, it can be concluded that the broken symmetry will be restored in three dimensions once the critical acceleration a_c is reached. Taking the near-horizon limit of $m\xi \to 0$, the leading order behavior of Eq. 5.27 is given by:

$$-\frac{m^2}{2} + \frac{\lambda a_c}{8\pi^3} \log\left(\frac{a_c}{m}\right) = 0. \tag{5.28}$$

By considering the Unruh temperature $a_c = 2\pi T_c$, it is possible to reproduce the results obtained in finite temperature field theory, as demonstrated in previous works [74, 75]. It is worth noting that attempting to obtain the logarithmic functional dependence on the critical acceleration using a Taylor expansion, as done in [93], is not feasible.

Similar to the finite temperature field theory [71], an accurate determination of the

critical acceleration necessitates higher-loop corrections in the effective potential [93]. However, the one-loop effective potential is a suitable approximation to study the observer dependence of spontaneous symmetry breaking.

5.4 Symmetry Restoration in Linear Sigma Model

Our current focus revolves around examining SSB within the $O(N)$ symmetric linear sigma model, specifically within the framework of Rindler space and under the assumption of the large N limit. In Section 5.3, we established the restoration of broken $\mathbb{Z}_2$ symmetry in the vacuum configuration of a single scalar field with ϕ^4 interaction at a critical acceleration. Furthermore, Section 4.4.1 presented evidence indicating the absence of $O(N)$ symmetry in the vacuum field configuration within three-dimensional spacetime, thereby manifesting spontaneous symmetry breaking . Consequently, our objective is to investigate whether the broken $O(N)$ symmetry can be restored in an accelerated frame, leveraging the large N limit as an approximation method. Following the same methodology as in Section 5.3, we derive the renormalized one-loop effective potential of the linear sigma model as

$$V_{eff}^{ren} = -\frac{N}{2\lambda}\sigma^2 + \frac{Nm^2}{\lambda}\sigma - \frac{2N\sigma^{\frac{d+1}{4}}}{(4\pi)^{\frac{d+2}{2}}\pi^{\frac{3}{2}}\xi^{\frac{d+3}{2}}} K_{\frac{d+1}{2}}(2\alpha)\,, \tag{5.29}$$

where m and λ are the renormalized parameters and $\alpha = \xi\sqrt{\sigma}$ which is a dimensionless parameter. With the effective potential in hand, one can study the symmetry behavior of the vacuum configurations in different dimensions.

In three dimensional spacetime, the one loop effective potential in the near horizon limit ($\alpha \to 0$) is

$$\lim_{\alpha\to 0} V_{eff}^{ren}\Big|_{d=1} = -\frac{N}{2\lambda}\sigma^2 + \frac{Nm^2}{\lambda}\sigma - \frac{N\sigma a}{8\pi^3}\log\left(\frac{\sigma}{a^2}\right), \tag{5.30}$$

where we choose the trajectory $\xi = 1/a$. Consider a theory with SSB in standard flat space, characterized by $m^2 < 0$. In accelerated frames, as indicated by Eq. 5.30, the effective mass becomes positive beyond a critical acceleration, leading to the symmetry restoration at high accelerations. At the same time, it is possible to

calculate the critical acceleration using conditions similar to Eq. 5.25 with $d = 1$, it should be noted that the critical acceleration depends on an arbitrary scale μ (even though the normalized effective potential is scale-independent). Hence, similar to finite temperature field theory [75], Eq. 5.30 may not be directly useful for predicting the critical acceleration. However, the underlying structure of Eq. 5.30 assures symmetry is restored for at least a particular class of Rindler observers. Moreover, our techniques are general and can be applied to shed light on symmetry-breaking aspects in Rindler space for arbitrary spacetimes.

An analogous analysis can be carried out in four-dimensional spacetime. Nevertheless, it is important to emphasize that the flat four-dimensional linear sigma model, as discussed in Section 4.4.1, does not exhibit SSB. Therefore, drawing definitive conclusions regarding the observer dependence of SSB based solely on four-dimensional results is not possible. However, through a comparison with results in flat space, it becomes apparent that acceleration introduces modifications to the effective mass of the theory. These corrections can be expressed as follows:

$$\frac{m_{eff}^2}{\lambda} = \frac{m^2}{\lambda} + \frac{a^2}{16\pi^3}. \tag{5.31}$$

In this study, we have investigated the observer dependence of SSB using two distinct models. The results obtained from both models lead to the conclusion that SSB does depend on the observer. By specifically focusing on the perspective of an accelerated observer and concurrently comparing these findings with those obtained from studying finite temperature effects, our results provide further support for the thermalization theorem.

Furthermore, since SSB is typically associated with a phase transition, the observer dependence of SSB suggests that the temperature experienced by an accelerated observer possesses physical significance. Thus, our analysis reinforces the notion that the temperature perceived by an accelerated observer is indeed a physically meaningful quantity.

Chapter 6

Symmetry Breaking in Anti-de Sitter Space

In this chapter, we explore the influence of curvature on spontaneous symmetry breaking (SSB) by investigating SSB in anti-de Sitter (AdS) spacetime, building upon the general framework of quantum field theory in curved spacetime. The analysis presented here is based on our previous work in [94] and follows a similar approach. We focus on the specific model of an $O(N)$ symmetric linear sigma model in the large N limit approximation. The AdS spacetime holds significant importance in the AdS/CFT correspondence, which establishes a connection between gravitational theories in AdS space and conformal field theories on the boundary. Furthermore, it is worth noting that Rindler space and AdS emerge as near-horizon geometries of non-extremal and extremal black holes, respectively, relating to our discussions in previous chapters.

6.1 Anti-de Sitter space

The $d+1$ dimensional Euclidean Anti-de Sitter (AdS) can be described using the Poincare coordinates as

$$ds^2 = \frac{L^2}{z^2}\left(dz^2 + \sum_{i=1}^{d} dx_i^2\right), \tag{6.1}$$

where L is the AdS scale. Note that the Poincare corrdinates only covers a portion of AdS space, called the Poincare patch. Some interesting properties of the AdS space is listed below [95, 96]

1. AdS is a maximally symmetric spacetime with $d(d+1)/2$ number of independent Killing vectors in d dimensional spacetime.

2. Solution to Einstein's field equation with a negative cosmological constant and constant negative curvature.

3. Asymptotic Structure: AdS space has a well-defined boundary at infinity. This boundary is topologically equivalent to a Euclidean space. The asymptotic behavior of AdS space plays a crucial role in the AdS/CFT correspondence, which relates theory in the bulk AdS space to a conformal field theory defined on its boundary.

Before proceeding with the calculation of SSB, examining the stability criteria for scalar fields in the AdS space is essential.

6.1.1 The Breitenlohner-Friedmann Bound

The Breitenlohner-Freedman (BF) bound is a stability condition in the AdS space. According to this bound, a negative mass for a scalar field does not result in instabilities, as in flat space, as long as $m^2L^2 > -d^2/4$ for AdS_{d+1} spacetime. This condition ensures the scalar field remains stable and well-behaved in the AdS background. One can obtain this bound in the following way [97]. Consider the action for a free massive scalar field $\phi = \phi(z)$ as

$$S = \int d^dxdz \frac{1}{z^{d+1}} \left(z^2\partial_z\phi\partial_z\phi + m^2L^2\phi^2\right). \tag{6.2}$$

Now introduce a new variable as $y = \log(z)$ and rescale the scalar field as $\phi = z^{d/2}\psi$ which gives the action upto a boundary term as

$$S = \int d^dxdy \left(\partial_y\psi\partial_y\psi + \left(m^2L^2 + \frac{d^2}{4}\right)\psi^2\right). \tag{6.3}$$

By comparing the action in Eq. 6.3 with the action in flat spacetime, we observe that $(m^2L^2 + d^2/4)$ serves as the effective mass of the theory. The potential is bounded if and only if $m^2L^2 > -d^2/4$, which corresponds to the BF bound. The BF bound can be derived using various approaches, all of which highlight the significance of this bound.

1. The stability of a static field configuration can be determined by examining the positivity of the conserved energy function. By applying this condition, it can be shown that the presence of normalizable negative energy modes is possible below the BF bound [98]. This method of analysis is similar to the original derivation of the BF bound [99, 100]

2. The BF bound ensures that the operator $\hat{K} = (-\Box + m^2)$ is positive definite. In various calculations, such as the effective action or perturbative analysis, it is crucial for $\hat{K}$ to be positive definite; otherwise, the Euclidean path integral would diverge. The BF bound can be derived by considering the condition for positive definiteness of $\hat{K}$.

3. Also, the BF bound can also be derived by examining the finiteness of the action in AdS space [101]. This requirement ensures the existence of normalizable modes and enables the quantization of the field.

Using any of these derivations, it can be shown that for an interacting field theory with a potential $U(\phi)$ that includes the mass term, the BF bound is given by $U''(\phi) > -d^2/4$ [102].

6.2 Symmetry Breaking

To investigate SSB, it is necessary to compute the one-loop effective potential. Analogously to the Rindler case, we calculate the one-loop effective potential using the propagator (as shown in equation 2.30). The bulk-to-bulk Green's function in AdS_{d+1} can be expressed as follows [103]:

$$G(W) = \frac{\alpha_0}{L^{d-1}} W^{\Delta}{}_2F_1\left(\Delta, \Delta + \frac{1-d}{2}, 2\Delta - d + 1; -4W\right), \tag{6.4}$$

where

$$W = \frac{1}{2}\frac{1}{\cosh\left(\frac{u}{L}\right)-1}; \quad \Delta = \frac{d}{2}+\frac{1}{2}\sqrt{d^2+4m^2L^2}; \quad \alpha_0 = \frac{\Gamma(\Delta)}{2\pi^{d/2}\Gamma\left(\Delta-\frac{d}{2}+1\right)}, \tag{6.5}$$

and ${}_2F_1$ is the Hypergeometric function. In the limit of coincidence ($u \to 0$), the propagator diverges, as expected. To calculate the effective potential in three and four-dimensional AdS space, we utilize Green's function given in equation 6.4.

6.2.1 Four Dimensions

To calculate the renormalized effective potential, it is necessary to regularize the Green's function in Eq. 6.4. Following a similar approach as in the previous chapter, we expand $G(W)$ around $u = 0$ in four-dimensional spacetime ($d = 3$ in equation Eq. 6.4) as

$$\begin{aligned}\lim_{u\to 0} G(W) = \frac{1}{12\pi^2}\Bigg(&\frac{3}{u^2}-\frac{16+3\Delta(\Delta-5)}{4L^2}\\ &+\frac{3}{4L^2}(\Delta-2)(\Delta-1)\left(2H_{\Delta-3}+2\log\left(\frac{u}{2L}\right)\right)\Bigg),\end{aligned} \tag{6.6}$$

where H_z is the harmonic number. In order to study the SSB, we focus on the linear sigma model in the large N limit as discussed in Section 4.4. Using Eq. 6.6 we can calculate the one loop corrections to the effective potential (using 4.15) as

$$\begin{aligned}\frac{8L^2\pi^2V_1}{N} =&\sigma\left(\gamma+\frac{L^2}{u^2}-\frac{5}{12}+\frac{\beta}{3}+\log\left(\frac{u}{2L}\right)+\frac{1}{2}\log\left(\Gamma(\beta)\right)+\beta\log\left(\Gamma(\beta)\right)-3\psi\left(-2,\beta\right)\right)\\ &+\frac{L^2\sigma^2}{4}\left(\log\left(\frac{u}{2L}\right)+\gamma-\frac{1}{2}\right)+\frac{\beta}{L^2}\left(\frac{3}{4}+2\log\left(\Gamma(\beta)\right)+6\psi\left(-3,\beta\right)\right)\\ &+\frac{1}{L^2}\left(\log\left(\Gamma(\beta)\right)-6\psi\left(-4,\beta\right)+3\psi\left(-3,\beta\right)\right)-\frac{13}{2L^2}\psi\left(-2,\beta\right),\end{aligned} \tag{6.7}$$

where γ is the Euler's constant, ψ is the polygamma function and for notational simplicity we choose

$$\beta = -\frac{1}{2}+\frac{1}{2}\sqrt{9+4L^2\sigma}. \tag{6.8}$$

Based on equation 6.8, it is evident that β is real when $-9/4L^2 < \sigma$, which corresponds to the BF bound discussed in Section 6.1.1. Therefore, within the BF bound, the effective potential is also real. Equation 6.7 provides a regularization scheme for

the effective potential, and as anticipated from previous results [102, 104], the divergences in the effective potential manifest as linear and quadratic terms in σ. So one can renormalize the theory by redefining m_0 and λ_0. By applying appropriate renormalization conditions (see Eq. 4.16), we can express the renormalized parameters as follows:

$$\begin{aligned}\frac{m^2}{\lambda} &= \frac{1}{48L^2\pi^2} + \frac{1}{8\pi^2u^2} + \frac{m_0^2}{\lambda_0} + \frac{1}{8L^2\pi^2}\log\left(\frac{u}{2L}\right)\\ -\frac{1}{\lambda} &= \frac{1}{144} - \frac{1}{96\pi^2} - \frac{1}{\lambda_0} + \frac{1}{16\pi^2}\log\left(\frac{u}{2L}\right).\end{aligned} \tag{6.9}$$

Note that in the renormalized parameters, we included the finite terms involving L. Using Eq. 6.9, one can write the renormalized effective potential as

$$\begin{aligned}V_{eff}^{ren} = \frac{Nm^2\sigma}{\lambda} - \frac{N\sigma^2}{2\lambda} + \frac{N}{8L^2\pi^2}\Bigg(&\frac{\sigma^2L^2}{4}\left(\gamma - \frac{1}{3} - \frac{\pi^2}{9}\right) + \frac{\beta}{L^2}\left(\frac{3}{4} + 2\log\left(\Gamma(\beta)\right) + 6\psi\left(-3,\beta\right)\right)\\ &+\frac{\sigma}{2}\left(2\gamma + \frac{2\beta}{3} + (2\beta+1)\log\left(\Gamma(\beta)\right) - 6\psi\left(-2,\beta\right) - \frac{7}{6}\right)\\ &+\frac{1}{L^2}\left(\log\left(\Gamma(\beta)\right) - 6\psi\left(-4,\beta\right) + 3\psi\left(-3,\beta\right) - \frac{13}{2}\psi\left(-2,\beta\right)\right)\Bigg).\end{aligned} \tag{6.10}$$

The one-loop renormalized effective potential is given by Eq. 6.10. Taking into account the tree-level contributions, we can express the full effective potential at the one-loop level as

$$V = \frac{1}{2}\sigma\phi^2 + V_{eff}^{ren}. \tag{6.11}$$

At this stage of our calculations, we can perform a consistency check by considering the limit as $L \to 0$. In this limit, we expect to recover the results obtained in flat spacetime, as discussed in Section 3.4. Taking $L \to 0$ in Eq. 6.11, we obtain

$$\lim_{L\to\infty} V = \frac{1}{2}\sigma\phi^2 + \frac{m^2N\sigma}{\lambda} - \frac{N\sigma^2}{2\lambda} + \frac{N\sigma^2}{64\pi^2}\log\left(\sigma L^2\right). \tag{6.12}$$

In the limit of flat spacetime, where L becomes an arbitrary parameter with dimensions of length, we can replace it with an energy parameter $2\mu^2 = 1/L^2$. This substitution allows us to reproduce the flat space result, as shown in Eq. 4.21.

The Ground State

We investigate spontaneous symmetry breaking (SSB) by examining the non-zero vacuum expectation value of the field. As discussed in Section 2.3, the vacuum field configuration corresponds to the stationary points of the effective potential V. The condition for the stationary points of the effective potential, as given by Eq. 4.18, can be applied in the AdS space to yield the following expression

$$\phi^2(\sigma) = \frac{N}{72L^2\pi^2\lambda}\Big(-144\pi^2L^2m^2 + 3\lambda L^2\sigma + \lambda\pi^2L^2\sigma + 144L^2\pi^2\sigma - 9\lambda\left(\beta + 1 + L^2\sigma\right)H_{\beta-1}\Big). \tag{6.13}$$

Similar to four-dimensional flat space (see Section 5.2), the function ϕ^2 exhibits two distinct branches as a function of σ, leading to the effective potential V being a double-valued function of σ. The variation of ϕ^2 with respect to σ is depicted in Figure 6.1, which is similar to the corresponding plot in flat space (see Figure 4.4). From Figure 6.1, we observe that ϕ^2 reaches its maximum value $\phi^2_{\max}$ at $\sigma = \sigma_0$ and subsequently decreases monotonically.

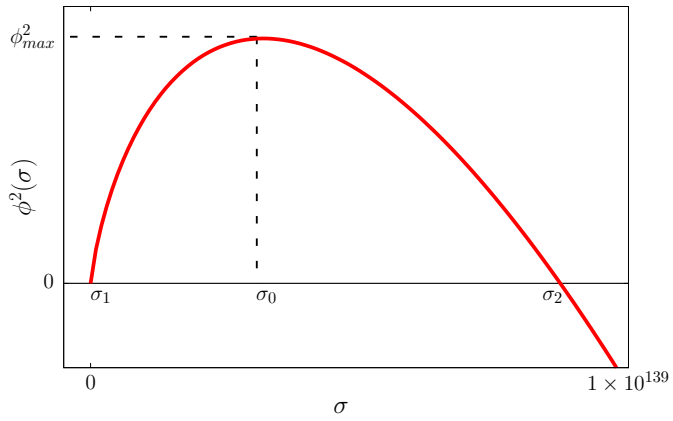

FIGURE 6.1: A plot illustrating ϕ^2 as a function of σ for $m^2 > 0$.

One can anticipate the existence of multiple local minima, corresponding to $\sigma = 0$ and $\phi = 0$. The determination of the ground state involves comparing the values of the effective potential at each minimum, and the configuration with the lowest effective potential corresponds to the ground state. Let us begin by considering $\sigma = 0$ which gives

$$V(0) = -\frac{0.003N}{L^4}. \tag{6.14}$$

But at this point

$$\phi^2(0) = -\frac{2m^2N}{\lambda}. \tag{6.15}$$

For $m^2 > 0$, the field becomes complex, so in order to have $\sigma = 0$, we require $m^2 \leq 0$. From Fig. 6.1, we observe that $\phi = 0$ for both σ_1 and σ_2. In the case of $m^2 < 0$ and $\phi^2(0) > 0$, we have $\sigma_1 < 0$. As discussed earlier, σ can take negative values within the BF bound. Our next task is to determine the global minima of the potential by comparing the values of effective potential. From Eq. 4.17, the effective potential at $\phi = 0$ is

$$V(\phi = 0) = V_{eff}^{ren}(\sigma). \tag{6.16}$$

Then for small values of σ

$$\lim_{\sigma \to 0} V_{eff}^{ren}(\sigma) = V(\sigma = 0) + \frac{Nm^2\sigma}{\lambda} + O(\sigma^2). \tag{6.17}$$

So, for $m^2 < 0$, we observe that the effective potential V_{eff} increases from $V(0)$ to $V(\sigma_1)$ since $\sigma_1 < 0$. However, it decreases from $V(0)$ to $V(\sigma_2)$. Thus, we can conclude that

$$V(\sigma_2) < V(0). \tag{6.18}$$

So, for $m^2 < 0$, the global minimum of the potential is located at $\phi = 0$. Therefore, the global minimum of the potential exhibits symmetry, and there is no spontaneous symmetry breaking.

Now, If $m^2 > 0$, the minimum of the potential can only occur at $\phi = 0$. Consequently, in this case, the system has no spontaneous symmetry breaking. However, the minimum of the potential can be at σ_1 or σ_2. For $m^2 > 0$, from Eq. 6.17, it can be observed that V_{eff}^{ren} decreases towards $V(\sigma_1)$ (since $\sigma_1 < 0$) and increases towards $V(\sigma_2)$. Thus

$$V(\sigma_1) < V(\sigma_2), \tag{6.19}$$

which makes σ_1 the global minima. Now, for $m^2 = 0$, we can apply the same reasoning as for $m^2 < 0$ and conclude that $\phi(\sigma_2)$ represents the global minimum configuration of the field.

In conclusion, in four-dimensional AdS, there is no spontaneous symmetry breaking for any values of m^2 with $\lambda > 0$.

6.2.2 Three Dimensions

The computation for the three-dimensional case follows a similar approach as the four-dimensional case. In three dimensions, we can expand the propagator near $u = 0$ as (from Eq. 6.4)

$$\lim_{u\to 0} G(W) = \frac{1}{4\pi L} + \frac{1}{4\pi u} - \frac{\Delta}{4\pi L} + O(u), \tag{6.20}$$

where Δ is defined in Eq. 6.5. Substituting this in Eq. 4.15 one can calculate V_1 as

$$V_1 = \frac{N\sigma}{8\pi u} - \frac{N}{12L\pi}\left(\sigma + \frac{1}{L^2}\right)\sqrt{1 + L^2\sigma}. \tag{6.21}$$

Here, the BF bound is given by $-1/L^2 < \sigma$, ensuring that the effective potential remains real valued. The divergence in V_1 is proportional to a linear power of σ. Therefore, it can be renormalized using Eq. 4.18, which give the renormalized parameters as

$$\frac{m^2}{\lambda} = \frac{1}{8\pi}\left(\frac{1}{u} + \frac{1}{L}\right) + \frac{m_0^2}{\lambda_0} \tag{6.22}$$

All the divergences in the effective potential are renormalized by Eq. 6.22. Similar to flat space (see Section 4.4.1), we can choose $\lambda = \lambda_0$. In Eq. 6.22, we included finite terms involving L in the renormalized parameters. By using this renormalization condition (4.16a), the renormalized effective potential becomes

$$V_{eff}^{ren} = \frac{N\sigma}{8\pi L} + \frac{Nm^2\sigma}{\lambda} - \frac{N\sigma^2}{2\lambda} - \frac{N}{12\pi}\left(\sigma + \frac{1}{L^2}\right)^{3/2}. \tag{6.23}$$

The Ground State

Continuing the analysis in the same manner as in four dimensions, the stationary points of the potential are determined by Eq. 4.18. By utilizing Eq. 4.18a, we obtain

$$\phi^2(\sigma) = -\frac{N}{4\pi L} - \frac{2Nm^2}{\lambda} + \frac{2N\sigma}{\lambda} + \frac{N}{4\pi L}\sqrt{1 + L^2\sigma}. \tag{6.24}$$

Here

$$\frac{d\phi^2}{d\sigma} > 0, \tag{6.25}$$

which implies that ϕ^2 is a monotonically increasing function of σ. From Eq. 4.20, we find that the stationary points of the potential V occur at $\phi = 0$ or $\sigma = 0$. Let's consider the extremum at $\sigma = 0$, the effective potential is given as

$$V(0) = -\frac{N}{12\pi L^3}, \tag{6.26}$$

For which we have

$$\phi^2(0) = -\frac{2Nm^2}{\lambda}. \tag{6.27}$$

Therefore, the value of $\sigma = 0$ is only possible if $m^2 \leq 0$. If we consider $m^2 < 0$, from Eq. 6.27 we find that $\phi^2(0) > 0$. As a monotonically increasing function, $\phi = 0$ is possible only if $\sigma < 0$. According to the BF bound $-1/L^2 < \sigma$, σ can indeed be negative. Now let's consider a σ_1 such that $-1/L^2 < \sigma_1 < 0$ and $\phi^2(\sigma_{10}) = 0$. We can expand V_{eff}^{ren} near $\sigma = 0$ as follows:

$$\lim_{\sigma \to 0} V_{eff}^{ren}(\sigma) = -\frac{N}{12\pi L^3} - N\sigma_1 \frac{m^2}{\lambda}. \tag{6.28}$$

It is important to note that the only extremum of $V_{\text{eff}}^{\text{ren}}(\sigma)$ occurs when $\sigma = \sigma_{10}$, which corresponds to $\phi = 0$. In the case of $m^2 < 0$, we find that $V_{\text{eff}}^{\text{ren}}(\sigma_{10}) > V_{\text{eff}}^{\text{ren}}(\sigma = 0)$. Therefore, the global minimum of the potential is located at $\sigma = 0$, representing an asymmetric minimum and indicating spontaneous symmetry breaking. However, for $m^2 > 0$ and $m^2 = 0$, the only possible ground state occurs at $\phi = 0$, which is a symmetric configuration.

In conclusion, in the AdS background, the qualitative results are similar to those obtained in flat space, as discussed in Section 3.4. In four dimensions, there is no spontaneous symmetry breaking for any values of m^2. However, in three-dimensional AdS, we observe spontaneous symmetry breaking for $m^2 < 0$. Furthermore, one-loop quantum effects introduce corrections proportional to $1/L$ and $1/L^2$ to the effective mass squared of the theory in three and four dimensions, respectively. Therefore, curvature's effect is to modify the effective mass squared of the scalar fields in this context.

Chapter 7

Conclusions and Future Work

In this thesis, we employ the concept of effective action as a fundamental mathematical tool to investigate various phenomena, including the Casimir effect, the Schwinger effect, and spontaneous symmetry breaking (SSB) in Rindler spacetime as well as in curved spacetime (anti-de Sitter space) or spacetime with non-trivial topology.

7.1 Summary

Our initial work (Chapter 3) delves into the impact of extra compact dimensions and background electromagnetic fields on the Casimir effect. We develop a closed-form expression for the one-loop effective potential of a massive complex scalar field minimally coupled to a constant electromagnetic field. Importantly, this analysis is conducted in arbitrary $p+k$ dimensional spacetime. Our approach provides a general framework that reproduces existing results and also yields new insights. Within this framework, we comprehensively examine the influence of several key factors on the Casimir force, including the number and size of extra compact dimensions, the mass of the complex scalar field, and the presence of constant electric and magnetic fields. Notably, a constant electric field leads to vacuum polarization, known as the Schwinger effect, with its signature manifested in the imaginary part of the effective potential. Leveraging the effective potential, we calculate the pair

production enhancement rate resulting from extra compact dimensions and finite boundary conditions, such as parallel plates.

Our research carries implications for experimental investigations. It suggests that more precise measurements of the Casimir force, capable of distinguishing corrections arising from extra compact dimensions, could provide experimental validation for their existence. Furthermore, while the Schwinger effect remains to be experimentally realized due to its requirement for intense electric fields, our findings indicate that pair production rates can be significantly enhanced by incorporating finite boundary conditions, potentially facilitating its experimental observation.

As a mathematical tool of remarkable potency, the effective potential enables further generalization of our findings. This encompasses extensions, including the twisted fields, quasi-periodic boundary conditions, and finite temperature effects.

In our subsequent research (Chapter 5 and Chapter 6), we directed our focus towards the phenomenon of spontaneous symmetry breaking (SSB). SSB is unmistakably characterized by the non-zero vacuum expectation value of a field, rendering the effective potential a natural tool for understanding this phenomenon.

To begin with, we pondered over the observer-dependent aspects of SSB. To that end, we explored SSB from the perspective of a uniformly accelerated observer. Our analysis revealed that the broken symmetries are restored from the perceptive of a uniformly accelerated observer, provided the proper acceleration is above a critical value. These findings had previously been found in the literature in the context of four-dimensional spacetime and relying on a specific renormalization procedure, which was incomplete. We have advanced these insights by extending their applicability to spacetimes of arbitrary dimensions. Furthermore, we introduced a more general renormalization procedure for calculating one-loop effective potential in the Euclidean Rindler frame. Connections with finite temperature field theory results are established, further reinforcing that Rindler space can be a proxy for Minkowski spacetime with finite temperature.

To comprehensively understand SSB, we employed two distinct models. The first model featured a single scalar field with $\lambda\phi^4$ interaction, while the second model

was an $O(N)$ symmetric scalar field theory in the large N limit. We examined scenarios encompassing discrete and continuous symmetry breaking with these models, employing two distinct perturbation methods to facilitate our analysis.

Additionally, we extended our effective potential calculations to study SSB in anti-de Sitter space. In this context, we focused purely on $O(N)$ symmetric scalar field theory in the large N limit. This work involved explicit calculations to understand the curvature-dependent aspects of SSB. Our work in anti-de Sitter space may pave the way for a deeper comprehension of SSB within the framework of quantum gravity theory, particularly through the lens of the AdS/CFT correspondence.

In summary, the effective action method provides a robust and systematic approach to studying the vacuum state of a theory and quantum field theory in curved spacetime in general. They offer a comprehensive understanding of quantum fluctuations, renormalization effects, vacuum stability, and non-perturbative phenomena, making them a valuable tool for theoretical physicists in various domains of physics. So, the effective action method can provide insight into a more general theory of quantum gravity.

7.2 Future Work

Some possible extensions of our work are listed below.

1. Understanding the Casimir effect in nontrivial topologies using different boundary conditions on the field, like the anti-periodic (twisted fields) and quasi-periodic boundary conditions. One can extend the results using Euclidean formalism to obtain finite temperature corrections.

2. One can study SSB in thermal anti-de Sitter space and address the following questions. Is broken symmetry restored after a critical acceleration? If so, it would be fascinating to investigate the role of the Hawking-Page transition in SSB and in the possible restoration of broken symmetry.

3. We can also study the symmetry breaking from the perspective of a uniformly accelerating observer in anti-de Sitter space. This is interesting since such a model would include the effects of both the curvature as well as the existence of an event horizon. Such an analysis can address the following questions. Is the Ads-Rindler frame equivalent to finite temperature AdS through Unruh temperature? Also, using AdS/CFT correspondence, one may calculate the CFT signature of symmetry restoration, and also provide us with insights on 'critical acceleration' in AdS spacetime.

4. One can also inquire the issue of electro-weak symmetry breaking in the early universe by considering the SSB in de-Sitter (dS) space from the perspectives of both geodesic as well as accelerating observers in dS spacetime.

Bibliography

[1] John H. Schwarz. "Introduction to Superstring Theory". In: *Techniques and Concepts of High-Energy Physics*. Ed. by Harrison B. Prosper and Michael Danilov. Dordrecht: Springer Netherlands, 2001, pp. 143–187. DOI: 10.1007/978-94-010-0522-7_4.

[2] Carlo Rovelli. *Quantum Gravity*. Cambridge Monographs on Mathematical Physics. Cambridge University Press, 2004. DOI: 10.1017/CBO9780511755804.

[3] Juan Maldacena. "The Large-N Limit of Superconformal Field Theories and Supergravity". In: *International Journal of Theoretical Physics* 38.4 (1999), pp. 1113–1133. DOI: 10.1023/A:1026654312961.

[4] Thomas Hartman. "Lectures on quantum gravity and black holes". In: *Cornell University* 21 (2015).

[5] Suvrat Raju. "Lessons from the information paradox". In: *Physics Reports* 943 (2022). Lessons from the information paradox, pp. 1–80. DOI: https://doi.org/10.1016/j.physrep.2021.10.001.

[6] Sean A. Hartnoll, Andrew Lucas, and Subir Sachdev. *Holographic quantum matter*. 2018.

[7] S. W. HAWKING. "Black hole explosions?" In: *Nature* 248.5443 (1974), pp. 30–31. DOI: 10.1038/248030a0.

[8] W. G. Unruh. "Notes on black-hole evaporation". In: *Phys. Rev. D* 14 (4 1976), pp. 870–892. DOI: 10.1103/PhysRevD.14.870.

[9] Stephen A. Fulling. "Nonuniqueness of Canonical Field Quantization in Riemannian Space-Time". In: *Phys. Rev. D* 7 (10 1973), pp. 2850–2862. DOI: 10.1103/PhysRevD.7.2850.

[10] N. D. Birrell and P. C. W. Davies. *Quantum Fields in Curved Space*. Cambridge Monographs on Mathematical Physics. Cambridge University Press, 1982. DOI: 10.1017/CBO9780511622632.

[11] H. B. G. Casimir. "On the Attraction Between Two Perfectly Conducting Plates". In: *Indag. Math.* 10 (1948), pp. 261–263.

[12] J. Goldstone. "Field theories with Superconductor solutions". In: *Il Nuovo Cimento (1955-1965)* 19.1 (1961), pp. 154–164. DOI: 10.1007/BF02812722.

[13] Jeffrey Goldstone, Abdus Salam, and Steven Weinberg. "Broken Symmetries". In: *Phys. Rev.* 127 (3 1962), pp. 965–970. DOI: 10.1103/PhysRev.127.965.

[14] Leonard Parker and David Toms. *Quantum Field Theory in Curved Spacetime: Quantized Fields and Gravity*. Cambridge Monographs on Mathematical Physics. Cambridge University Press, 2009. DOI: 10.1017/CBO9780511813924.

[15] Thanu Padmanabhan. "Real Life I: Interactions". In: *Quantum Field Theory: The Why, What and How*. Cham: Springer International Publishing, 2016, pp. 131–187. DOI: 10.1007/978-3-319-28173-5_4.

[16] Michael F. Wondrak, Walter D. van Suijlekom, and Heino Falcke. "Gravitational Pair Production and Black Hole Evaporation". In: *Phys. Rev. Lett.* 130 (22 2023), p. 221502. DOI: 10.1103/PhysRevLett.130.221502.

[17] Sidney Coleman. *Aspects of Symmetry: Selected Erice Lectures*. Cambridge University Press, 1985. DOI: 10.1017/CBO9780511565045.

[18] Eduardo Fradkin. *Quantum Field Theory: An Integrated Approach*.

[19] M. R. Brown and M. J. Duff. "Exact results for effective Lagrangians". In: *Phys. Rev. D* 11 (8 1975), pp. 2124–2135. DOI: 10.1103/PhysRevD.11.2124.

[20] R. J. Rivers. *Path Integral Methods in Quantum Field Theory*. Cambridge Monographs on Mathematical Physics. Cambridge University Press, 1987. DOI: 10.1017/CBO9780511564055.

[21] K. Symanzik. "Renormalizable models with simple symmetry breaking". In: *Communications in Mathematical Physics* 16.1 (1970), pp. 48–80. DOI: 10.1007/BF01645494.

[22] J. Iliopoulos, C. Itzykson, and A. Martin. "Functional methods and perturbation theory". In: *Rev. Mod. Phys.* 47 (1 1975), pp. 165–192. DOI: 10.1103/RevModPhys.47.165.

[23] Erick J. Weinberg and Aiqun Wu. "Understanding complex perturbative effective potentials". In: *Phys. Rev. D* 36 (8 1987), pp. 2474–2480. DOI: 10.1103/PhysRevD.36.2474.

[24] Sidney Coleman. *Lectures of Sidney Coleman on Quantum Field Theory*. Ed. by Bryan Gin-ge Chen et al. Hackensack: WSP, Dec. 2018. DOI: 10.1142/9371.

[25] R. Jackiw. "Functional evaluation of the effective potential". In: *Phys. Rev. D* 9 (6 1974), pp. 1686–1701. DOI: 10.1103/PhysRevD.9.1686.

[26] Viatcheslav Mukhanov and Sergei Winitzki. *Introduction to quantum effects in gravity*. Cambridge University Press, June 2007.

[27] Julian Schwinger. "On Gauge Invariance and Vacuum Polarization". In: *Phys. Rev.* 82 (5 1951), pp. 664–679. DOI: 10.1103/PhysRev.82.664.

[28] Sang Pyo Kim, Hyun Kyu Lee, and Yongsung Yoon. "Effective action of QED in electric field backgrounds". In: *Phys. Rev. D* 78 (10 2008), p. 105013. DOI: 10.1103/PhysRevD.78.105013.

[29] David J. Toms. "Mathematical appendices". In: *The Schwinger Action Principle and Effective Action*. Cambridge Monographs on Mathematical Physics. Cambridge University Press, 2007, 447–461. DOI: 10.1017/CBO9780511585913.010.

[30] Mikko Laine and Aleksi Vuorinen. *Basics of Thermal Field Theory*. Springer International Publishing, 2016. DOI: 10.1007/978-3-319-31933-9.

[31] S.R. Haridev and Prasant Samantray. "Revisiting vacuum energy in compact spacetimes". In: *Physics Letters B* 835 (2022), p. 137489. DOI: https://doi.org/10.1016/j.physletb.2022.137489.

[32] S. A. Fulling. *Aspects of Quantum Field Theory in Curved Space-time*. Vol. 17. 1989.

[33] Rafael I. Nepomechie. "Calculating heat kernels". In: *Phys. Rev. D* 31 (12 1985), pp. 3291–3292. DOI: 10.1103/PhysRevD.31.3291.

[34] Kenneth G. Wilson. "Renormalization Group and Critical Phenomena. I. Renormalization Group and the Kadanoff Scaling Picture". In: *Phys. Rev. B* 4 (9 1971), pp. 3174–3183. DOI: 10.1103/PhysRevB.4.3174.

[35] Kenneth G. Wilson. "The renormalization group and critical phenomena". In: *Rev. Mod. Phys.* 55 (3 1983), pp. 583–600. DOI: 10.1103/RevModPhys.55.583.

[36] A Zee. *Quantum Field Theory in a Nutshell; 1st ed.* In a nutshell. Princeton, NJ: Princeton Univ. Press, 2003.

[37] Ashok Sen. *Lectures on quantum field theory 2 home.icts.res.in/ sen*.

[38] Zhang Hong-Hao et al. "On analytic formulas of Feynman propagators in position space". In: *Chinese Physics C* 34.10 (2010), p. 1576. DOI: 10.1088/1674-1137/34/10/005.

[39] Michael Edward Peskin and Daniel V. Schroeder. *An Introduction to Quantum Field Theory*. Reading, USA: Addison-Wesley (1995) 842 p. Westview Press, 1995.

[40] Tom Banks. *Modern Quantum Field Theory: A Concise Introduction*. Cambridge University Press, 2008. DOI: 10.1017/CBO9780511811500.

[41] Theodor Kaluza. "Sitzungsber". In: *Preuss. Akad. Wiss. Phys. Math. Klasse* 996 (1921), p. 1921.

[42] Oskar Klein. "Quantum theory and five-dimensional relativity theory". In: *The Oskar Klein Memorial Lectures: Vol 1: Lectures by CN Yang and S Weinberg*. World Scientific, 1991, pp. 67–80.

[43] TH. Kaluza. "On the Unification Problem in Physics". In: *International Journal of Modern Physics D* 27.14 (2018), p. 1870001. DOI: 10.1142/s0218271818700017.

[44] Hongbo Cheng. "The asymptotic behavior of Casimir force in the presence of compactified universal extra dimensions". In: *Physics Letters B* 643.6 (2006), pp. 311–314. DOI: https://doi.org/10.1016/j.physletb.2006.10.051.

[45] Hongbo Cheng. "The Casimir force on a piston in the spacetime with extra compactified dimensions". In: *Physics Letters B* 668.1 (2008), pp. 72–77. DOI: https://doi.org/10.1016/j.physletb.2008.08.013.

[46] AC Pinto et al. "Casimir effect for a massive scalar field under mixed boundary conditions". In: *Brazilian Journal of Physics* 33.4 (2003), pp. 860–866. DOI: 10.1590/S0103-97332003000400042.

[47] S.A. Fulling and Klaus Kirsten. "Comment on: "The Casimir force on a piston in the spacetime with extra compactified dimensions" [Phys. Lett. B 668 (2008) 72]". In: *Physics Letters B* 671.1 (2009), pp. 179–180. DOI: https://doi.org/10.1016/j.physletb.2008.11.037.

[48] Klaus Kirsten and S. A. Fulling. "Kaluza-Klein models as pistons". In: *Phys. Rev. D* 79 (6 2009), p. 065019. DOI: 10.1103/PhysRevD.79.065019.

[49] R. M. Cavalcanti. "Casimir force on a piston". In: *Phys. Rev. D* 69 (6 2004), p. 065015. DOI: 10.1103/PhysRevD.69.065015.

[50] S. Mobassem. "Casimir effect for massive scalar field". In: *Modern Physics Letters A* 29.31 (2014), p. 1450160. DOI: 10.1142/S0217732314501600.

[51] S. K. Lamoreaux. "Demonstration of the Casimir Force in the 0.6 to 6μm Range". In: *Phys. Rev. Lett.* 78 (1 1997), pp. 5–8. DOI: 10.1103/PhysRevLett.78.5.

[52] M. Bordag et al. *Advances in the Casimir effect*. Vol. 145. Oxford University Press, 2009.

[53] A.M. Sirunyan et al. "A measurement of the Higgs boson mass in the diphoton decay channel". In: *Physics Letters B* 805 (2020), p. 135425. DOI: https://doi.org/10.1016/j.physletb.2020.135425.

[54] Katja Poppenhaeger et al. "The Casimir effect in the presence of compactified universal extra dimensions". In: *Physics Letters B* 582.1 (2004), pp. 1–5. DOI: https://doi.org/10.1016/j.physletb.2003.12.015.

[55] M V Cougo-Pinto et al. "Bosonic Casimir effect in external magnetic field". In: *Journal of Physics A: Mathematical and General* 32.24 (1999), pp. 4457–4462. DOI: 10.1088/0305-4470/32/24/310.

[56] W. Heisenberg and H. Euler. *Consequences of Dirac Theory of the Positron*. 2006.

[57] Y. M. Cho and D. G. Pak. "A Convergent Series for the QED Effective Action". In: *Phys. Rev. Lett.* 86 (10 2001), pp. 1947–1950. DOI: 10.1103/PhysRevLett.86.1947.

[58] W. S. Bae, Y. M. Cho, and D. G. Pak. "Electric-magnetic duality in the QED effective action". In: *Phys. Rev. D* 64 (1 2001), p. 017303. DOI: 10.1103/PhysRevD.64.017303.

[59] Yu. A. Sitenko and S. A. Yushchenko. "The Casimir effect with quantized charged scalar matter in background magnetic field". In: *International Journal of Modern Physics A* 29.09 (2014), p. 1450052. DOI: 10.1142/S0217751X14500523.

[60] Mehran Kardar. *Statistical Physics of Fields*. Cambridge University Press, 2007. DOI: 10.1017/CBO9780511815881.

[61] Steven Weinberg. *The Quantum Theory of Fields*. Vol. 2. Cambridge University Press, 1996. DOI: 10.1017/CBO9781139644174.

[62] Lewis H. Ryder. *Quantum Field Theory*. 2nd ed. Cambridge University Press, 1996. DOI: 10.1017/CBO9780511813900.

[63] Yoichiro Nambu. "Quasi-Particles and Gauge Invariance in the Theory of Superconductivity". In: *Phys. Rev.* 117 (3 1960), pp. 648–663. DOI: 10.1103/PhysRev.117.648.

[64] N. D. Mermin and H. Wagner. "Absence of Ferromagnetism or Antiferromagnetism in One- or Two-Dimensional Isotropic Heisenberg Models". In: *Phys. Rev. Lett.* 17 (22 1966), pp. 1133–1136. DOI: 10.1103/PhysRevLett.17.1133.

[65] P. C. Hohenberg. "Existence of Long-Range Order in One and Two Dimensions". In: *Phys. Rev.* 158 (2 1967), pp. 383–386. DOI: 10.1103/PhysRev.158.383.

[66] Sidney Coleman. "There are no Goldstone bosons in two dimensions". In: *Communications in Mathematical Physics* 31.4 (1973), pp. 259–264. DOI: 10.1007/BF01646487.

[67] Sidney Coleman, R. Jackiw, and H. D. Politzer. "Spontaneous symmetry breaking in the O(N) model for large N". In: *Phys. Rev. D* 10 (8 1974), pp. 2491–2499. DOI: 10.1103/PhysRevD.10.2491.

[68] L. F. Abbott, J. S. Kang, and Howard J. Schnitzer. "Bound states, tachyons, and restoration of symmetry in the $\frac{1}{N}$ expansion". In: *Phys. Rev. D* 13 (8 1976), pp. 2212–2226. DOI: 10.1103/PhysRevD.13.2212.

[69] Makoto Kobayashi and Taichiro Kugo. "On the Ground State of $O(N) - \lambda\phi^2$ Model". In: *Progress of Theoretical Physics* 54.5 (Nov. 1975), pp. 1537–1545. DOI: 10.1143/PTP.54.1537.

[70] D.A. Kirzhnits and A.D. Linde. "Macroscopic consequences of the Weinberg model". In: *Physics Letters B* 42.4 (1972), pp. 471–474. DOI: https://doi.org/10.1016/0370-2693(72)90109-8.

[71] L. Dolan and R. Jackiw. "Symmetry behavior at finite temperature". In: *Phys. Rev. D* 9 (12 1974), pp. 3320–3341. DOI: 10.1103/PhysRevD.9.3320.

[72] Steven Weinberg. "Gauge and global symmetries at high temperature". In: *Phys. Rev. D* 9 (12 1974), pp. 3357–3378. DOI: 10.1103/PhysRevD.9.3357.

[73] D. G. Caldi and S. Nussinov. "Simple approach to finite-temperature symmetry restoration". In: *Phys. Rev. D* 29 (4 1984), pp. 739–742. DOI: 10.1103/PhysRevD.29.739.

[74] M.B. Einhorn and D.R.T. Jones. "phi4 in three dimensions at finite temperature". In: *Nuclear Physics B* 398.3 (1993), pp. 611–621. DOI: https://doi.org/10.1016/0550-3213(93)90606-P.

[75] Y. Fujimoto, A. Wipf, and H. Yoneyama. "Finite temperature $\lambda\phi 4$ theory in two and three dimensions and symmetry restoration". In: *Zeitschrift für Physik C Particles and Fields* 35.3 (1987), pp. 351–354. DOI: 10.1007/BF01570771.

[76] Pallab Basu, Haridev S R, and Prasant Samantray. *On the Observer Dependence of the Quantum Effective Potential*. 2023.

[77] P C W Davies. "Scalar production in Schwarzschild and Rindler metrics". In: *Journal of Physics A: Mathematical and General* 8.4 (1975), p. 609. DOI: 10.1088/0305-4470/8/4/022.

[78] T.D. Lee. "Are black holes black bodies". In: *Nuclear Physics B* 264 (1986), pp. 437–486. DOI: https://doi.org/10.1016/0550-3213(86)90493-1.

[79] S.M. Christensen and M.J. Duff. "Flat space as a gravitational instanton". In: *Nuclear Physics B* 146.1 (1978), pp. 11–19. DOI: https://doi.org/10.1016/0550-3213(78)90428-5.

[80] T. Padmanabhan. "Thermality of the Rindler horizon: A simple derivation from the structure of the inertial propagator". In: *Phys. Rev. D* 100 (4 2019), p. 045024. DOI: 10.1103/PhysRevD.100.045024.

[81] Shin Takagi. "Vacuum Noise and Stress Induced by Uniform Acceleration: Hawking-Unruh Effect in Rindler Manifold of Arbitrary Dimension". In: *Progress of Theoretical Physics Supplement* 88 (Mar. 1986), pp. 1–142. DOI: 10.1143/PTP.88.1.

[82] Lu's C. B. Crispino, Atsushi Higuchi, and George E. A. Matsas. "The Unruh effect and its applications". In: *Rev. Mod. Phys.* 80 (3 2008), pp. 787–838. DOI: 10.1103/RevModPhys.80.787.

[83] J. S. Ben-Benjamin et al. "Unruh acceleration radiation revisited". In: *International Journal of Modern Physics A* 34.28 (2019), p. 1941005. DOI: 10.1142/S0217751X19410057.

[84] R. Emparan. "Heat kernels and thermodynamics in Rindler space". In: *Phys. Rev. D* 51 (10 1995), pp. 5716–5719. DOI: 10.1103/PhysRevD.51.5716.

[85] S. P. de Alwis and N. Ohta. "Thermodynamics of quantum fields in black hole backgrounds". In: *Phys. Rev. D* 52 (6 1995), pp. 3529–3542. DOI: 10.1103/PhysRevD.52.3529.

[86] B. Linet. *Euclidean scalar and spinor Green's functions in Rindler space*. 1995. DOI: 10.48550/ARXIV.GR-QC/9505033.

[87] E. T. Akhmedov and D. V. Diakonov. "Free energy and entropy in Rindler and de Sitter space-times". In: *Phys. Rev. D* 105 (10 2022), p. 105003. DOI: 10.1103/PhysRevD.105.105003.

[88] Daniel Kabat. "Black hole entropy and entropy of entanglement". In: *Nuclear Physics B* 453.1 (1995), pp. 281–299. DOI: https://doi.org/10.1016/0550-3213(95)00443-V.

[89] Alireza Ansari and Shiva Eshaghi. "Macdonald's identities and integral representations of products of Airy functions". In: *Integral Transforms and Special Functions* 31.9 (2020), pp. 744–757. DOI: 10.1080/10652469.2020.1737529.

[90] I. S. Gradshteyn and I. M. Ryzhik. *Table of integrals, series, and products*. Seventh. Translated from the Russian, Translation edited and with a preface by Alan Jeffrey and Daniel Zwillinger, With one CD-ROM (Windows, Macintosh and UNIX). Elsevier/Academic Press, Amsterdam, 2007, pp. xlviii+1171.

[91] Antonio Dobado. *Spontaneous symmetry breaking and the Unruh effect*. 2017. DOI: 10.48550/ARXIV.1703.05675.

[92] T Padmanabhan. "Symmetry breaking in the early universe and accelerated frames". In: *Journal of Physics A: Mathematical and General* 16.2 (1983), p. 335. DOI: 10.1088/0305-4470/16/2/016.

[93] Paolo Castorina and Marco Finocchiaro. "Symmetry Restoration by Acceleration". In: *Journal of Modern Physics* 03.11 (2012), pp. 1703–1708. DOI: 10.4236/jmp.2012.311209.

[94] Pallab Basu, S. R. Haridev, and Prasant Samantray. "Aspects of spontaneous symmetry breaking in Rindler and anti–de Sitter spacetimes for the $O(N)$ linear sigma model". In: *Phys. Rev. D* 107 (10 2023), p. 105004. DOI: 10.1103/PhysRevD.107.105004.

[95] S. Weinberg. *Gravitation and cosmology*. New York: John Wiley and Sons, 1972.

[96] S. W. Hawking and G. F. R. Ellis. *The Large Scale Structure of Space-Time*. Cambridge Monographs on Mathematical Physics. Cambridge University Press, 1973. DOI: 10.1017/CBO9780511524646.

[97] Martin Ammon and Johanna Erdmenger. *Gauge/Gravity Duality: Foundations and Applications*. Cambridge University Press, 2015. DOI: 10.1017/CBO9780511846373.

[98] John McGreevy. "8.821 F2008 Problem Set 4 Solutions". In: (). DOI: https://ocw.mit.edu/courses/8-821-string-theory-fall-2008/.

[99] Peter Breitenlohner and Daniel Z. Freedman. "Positive energy in anti-de Sitter backgrounds and gauged extended supergravity". In: *Physics Letters B* 115.3 (1982), pp. 197–201. DOI: https://doi.org/10.1016/0370-2693(82)90643-8.

[100] Peter Breitenlohner and Daniel Z Freedman. "Stability in gauged extended supergravity". In: *Annals of Physics* 144.2 (1982), pp. 249–281. DOI: https://doi.org/10.1016/0003-4916(82)90116-6.

[101] Igor R. Klebanov and Edward Witten. "Ads/CFT correspondence and symmetry breaking". In: *Nuclear Physics B* 556.1 (1999), pp. 89–114. DOI: https://doi.org/10.1016/S0550-3213(99)00387-9.

[102] C.P. Burgess and C.A. Lütken. "Propagators and effective potentials in anti-de Sitter space". In: *Physics Letters B* 153.3 (1985), pp. 137–141. DOI: https://doi.org/10.1016/0370-2693(85)91415-7.

[103] David Berenstein et al. "Operator product expansion for Wilson loops and surfaces in the large N limit". In: *Phys. Rev. D* 59 (10 1999), p. 105023. DOI: 10.1103/PhysRevD.59.105023.

[104] Takeo Inami and Hirosi Ooguri. "One-Loop Effective Potential in Anti-de Sitter Space". In: *Progress of Theoretical Physics* 73.4 (Apr. 1985), pp. 1051–1054. DOI: 10.1143/PTP.73.1051.

List of Publications and Presentations

Publications

1. P. Basu, S.R. Haridev and P. Samantray, Aspects of spontaneous sym- metry breaking in rindler and anti–de sitter spacetimes for the o(N) linear sigma model, *Phys. Rev. D* **107** (2023) 105004

2. S. Haridev and P. Samantray, Revisiting vacuum energy in compact spacetimes, *Physics Letters B* **835** (2022) 137489

3. P. Basu, H.S. R and P. Samantray, On the observer dependence of the quantum effective potential, 2023, *arXiv.2303.04039*.

Conference Presentations

1. **[Poster Presentation]** Frontier Symposium in Physics 2023,
   Indian Institutes of Science Education and Research, Thiruvananthapuram, India, February 2023

2. **[Poster Presentation]** 23^{rd} International Conference on General Relativity and Gravitation (IAGRG)
   Indian Institutes of Science Education and Research, Kolkata, India,December 2022

3. **[Oral Presentation]** An Inaugural Conference on Current Status of Cosmology
   The Thanu Padmanabhan Center for Cosmology and Science Popularization (Online), October 2022

4. [**Poster Presentation**] 23^{rd} International Conference on General Relativity and Gravitation
   Institute of Theoretical Physics, Chinese Academy of Sciences,Liyang, China (Online), July 2022

Invited Talks

1. **Seminar**
   INTER-UNIVERSITY CENTRE FOR ASTRONOMY AND ASTROPHYSICS (IUCAA), September 2023

2. **High Energy Theory Seminar**
   Indian Institutes of Science Education and Research, Pune (IISER-Pune) Department of Physics, September 2023

3. **High Energy Theory Seminar**
   Indian Institute of technology, Hyderabad (IITH)
   Strings, Fields, and Gravity group, August 2023

4. **One day workshop on Research facility training program**
   Osmania University, Hyderabad, India
   Department of Astronomy In association with DST SERB Under scientific social responsibility, August 2022

Brief Biography of the Candidate

Mr. Haridev S R obtained Bachelor's degree (B. Sc in Physics) in the year 2016 from the University of Calicut, Kerala. He obtained Master's degree in Physics (M. Sc Physics) from the Indian Institute of Technology, Indore (IIT Indore) in the year 2018. He joined as a research scholar in the Department of Physics, BITS-Pilani, Hyderabad campus in the year 2019 under the supervision of Dr. Prasant Samantray.

Breif Biography of the Supervisor

Prof. Prasant Kumar Samantray currently serves as an Associate Professor in the Department of Physics at BITS - PILANI, Hyderabad Campus, Hyderabad. He joined BITS-Pilani Hyderabad as an assistant professor in 2017. Before joining BITS Pilani, Hyderabad, he was a visiting faculty at ICTS-TIFR, Bangalore, and IUCAA Pune. Between 2014 and 2017, he was an assistant professor at the Centre of Astronomy at IIT Indore. Prof. Samantray also gained valuable experience as a post-doctoral fellow at ICTS-TIFR, Bengaluru, from 2013 to 2014, following his time as an official visitor at IUCAA Pune.

He earned his Ph.D. in Physics from Arizona State University in 2012 and completed his Bachelor's degree (B.Tech) at IIT Madras. Prof. Samantray's research interests span a wide array of topics, including AdS/CFT Correspondence, Phase Transitions in Matrix Models, Quantum Fields in Curved Spacetimes, and Foundations of Quantum Mechanics.